Εθνικό Μετσόβιο Πολυτεχνείο
Σχολή Πολιτικών Μηχανικών
Εργαστήριο Μεταλλικών Κατασκευών

ΙΚΑΝΟΤΙΚΟΣ ΣΧΕΔΙΑΣΜΟΣ ΚΑΙ ΜΕΛΕΤΗ ΣΥΜΠΕΡΙΦΟΡΑΣ ΠΟΛΥΩΡΟΦΩΝ ΜΕΤΑΛΛΙΚΩΝ ΚΤΙΡΙΩΝ ΚΑΤΑ ΤΟΝ ΕΥΡΩΚΩΔΙΚΑ 8

Κέντρο John Hancock, Σικάγο

Διπλωματική Εργασία

Ελεονώρα Μπαλαούρα

ΕΜΚ ΔΕ 2016 46

Επιβλέπων: Χάρης Γαντές, Δρ. Πολιτικός Μηχανικός, Καθηγητής ΕΜΠ

Αθήνα, Οκτώβριος 2016

National Technical University of Athens
School of Civil Engineering
Institute of Steel Structures

CAPACITY DESIGN AND INVESTIGATION OF THE BEHAVIOR OF MULTI-STOREY STEEL BUILDINGS ACCORDING TO EUROCODE 8

John Hancock Centre, Chicago

Diploma Thesis

Eleonora Balaoura

ΕΜΚ ΔΕ 2016 46

Supervisor: Charis Gantes, Professor NTUA

Athens, October 2016

Ελεονώρα Μπαλαούρα (2016)

Ικανοτικός σχεδιασμός και μελέτη συμπεριφοράς πολυώροφων μεταλλικών κτιρίων κατά τον Ευρωκώδικα 8

Διπλωματική Εργασία ΕΜΚ ΔΕ 2016 46

Εργαστήριο Μεταλλικών Κατασκευών, Εθνικό Μετσόβιο Πολυτεχνείο, Αθήνα.

Eleonora Balaoura (2016)

Diploma Thesis EMK ΔΕ 2016 46

Capacity design and investigation of the behavior of multi-storey steel buildings according to Eurocode 8

Institute of Steel Structures, National Technical University of Athens, Greece

Στον παππού μου Νίκο και τη μητέρα μου Αμαλία,
τους πρώτους μου δασκάλους που με ταξίδεψαν
με υπομονή και αγάπη στο δρόμο της γνώσης

ΕΥΧΑΡΙΣΤΙΕΣ

Η παρούσα διπλωματική εργασία σηματοδοτεί το πέρας μιας πολύμηνης προσπάθειας, αλλά και της προπτυχιακής φοίτησής μου στη Σχολή Πολιτικών Μηχανικών του Ε.Μ.Π. Σε όλη αυτή την πορεία, καθοριστική ήταν η συμβολή και η καθοδήγηση των ανθρώπων που συμπορευτήκαμε, προσφέροντας μου άλλες φορές γνωστικά και άλλες ηθικά και συναισθηματικά εφόδια.

Πρωτίστως θα ήθελα να ευχαριστήσω θερμά τον Καθηγητή και επιβλέποντα της παρούσας διπλωματικής εργασίας κ. Χάρη Γαντέ. Το υψηλού επιπέδου επιστημονικό του υπόβαθρο σε συνδυασμό με την πολυετή εμπειρία και εποπτεία που διαθέτει επί των προβλημάτων μηχανικού, μου προσέφεραν τις βάσεις για να καλλιεργήσω έναν οργανωμένο και ταυτόχρονα σφαιρικό τρόπο σκέψης. Αξιοθαύμαστη αποτελεί η πολύωρη αφοσίωσή του, παρά το απαιτητικό του πρόγραμμα, στην αντιμετώπιση των προβλημάτων που προέκυψαν μέχρι την ολοκλήρωση αυτής της προσπάθειας. Παρά τις αντίξοες συνθήκες που επικρατούν στο ελληνικό πανεπιστήμιο σήμερα, αποτελεί λαμπρό πρότυπο διδάσκοντα και ερευνητή, καθώς μεταβιβάζει όρεξη, έμπνευση και άνευ όρων επιστημονική γνώση στους νέους μηχανικούς.

Οφείλω, επίσης, ένα μεγάλο ευχαριστώ στο εκπαιδευτικό προσωπικό του εργαστηρίου μεταλλικών κατασκευών κ. Δημήτρη Βαμβάτσικο, κ. Παύλο Θανόπουλο και κ. Ανδρέα Σπηλιόπουλο για την εμπειρία και τις αμέριστες συμβουλές που μοιράστηκαν μαζί μου. Η συμβολή τους υπήρξε καθοριστική στη διαμόρφωση της μεθόδου διαστασιολόγησης μεταλλικών κτιρίων κατά τον Ευρωκώδικα 8.

Πολύτιμη ήταν, επίσης, η βοήθεια του υποψήφιου διδάκτορα Ηλία Θανάσουλα, τόσο στην εκμάθηση του λογισμικού πεπερασμένων στοιχείων ADINA, όσο και στην αντιμετώπιση των αριθμητικών προβλημάτων που προέκυψαν κατά τη διάρκεια της εκπόνησης της παρούσας εργασίας.

Θα ήθελα να ευχαριστήσω ακόμη την ομάδα του φόρουμ της σχολής www.mqn.gr για όλες τις όμορφες και μοναδικές στιγμές που περάσαμε μαζί. Το κοινό όραμα για ελεύθερη διάδοση της γνώσης, αλλά και η ακατάπαυστη μάχη για τη διατήρηση ομαδικών θεσμών στο ελληνικό πανεπιστήμιο, μας συνδιαμόρφωσαν και μας ένωσαν σε μια από τις ομορφότερες εμπειρίες των φοιτητικών μας χρόνων.

Ωστόσο, πέρα από τη βοήθεια στη συγγραφή αυτής της εργασίας, θα ήθελα να αναφερθώ στους αγαπητούς μου φίλους που αποτελούν αναπόσπαστο ηθικό και συναισθηματικό μου στήριγμα. Ευχαριστώ τους Ανδρόνικο, Κώστα, Πέτρο, Ορέστη, Λάζαρο και Μάνο για την όμορφη καθημερινότητα που μοιραστήκαμε στη σχολή, καθώς και τους Χριστίνα, Έμμα και Χρύσα για τη συνεχή υποστήριξη και αγάπη τους.

Θα ήθελα να ευχαριστήσω ιδιαιτέρως τον Νίκο Λαντζούνη για τις καίριες παρατηρήσεις επί του περιεχομένου και του κειμένου της διπλωματικής, αλλά και για τη διαρκή συμπαράσταση και την ηθική υποστήριξη που προσέφερε όλο αυτό το διάστημα.

Ολοκληρώνοντας, το μεγαλύτερο ευχαριστώ το οφείλω στους γονείς μου Αμαλία και Σπύρο καθώς και στον αδερφό μου Νίκο για την υπομονή, την εμπιστοσύνη και την ανιδιοτελή αγάπη που μου δείχνουν όλα αυτά τα χρόνια.

Ελεονώρα Μπαλαούρα

Οκτώβριος 2016

ΕΘΝΙΚΟ ΜΕΤΣΟΒΙΟ ΠΟΛΥΤΕΧΝΕΙΟ
ΣΧΟΛΗ ΠΟΛΙΤΙΚΩΝ ΜΗΧΑΝΙΚΩΝ
ΕΡΓΑΣΤΗΡΙΟ ΜΕΤΑΛΛΙΚΩΝ ΚΑΤΑΣΚΕΥΩΝ

ΔΙΠΛΩΜΑΤΙΚΗ ΕΡΓΑΣΙΑ
ΕΜΚ ΔΕ 2016 46

Ικανοτικός σχεδιασμός και μελέτη συμπεριφοράς πολυώροφων μεταλλικών κτιρίων κατά τον Ευρωκώδικα 8

Ελεονώρα Μπαλαούρα

Επιβλέπων: Χάρης Γαντές, Καθηγητής ΕΜΠ

ΠΕΡΙΛΗΨΗ

Η παρούσα διπλωματική εργασία πραγματεύεται τον ικανοτικό σχεδιασμό κανονικών πολυώροφων μεταλλικών κτιρίων με χιαστί συνδέσμους δυσκαμψίας, ενώ παράλληλα διερευνάται η φέρουσα ικανότητα και συμπεριφορά της με χρήση μη γραμμικών αναλύσεων. Συγκεκριμένα, μελετάται αναλυτικά η επιρροή της διάταξης 6.7.2(2) του Ευρωκώδικα 8 στη φέρουσα ικανότητα της κατασκευής υπό σεισμικά φορτία, η οποία διευκρινίζει πως η συνεισφορά του θλιβόμενου συνδέσμου δυσκαμψίας πρέπει να αγνοείται στην ανάλυση και, κατά συνέπεια, στη διαστασιολόγηση της κατασκευής.

Στο πρώτο κεφάλαιο παρουσιάζονται οι θεμελιώδεις αρχές που διέπουν τον ικανοτικό σχεδιασμό μεταλλικών κτιρίων κατά τον Ευρωκώδικα 8, με ιδιαίτερη έμφαση στην εμβάθυνση της σημασίας εφαρμογής τους. Ορίζονται οι απαιτούμενες παράμετροι του αντισεισμικού σχεδιασμού, οι οποίες καθορίζουν τόσο τη μέθοδο ανάλυσης, όσο και τα σεισμικά φορτία σχεδιασμού που επιβάλλονται στην κατασκευή. Ακολούθως, παρουσιάζονται συγκεντρωτικά οι απαιτούμενες κανονιστικές διατάξεις και έλεγχοι για όλα τα κύρια μέλη ενός μεταλλικού κτιρίου υπό σεισμικά και μη φορτία, τόσο για συστήματα πλαισίων ροπής, όσο και για συστήματα χιαστί συνδέσμων δυσκαμψίας.

Στο δεύτερο κεφάλαιο διατυπώνονται 4 δυνατά σενάρια διαστασιολόγησης ενός τριώροφου μεταλλικού κτιρίου με χρήση γραμμικών αναλύσεων για την ορθότερη διερεύνηση της υπό έρευνα διάταξης. Προκειμένου τα συμπεράσματα που θα εξάγονταν από τις μη γραμμικές αναλύσεις που θα εκτελεστούν στη συνέχεα να είναι όσο το δυνατόν ρεαλιστικά, η κατασκευή επαναδιαστασιολογείται σε κάθε περίπτωση ώστε να υπακούει σε όλες τις κανονιστικές διατάξεις των Ευρωκωδίκων 3 και 8. Για το λόγο αυτό, αναπτύχθηκε μία μεθοδολογία βέλτιστου σχεδιασμού κανονικών μεταλλικών κτιρίων, που αποσκοπεί τόσο στην οικονομία υλικού, όσο και στην ελαχιστοποίηση του πλήθους των απαιτούμενων αναλύσεων.

Στο τρίτο κεφάλαιο μελετάται η συμπεριφορά του τριώροφου κτιρίου με χρήση μη γραμμικών αναλύσεων γεωμετρίας και υλικού για σεισμική διέγερση στη διεύθυνση των συνδέσμων δυσκαμψίας για κάθε σενάριο διαστασιολόγησης. Στόχος είναι η εκτίμηση του 'πραγματικού' οριακού φορτίου της

κατασκευής, όταν λαμβάνεται υπόψη ο θλιβόμενος σύνδεσμος και, κατ' επέκταση, η μεταλυγισμική του συμπεριφορά. Εξετάζεται, ύστερα, η τήρηση και μη του κριτηρίου λυγηρότητας στη φέρουσα ικανότητα της κατασκευής, καθώς αποτελεί εξαιρετικά καθοριστικό κριτήριο του Ευρωκώδικα 8 στη διαστασιολόγηση των συνδέσμων δυσκαμψίας.

Στη συνέχεια του ίδιου κεφαλαίου εισάγεται ένα πέμπτο σενάριο διαστασιολόγησης, στο οποίο η υπό μελέτη κατασκευή διαστασιολογείται αποκλειστικά ως προς τα αναπτυσσόμενα εντατικά μεγέθη των συνδυασμών σχεδιασμού, ενώ αγνοούνται πλήρως οι απαιτήσεις του ικανοτικού σχεδιασμού. Σκοπός αυτής της μελέτης είναι να αναδειχθεί η αξία του ικανοτικού σχεδιασμού στην περίπτωση όπου οι χαρακτηριστικές τιμές, είτε της σεισμικής έντασης ή των αντοχών, δεν είναι οι αναμενόμενες κατά το σχεδιασμό. Με αφορμή τη δεύτερη περίπτωση, διεξάγεται παραμετρική διερεύνηση ως προς το υλικό των συνδέσμων δυσκαμψίας αλλά και των άμεσα συνδεδεμένων στύλων. Τέλος, η κατασκευή αποτιμάται σε όρους οριακού φορτίου για κάθε σενάριο ως προς την απαιτούμενη σεισμική τέμνουσα , ενώ το αποτελεσματικότερο σενάριο διαστασιολόγησης προτείνεται ως μία πιο ρεαλιστική προσέγγιση της συμμετοχής του θλιβόμενου συνδέσμου στη φέρουσα ικανότητα της κατασκευής.

Τέλος, στο τέταρτο και τελευταίο κεφάλαιο παρουσιάζονται τα γενικά συμπεράσματα της διπλωματικής εργασίας και διατυπώνονται ορισμένες προτάσεις για την περαιτέρω διερεύνηση της συμπεριφοράς πολυώροφων μεταλλικών κτιρίων με συνδέσμους δυσκαμψίας υπό σεισμικά φορτία.

NATIONAL TECHNICAL UNIVERSITY OF ATHENS
SCHOOL OF CIVIL ENGINEERING
INSTITUTE OF STEEL STRUCTURES

DIPLOMA THESIS
ΕΜΚ ΔΕ 2016 46

Capacity design and investigation of the behavior of multi-storey steel buildings according to Eurocode 8

Eleonora Balaoura

Supervisor: Charis Gantes, Professor NTUA

ABSTRACT

The present diploma thesis deals with the capacity design of regular multi-storey steel buildings with concentric bracing systems in conjunction with the investigation of the behavior and load-bearing capacity of a regular three-storey structure using non-linear analyses. In particular, an extensive research is carried out regarding the influence of guideline 6.7.2(2) of Eurocode 8, which stipulates that the contribution of the compressed bracing should be ignored during the analysis and, as a result, the design of the structure.

In the first chapter, the fundamental principles concerning the capacity design of steel buildings according to Eurocode 8 are presented, with emphasis on a deeper understanding of their application. The required seismic design components are introduced, which are necessary in order to define the analysis method as well as the seismic design loads imposed in the structure. Moreover, the regulatories and checks for all structural members of a steel building under seismic and non-seismic loads are summarized, especially for moment resisting and concentrically braced framing systems.

In the second chapter, 4 possible design scenarios of a regular three-storey steel building are presented using non-linear analyses for the more accurate investigation of the aforementioned guideline. In order to reach rather realistic conclusions regarding the 'actual' behavior of the structure, it is re-designed for each scenario from the beginning so as to fully comply with all regulatories of Eurocodes 3 and 8. For this reason, a design methodology for regular steel buildings was developed that aims to achieve material economy as well as the minimum required number of linear analyses.

In the third chapter, the behavior of the three-storey steel building is extensively investigated using non-linear analyses of material and geometry for seismic loading in the direction of the bracing systems and for all design scenarios. The main purpose of this chapter is the estimation of the structure's ultimate load when the compressed bracing and its post-buckling behavior are taken into account. Subsequently, the non-compliance of the slenderness limitation in the load-bearing capacity of the structure is investigated, as it is a rather definitive criterion for the design of the bracings.

In the same chapter, a fifth design scenario is introduced, where the structure under investigation is designed based entirely on the resistance checks, while the requirements of the seismic code are completely ignored. This approach aims to highlight the necessity of capacity design in the case where the nominal values of either the seismic actions or the resistance of the members are, in fact, different compared to the design. Therefore, a parametric study for the material of the bracings, as well as the columns directly connected to them, is carried out. The load-bearing capacity of the structure in correspondence to the developed seismic shear is assessed for each design scenario and the most effective scenario is suggested as a more realistic approach of the contribution of the compressed bracing in the total behavior of the structure.

Finally, in the fourth and final chapter the general conclusions of this diploma thesis are summarized and proposals for the further investigation of the behavior of steel buildings with bracing systems under seismic loads are suggested.

Contents

1 CHAPTER 1: THE BASIC PRINCIPLES OF CAPACITY DESIGN FOR STEEL BUILDINGS ACCORDING TO EC8

1.1 INTRODUCTION

Eurocodes are technical rules, unified at a European level, that constitute a set of unanimously accepted and applicable standards. They provide the basis for the analysis and design of structures in terms of strength and stability against live and extreme loads, such as earthquakes. The most recent technical developments regarding structural design are included, as they aim to bridge the gap between the tradition of the practitioner engineers and the theoretical innovation of the researchers.

Eurocode 8, denoted in general as EN 1998, applies to the design and construction of buildings and civil engineering works in seismic regions and covers all common structures with provisions of general validity. Part 1 of EN 1998, in particular, comprises of a two-level seismic design, establishing explicitly the following requirements that balance both concepts of safety and economy at the same time:

- No-collapse requirement

The structure should be designed in order to resist the seismic design actions, without any danger of local or global collapse occurring. It should also be able to maintain its load bearing capacity after the seismic event, in order to allow safe evacuation as well as sufficient lateral resistance in case of possible aftershocks (JRC European Commission 2012). In particular, any type of failure that poses a risk of collapse, such as the formation of soft-storey mechanism and shear types of failure, should be avoided. The no-collapse requirement is associated with the Ultimate Limit State (ULS), since it deals with the safety of people and the entire structure. For ordinary structures, this requirement should be applied to a reference seismic action with a 10% probability of exceedance in 50 years or a return period of 475 years.

- Damage limitation requirement

The structure should be designed and constructed with the ability to resist a seismic action with a larger probability of occurrence than the design seismic action. This requirement stipulates that no damage should occur for seismic actions that are more frequent than the design action. After the design seismic event, however, the structure may present substantial damages in its structural elements, including permanent drifts, to the point that it may be economically unrecoverable. Some damage to non-structural elements is acceptable but they should not impose significant limitations of use and should be repairable economically. The damage limitation requirement is associated with the Serviceability Limit State (SLS), since it deals with the use of the building, the comfort of the occupants and economic losses. For ordinary structures this requirement should be applied to a reference seismic action with a 10% probability of exceedance in 10 years or a return period of 95 years. For earthquakes smaller than the design seismic event, an ordinary structure performs in the elastic region due to the compliance to the damage limitation requirement that refers to the design earthquake. (I. Psycharis 2016)

1.2 DEFINITION OF SEISMIC DESIGN COMPONENTS

1.2.1.1 Ductility class

Ductility is defined as the ability of the structure to sustain large deformations beyond the yielding point without collapse and is expressed in terms of demand and availability. The ductility demand is the maximum level of ductility that the structure can reach during a seismic situation and depends on the characteristics of both the earthquake and the structure. Available ductility, on the other hand, is a characteristic of the structure and is defined as the maximum ductility that the structure is capable to develop by undergoing severe damages that lead to collapse. Therefore, the seismic code aims to ensure the existence of a stable and trustworthy model of absorbing energy in predefined critical areas that restrict no inertial loading that appears in other parts of the structure. (A. Elghazouli 2009).

The seismic energy dissipation capacity of a structure depends on the level of exploitation of its non-linear response. This capacity can be described by the values of behavior factor q and the associated ductility classification (low, medium or high) provided by Part 6.1.2 of EN 1998-1:2004.

Table 1-1: Design concepts, structural ductility classes and upper limit reference values of the behavior factor

Design concept	**Structural ductility class**	**Range of the reference values of the behavior factor q**
Low dissipative structural behavior	DCL (Low)	$\leq 1.5 - 2.0$
Dissipative structural behavior	DCM (Medium)	≤ 4.0 also limited by the values of Table 1-2
	DCH (High)	only limited by the values of Table 1-2

In the case of structures that are classified as low-dissipative (Ductility Class Low or DCL), no account of hysteretic energy dissipation is considered and, as a result, the behavior factor is not greater than 1.5-2.0 in order to take into account the overstrengths (EN 1998-1: 2004). However, for dissipative

structures (Ductility Class Medium or DCM and Ductility Class High or DCH), the behavior factor is taken as being greater than these limiting values accounting for the hysteretic energy dissipation that mainly occurs in specifically designed zones, called dissipative zones or critical regions (EN 1998-1: 2004).

1.2.2 **Behavior factor**

The seismic design situation lasts only a few seconds during a structure's lifespan and would be, therefore, uneconomic to design the structure based on the assumption that no damages occur (elastic behavior) and not take advantage of its ability to retain its strength and rigidity in the plastic region through large deformations. The structure is allowed to present a certain level of damage during the design earthquake, which should be limited and recoverable. The ability of a structure to develop large deformations in the plastic range without collapse defines the degree of its dissipative behavior for seismic loads. In regions of low seismicity or structures of special use or importance, the design aims for an elastic response in the design earthquake situation. On the other hand, in areas of high seismicity, such as Greece, the seismic codes aim to achieve economical design by employing dissipative behavior in which considerable inelastic deformations can be accommodated under significant seismic events.

This is also supplemented by the capacity design concept which predetermines an acceptable failure mechanism in case of extreme seismic loads that exceed the design situation. It is achieved by ensuring sufficient ductility in plastic zones as well as adequate overstrength to the non-dissipative elements in order to steer seismic energy towards the dissipative members, in case the structure undergoes plastic deformations. Consequently, Eurocode 8 suggests that structures should be designed in the elastic range for a reduced design seismic load, while the rest of the seismic action should be resisted through large but allowable deformations in the plastic range. This reductive factor is called behavior factor and quantifies the ability of the structure to dissipate energy with the following definition:

$$q = F_e / F_d \tag{1-1}$$

where

F_e is the maximum developed force during the design earthquake supposing that the structure had sufficient strength as to respond entirely in the elastic range

The higher the behavior factor, the higher the expected energy dissipation, as well as the ductility demand on critical zones. Using Newton's second law of motion, the equivalent elastic seismic force can be acquired as $F_e = ma_e$, where a_e is the maximum elastic acceleration from the elastic design spectrum according to the respective frequency of vibration T of the structure. This means that for this specific frequency, the structure behaves as a single degree of freedom oscillator, thus ignoring the contribution of all other modes of vibration.

After selecting one of the suggested values of q considering that the given values are upper limits, the next step is to estimate the design seismic load which can be defined according to equation (1-1) as:

$$F_d = \frac{F_e}{q} = m\left(\frac{S_e(T,\xi)}{q}\right) \tag{1-2}$$

An elastic analysis is then carried out for the horizontal load distribution F_d and the structure is designed based on the results of this analysis. However, due to the overstrength of materials and the capacity

design of plastic zones, the load bearing capacity of the structure is ultimately increased. The ability of the structure to resist higher seismic loads compared to the design situation is referred to as overstrength.

Therefore, in correspondence with the design behavior factor, the yielding behavior factor is defined as:

$$q_y = F_e / F_y \quad (1\text{-}3)$$

where

F_y is the actual horizontal load for which the structure yields due to overstrength

It should also be mentioned that the yielding behavior factor is a quantity that can only be measured after a typical pushover analysis for a specific mode and its respective frequency of vibration is carried out. In particular, the extracted pushover curve is displaced by a bilinear curve with the assumption that all plastic hinges are concentrated on a single yielding point with coordinates (F_y, d_y), as illustrated in the following figure.

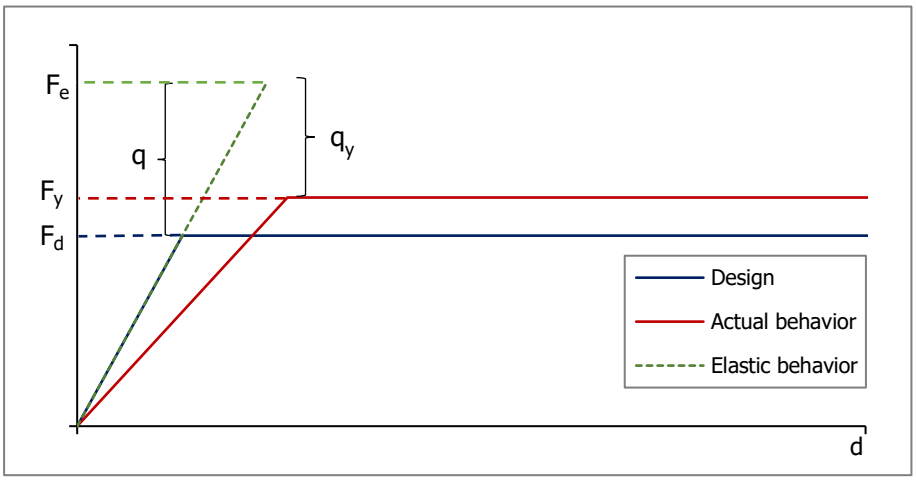

Figure 1-1: Structure's typical response according to design and actual inelastic behavior

On the other hand, the design behavior factor used to calculate the design seismic loads is provided by Eurocode 8 and does not depend on the value of the yielding behavior factor. The suggested values are a result of numerous observations through extensive experimental and analytical investigations. Behavior factor q implicitly aims to satisfy the damage limitation requirement by defining the maximum allowed value of ductility according to material and structural configuration. The following table represents the maximum suggested values of the design behavior factor for a few types of frames.

Table 1-2: Upper limit of reference values of behavior factors for systems regular in elevation

Structural type	**Ductility class**	
	DCM	**DCH**
(a) Moment resisting frames	4	$5\,a_u/a_1$
(b) Frame with concentric bracings		
Diagonal bracings	4	4

1.2.3 **Criteria for regularity**

1.2.3.1 Regularity in plan

For the purpose of seismic design, buildings are categorised into being regular or irregular. Regularity of the structure influences the required structural model (planar or spatial), the required method of analysis, which can be either a simplified response spectrum analysis (equivalent lateral force) or a modal one, and the value of the behavior factor q, which shall be decreased for buildings non-regular in elevation (EN 1998-1: 2004, §4.2.3.1).

For a building to be categorized as being regular in plan, it should satisfy all the conditions listed in EN 1998-1: 2004, §4.2.3.2:

- With respect to the lateral stiffness and mass distribution, the building structure shall be approximately symmetrical in plan with respect to two orthogonal axes.
- The plan configuration shall be compact, which means that each floor shall be delimited by a polygonal convex line.
- Regarding the global behavior of the building, the in-plan stiffness of the floors shall be sufficiently large in comparison to the lateral stiffness of the vertical structural elements, so that the deformation of the floor shall have a small effect on the distribution of the forces among the vertical structural elements. They act as a horizontal tie, preventing excessive relative deformations between the vertical elements and, thus, help distribute seismic loads. This criteria is met in case the floor is a concrete slab which can be accurately assumed to be a rigid diaphragm with almost infinite axial rigidity. However, if they have very elongated plan shapes or large openings, they are likely to be inefficient in distributing seismic loads to the vertical elements.
- The slenderness $\lambda = L_{max}/L_{min}$ of the building in plan shall not be higher than 4, where L_{max} and L_{min} are respectively the larger and smaller dimension of the building, measured in orthogonal directions.
- At each level and for each direction, the structural eccentricity shall be smaller than 30% of the torsional radius, meaning that (a) $e_{ox} \leq 0.30 r_X$ & $e_{oy} \leq 0.30 r_Y$ and (b) $r_X \geq l_s$ & $r_Y \geq l_s$. In the case of a symmetrical building, however, where the center of mass coincides with the center of rigidity for all storeys, there is no structural eccentricity in any direction and, therefore, requirement (a) is immediately fulfilled. Regarding requirement (b), in the case of a rectangular floor area with dimensions l_x and l_y with uniformly distributed mass over the floor, l_s is defined as:

$$l_s = \sqrt{\frac{(l_x^2 + l_y^2)}{12}} \tag{1-4}$$

$$r_{X,i} = \sqrt{\frac{K_{M,i}}{K_{FY,i}}} \text{ and } r_{Y,i} = \sqrt{\frac{K_{M,i}}{K_{FX,i}}} \tag{1-5}$$

$$K_{M,i} = \frac{1}{R_{Z,i}(M_{t,i}=1)},\ K_{FX,i} = \frac{1}{u_{X,i}(F_{tX,i}=1)} \text{ and } K_{FY,i} = \frac{1}{u_{Y,i}(F_{tY,i}=1)} \tag{1-6}$$

where

$R_{Z,i}(M_{t,i}=1)$ is the rotation of storey i about the vertical axis due to the unit moment

$u_{X,i}(F_{tX,i}=1)$ is the displacement at storey level i in direction X due to unit force F_{tX}

$u_{Y,i}(F_{tY,i}=1)$ is the displacement in direction Y due to unit force F_{tY}

1.2.3.2 Regularity in elevation

For a building to be categorized as being regular in plan, it should satisfy all the conditions listed in EN 1998-1: 2004, §4.2.3.3:

- The lateral stiffness and the mass of the individual storeys should remain constant or reduce gradually, without abrupt changes, from the base to the top of the building.
- When setbacks are present, they should satisfy criteria (a), (b) and (c) of the same paragraph.

With regard to the category that the building under investigation falls into, the seismic analysis and design are stipulated by EN 1998-1: 2004, §4.2.3.1(3), Table 4.1.

1.2.4 **Cross-section classification**

According to §6.3.1(1) of EN1998-1, all steel buildings should be assigned to one of the following structural types according to the behavior of their primary resisting configuration under seismic actions.

- Moment resisting frames

  where the resistance to lateral forces is primarily provided by the development of bending moments and shear forces in the framing members and joints.

- Frames with concentric bracings

  where horizontal loads are mainly resisted through axial forces developed in the bracings.

- Frames with eccentric bracings

  where horizontal forces are mainly resisted by axially loaded members, but the eccentricity of the layout is such that energy can be dissipated in seismic links by means of either cyclic bending or cyclic shear (EN 1998-1: 2004).

The application of the behavior factor with a value greater than 1.5-2.0 should be coupled with sufficient local ductility demand in the predefined dissipative zones. The cross-sectional class requirement aims to ensure that members in compression or bending have an acceptably small b/t ratio that ensures sufficient local ductility of the dissipative members. The occurrence of local buckling results in lower element ductility, thus leading to a reduction in the energy dissipation capacity and a lower factor q. The cross-section requirements apply to all types of frame considered in Eurocode 8 and implicitly accounts for the relationship between local buckling and rotational ductility of steel members that has been extensively investigated in the past (A. Elghazouli 2009).

Table 1-3: Requirements on cross-sectional class for dissipative elements (EN 1998-1: 2004 Table 6.3)

Ductility class	**Reference value of behavior factor q**	**Required cross-sectional class**
DCM	1.5≤q≤2.0	Class 1, 2 or 3
	2.0≤q≤4.0	Class 1 or 2
DCH	q>4.0	Class 1

The area below the diagram in each case represents the level of ductile behavior of the cross-section. Cross-sections classified as Class 3 and 4 do not perform ductile behavior, due to their vulnerability to local buckling that takes effect after the section reaches its yielding moment.

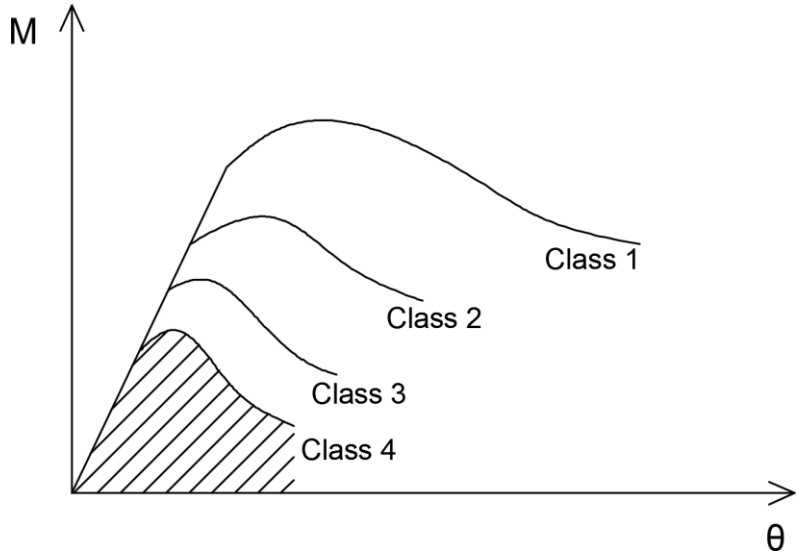

Figure 1-2: Typical moment resistance to rotational capacity diagram according to the cross-section classification

1.2.5 **Seismic loads**

The inertial loads, ultimately imposed in the building, are directly related to the motion of the ground upon which the structure is built. The seismic design is based on representing the earthquake actions in the form of an equivalent static force applied to the center of mass of the structure. According to EN 1998-1: 2004, §3.2.2.1 the earthquake motion can be represented by the elastic response spectrum, which is subsequently reduced by factors that account for the capacity of the structure to dissipate the seismic energy through inelastic deformations. For non-critical structures, it is generally considered sufficient to estimate the seismic actions through this elastic response spectrum.

1.2.5.1 Horizontal component of seismic force

The seismic loads are evaluated based on the design response spectrum in conjunction with the respective period of vibration of the structure. The period of vibration is a combination of the existing rigidity of the members, activated in the direction of the seismic motion, and the total mass acquired from all imposed loads in the seismic design situation (G+0.3Q) as:

$$T=2\pi\sqrt{\frac{m}{k}} \tag{1-7}$$

The horizontal seismic action is described by two orthogonal components assumed as being independent and represented by the same response spectrum. In addition, the elastic response spectrum recommended by Eurocode 8 takes into account the effect of the soil through parameter S for different ground types (A , B, C, D or E – rock to soft soil). The different soil classes reflect the amplifying effect of softer layers as well as the effect on the frequency content, which leads to a wider constant acceleration plateau and higher ordinates at intermediate and long response periods (Kumar, Stafford, Elghazouli 2013). The design response spectrum provides the engineer with the advantage to bypass the very considerable effort, expense and time required for a full site-specific hazard assessment.

It should be mentioned that the elastic spectrum provided by Eurocode 8 is suggested for a 5% damping. In any other case, the correction factor η should be introduced in the spectral acceleration with regard to the viscous damping ratio ξ of the structure, determined by the following expression:

$$\eta=\sqrt{10/(5+\xi)} \geq 0.55 \quad (1\text{-}8)$$

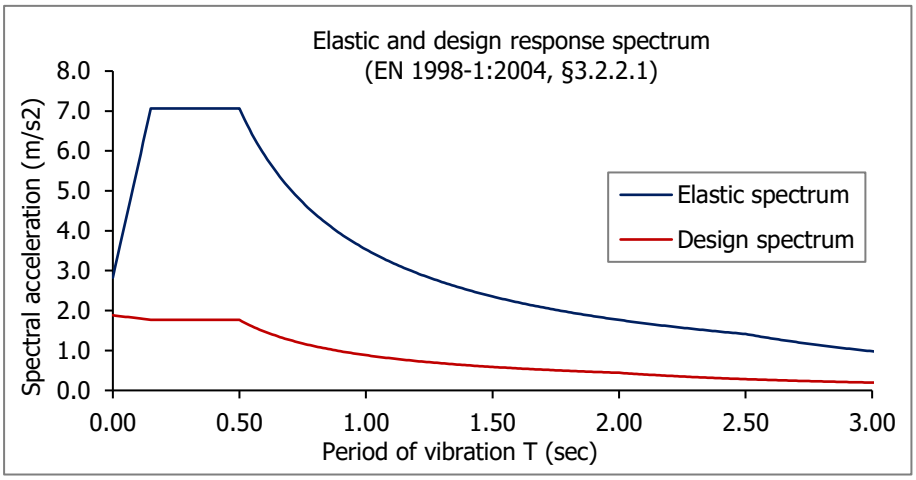

Figure 1-3: Example of elastic and design response spectrum (Type 1) for importance class II and soil type B

1.2.5.2 Vertical component of seismic force

The seismic force is a vector that comprises of 3 components in a spatial model, one for its projection in each level of direction. Therefore, apart from the two horizontal components, a vertical component is also developed, that should be determined whether or not it contributes with significantly in the seismic response of the building. According to EN 1998-1: 2004, §4.3.3.5.2, the vertical component of the seismic action should be taken into account if a_{vg} is greater than 0.25g in the following cases:

- for horizontal or nearly horizontal structural members spanning 20 m or more as well as cantilever components longer than 5 m
- for horizontal or nearly horizontal pre-stressed components
- for beams supporting columns

The vertical ground spectral acceleration a_{vg} is defined in EN 1998-1: 2004, §3.2.2.3, Table 3.4 for Type 1 spectrum as $a_{vg}=0.9 \cdot a_g$.

1.2.5.3 Accidental eccentricity

In order to account for uncertainties in the location of masses and in the spatial variation of the seismic motion, the calculated center of mass at each floor i should be considered as being displaced from its nominal location in each direction by an accidental eccentricity equal to 5% of the floor dimensions L_{xi} and L_{yi} (EN 1998-1: 2004, §4.3.2(1)) as:

$$e_{ai}=\pm 0.05 \cdot L_i \tag{1-9}$$

where

e_{ai} is the accidental eccentricity of storey mass i from its nominal location, applied in the same direction at all floors

L_i is the floor-dimension perpendicular to the direction of the seismic action

When a modal analysis is carried out, two separate analyses should be carried out for each seismic direction, one for $e_{ai}=+0.05 \cdot L_i$ and a second for $e_{ai}=-0.05 \cdot L_i$. Alternatively, instead of assuming the displacement of the center of mass, torsional moments about the vertical axis of each storey i can be introduced (EN 1998-1: 2004, §4.3.3.3.3):

$$M_{ai}=e_{ai} \cdot F_i \tag{1-10}$$

where

F_i is the horizontal force acting on storey i is derived from the lateral force method of analysis

However, when a lateral force method of analysis is carried out, where it is assumed that the deformation of the structure occurs in the level of the seismic force, the displacement of the centre of mass perpendicular to the direction of the of the earthquake, does not have any significant effect in the final results (I. Psycharis 2016). In this case, the effect of accidental eccentricity can be taken into account using quantity δ, which is multiplied with the developed internal forces and displacements (EN 1998-1: 2004, §4.3.3.2.4):

$$\delta=1+0.6\frac{x}{L_e} \tag{1-11}$$

where

x is the distance of the element under consideration from the centre of the mass of the building in plan, measured perpendicularly to the direction of the imposed seismic action

L_e is the distance between the two outermost lateral load resisting elements, measured perpendicularly to the direction of the seismic action

The effects of accidental eccentricity is taken into account with the same direction in each floor in order to maximise its torsional effects (I. Psycharis 2016).

1.2.6 **Methods of analysis**

When designing structures by taking into account their non-linear seismic response, a variety of analysis options is available. The simplest and most widely used approach is to use either the modal or the lateral force method of analysis (EN 1998-1: 2004, §4.3.3.1(3)), depending on the structural characteristics of the building. The method of analysis is selected based on the dynamic characteristics of the structure which are estimated from a modal analysis.

1.2.6.1 Lateral force method of analysis

The response of multi-storey buildings, symmetric in plan, is dominated by the fundamental mode of vibration and their response is not significantly affected by contributions from higher modes. In this case, a simplified method of analysis, namely lateral force method of analysis, can be applied that does not require to determine usually more than two fundamental modes of vibration, one for each principal direction of the building. This method should only be applied for buildings meeting both of the following conditions imposed by EN 1998-1: 2004, §4.3.3.2(2):

- they have fundamental periods of vibration T_1 in the two main directions that are smaller than the following values

$$T_1 \leq \begin{cases} 4T_c \\ 2.0 \text{ sec} \end{cases} \quad (1\text{-}12)$$

- they meet the criteria for regularity in elevation.

1.2.6.2 Base shear

The total seismic load should be estimated in the direction of the earthquake, which is imposed in the form of a shear force in the base of the building, according to the d' Alembert system of inertia. The design seismic shear is determined from the following equation:

$$F_b = \lambda \cdot m \cdot S_d(T_1, \xi) \quad (1\text{-}13)$$

where

λ is the correction factor equal to 0.85 if $T_1 \leq 2T_c$ and the building has more than two storeys; otherwise $\lambda = 1.00$

m is the total mass of the building in the seismic design situation (G+0.3Q)

T_1 is the fundamental period of vibration of the building for lateral motion in the considered direction

$S_d(T_1, \xi)$ is the ordinate of the design spectrum for period T_1

The correction factor λ accounts for the fact that in buildings with at least three storeys and translational degrees of freedom in each horizontal direction, the effective modal mass of the fundamental mode is smaller on average by 15% of the total mass of the building. The fundamental period of vibration can be estimated from a modal analysis, from the Rayleigh method or even using approximate expressions provided by EN 1998-1: 2004, §4.3.3.2.2(3).

1.2.6.3 Modal response spectrum analysis

This type of analysis should be applied to buildings that do not satisfy the conditions for applying the lateral force method of analysis (EN 1998-1: 2004, §4.3.3.3.1(2)). This means that for buildings irregular in elevation, the modal response spectrum analysis is the only option. The contribution of all modes of vibration that contribute significantly to the global response of the structure should be taken into account, according to the following conditions (EN 1998-1: 2004, §4.3.3.3.1(3)):

- the sum of the effective modal masses for the modes taken into account amounts to at least 90% of the total mass of the structure

$$\sum_{i=1}^{k} m_i^* \geq 0.90 \cdot m_{tot} \tag{1-14}$$

where

m_i^* is the effective modal mass of the i mode shape

m_{tot} is the total mass of the structure in the seismic design situation (G+0.3Q)

- all modes with effective modal masses greater than 5% of the total mass are taken into account

$$m_i^* > 0.05 \cdot m_{tot} \tag{1-15}$$

The horizontal loads in the seismic design situation are calculated for each mode shape i that activates the j degree of freedom as:

$$F_{d,ji} = \Gamma_i \cdot S_d(T_i, \xi_i) \cdot m_j \cdot \varphi_{ji} \tag{1-16}$$

After the estimation of the design seismic loads' matrix, the developed internal forces and displacements are calculated for each mode shape. The assumption that these forces are applied in the center of mass of each diaphragm is made and, according to a static analysis, their displacements are calculated using the following equation:

$$u_{d,i} = K^{-1} F_{d,i} \tag{1-17}$$

Afterwards, the displacements at the beginning and end of each member are calculated based on the displacement of the center of mass, as well as the internal forces using the rigidity of each member. It is important to mention that the actual displacements of the structure in the seismic design situation should be multiplied by the behavior factor q as:

$$u_{d,i} = q \cdot u_{d,i} \tag{1-18}$$

The final internal forces and displacements are calculated using either the SRSS or the CQC method to superposition the contribution of each mode shape.

1.2.6.4 Distribution of seismic loads

For the distribution of the base shear in the center of mass at each storey i, the fundamental mode of vibration should be calculated in the respective direction. Due to the fact that seismic loads are only

estimated in the direction under investigation, only the degrees of freedom developed in this direction are considered, whereas all others are ignored. The imposed seismic loads in each storey can be estimated as:

$$F_j = F_b \frac{m_j \cdot \varphi_j}{\sum_i m_i \cdot \varphi_i} \tag{1-19}$$

When the fundamental mode shape is approximated by horizontal displacements increasing linearly along the height, they can be approached by an inverted triangle where $\varphi_j = z_j/H$:

$$F_j = F_b \frac{m_j \cdot z_j}{\sum_i m_i \cdot z_i} \tag{1-20}$$

In regular structures, where inelasticity can be expected to be uniformly distributed, the design forces are reduced on the basis of a single, global behavior factor q that Eurocode 8 suggests for common structural forms. However, in irregular buildings, the q-factor approach can become inaccurate and a more realistic description of the distribution of inelasticity throughout the structure may be required. In these cases, a full non-linear analysis should be performed. Rather than using a single behavior factor, a representation of the non-linear load-deformation characteristics of each member within the structure is necessary.

1.3 CAPACITY DESIGN OF FRAMES

1.3.1 Moment resisting frames

In moment resisting frames (MRFs), the dissipative zones should be mainly located in plastic hinges in the beams or the beam-column joints, so that energy is dissipated by means of cyclic bending (EN 1998-1: 2004). Plastic hinges should predominantly occur in the beams or in the connections of the beams to the columns, but in no case in the columns (weak beam/strong column design). For frames that belong to multi-storey buildings, this requirement is waived in the base of the columns and at the top of the upper storey. The weak beam/strong column design provides favourable performance in the avoidance of premature and undesirable storey collapse mechanisms. Another benefit is that relatively strong columns are obtained, such that beam rather than column yielding dominates over several storeys, hence achieving adequate overall performance (A. Elghazouli 2009).

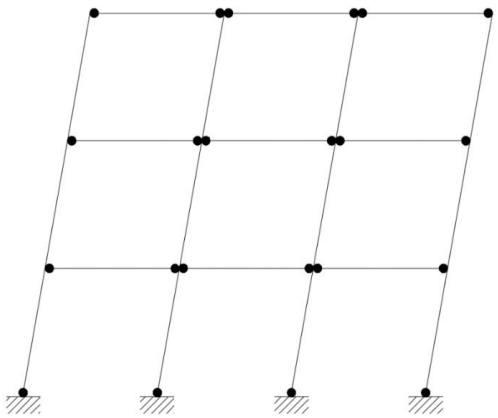

Figure 1-4: Acceptable mode of failure and desired uniform distribution of plastic hinges in a typical MRF system

1.3.1.1 Columns

To obtain ductile plastic hinges in the beams, coexisting compression and shear forces should be checked so as the full plastic moment resistance and rotation of the hinge are not reduced (A. Elghazouli 2009). For this reason, it is mandatory that the cross-section in the base of the columns is classified as Class 1 or 2, in order to be able to develop its full plastic resistance. These criteria should be met for each critical section according to the most unfavourable combination of bending moments M_{Ed}, shear forces V_{Ed} and axial forces N_{Ed}, according to the requirements summarized in the following table.

Table 1-4: Summary table of capacity design requirements and checks according to EN1998-1 for MRF columns

Capacity design requirements	**Checks**	**Eurocode 8 reference**
Cross-section classification	Class 1 or 2	EN 1998-1, §6.3.1(5), Figure 6.1 EN 1998-1, §6.5.3(2), Table 6.3
$M_{Ed}=M_{Ed,G}+1.1\gamma_{ov}\Omega M_{Ed,E}$	Section and member checks in bending and compression according to EC3	EN 1993-1-1, §6.3.3(4), Equation 6.61
$N_{Ed}=N_{Ed,G}+1.1\gamma_{ov}\Omega N_{Ed,E}$		EN 1993-1-1, §6.3.3(4), Equation 6.62
$V_{Ed}=V_{Ed,G}+1.1\gamma_{ov}\Omega V_{Ed,E}$		EN 1993-1-1, §6.2.6(1), Equation 6.17

where

$\Omega=\min(M_{pl,Rd,i}/M_{Ed,i})$ is the minimum overstrength in the respective critical section i

$M_{Ed,G}$ and $M_{Ed,E}$ are the bending moments in the seismic design situation due to the gravity loads and lateral earthquake forces respectively

1.3.1.2 Beams

According to the weak beam/strong column requirement, hinges formed in the beams that constitute as energy dissipation zones, should be able to develop their full plastic moment resistance. This criterion should be satisfied not only for material economy, but also in order to provide sufficient ductility and, therefore, stability during the structure's response in the non-linear range, where a significant number of plastic hinges is formed.

Table 1-5: Summary table of capacity design requirements and checks according to EN1998-1 for MRF beams

Capacity design requirements	**Checks**	**Eurocode 8 reference**
Cross-section classification	Class 1 or 2	EN 1998-1, §6.3.1(5), Figure 6.1 EN 1998-1, §6.5.3(2), Table 6.3
$M_{Ed}=M_{Ed,G}+M_{Ed,E}$	$M_{Ed}/M_{pl,Rd}\leq 1$	EN 1998-1, §6.6.2(2)
$N_{Ed}=N_{Ed,G}+N_{Ed,E}$	$N_{Ed}/N_{pl,Rd}\leq 0.15$	EN 1998-1, §6.6.2(2)
$V_{Ed}=V_{Ed,G}+V_{Ed,M}$ where $V_{Ed,M}=(M_{pl,Rd,A}+M_{pl,Rd,B})/L$	$V_{Ed}/V_{pl,Rd}\leq 0.5$	EN 1998-1, §6.6.2(2)
Local ductility condition	$\sum MR_c \geq 1.3\sum MR_b$	EN 1998-1, §4.4.2.3(4)

1.3.2 **Concentrically braced frames**

Due to their geometry, concentrically braced frames (CBFs) provide truss action with members largely subjected to axial forces in the elastic range. Although CBFs present relatively higher stiffness than moment resisting frames, they can suffer from reduced ductility once the compression bracings buckle (A. Elghazouli 2009). For this reason the dissipative zones should be mainly located in the tensile diagonals. This ultimately leads to the application of capacity design procedures for the non-dissipative elements, which ensures that seismic energy is primarily dissipated by the tensile bracings and not the beams or columns directly connected to them.

1.3.2.1 Columns

The columns directly connected to the bracings should be capacity designed using the following equation, where the design resistance of the beam or column under consideration $N_{b,Rd}$ with due account of the interaction with the bending moment (M_{Ed}) is determined as:

$$N_{b,Rd}(M_{Ed}) \geq N_{Ed,G} + 1.1\gamma_{ov}\Omega N_{Ed,E} \tag{1-21}$$

where

$N_{Ed,G}$ and $N_{Ed,E}$ are the axial loads due to gravity and lateral actions respectively in the seismic design situation

$\Omega = \min(N_{pl,Rd,i}/N_{Ed,i})$ is the minimum value of axial brace overstrength over all the diagonals of the frame

The Ω of each diagonal should not differ from the minimum value more than 25% in order to ensure reasonable distribution of ductility. The alternate approach of equation (1-21) is to acquire the most unfavourable value of axial force as:

$$N_{Ed} = N_{Ed,G} + 1.1\gamma_{ov}\Omega N_{Ed,E} \tag{1-22}$$

in order to concentrate the seismic energy dissipation mechanism in the bracings, in conjunction with the combined section and member check that take into account the interaction of bending moment and axial force according to one of the equations (6.61) and (6.62) of Eurocode 3. In the case where the structure comprises of MRF systems in both directions, the section and member checks in bending and compression according to EN 1993-1-1, §6.3.3(4), Equations (6.61) and (6.62) are the following:

$$\frac{N_{Ed}}{\chi_y N_{Rk}} + k_{yy}\frac{M_{y,Ed}}{\chi_{LT} M_{y,Rk}} + k_{yz}\frac{M_{z,Ed}}{M_{z,Rk}} \leq 1 \tag{1-23}$$

$$\frac{N_{Ed}}{\chi_z N_{Rk}} + k_{zy}\frac{M_{y,Ed}}{\chi_{LT} M_{y,Rk}} + k_{zz}\frac{M_{z,Ed}}{M_{z,Rk}} \leq 1 \tag{1-24}$$

Alternatively, in case the CBF column belongs to two different types of frames in the two main directions, such as a CBF and an MRF at the same time, the columns are not subjected to any bending moment in the CBF direction. For example, in case $M_{z,Ed} \approx 0$ due to a CBF system in the Y direction, the column should be checked by considering the interaction between the axial force and the bending moment $M_{y,Ed}$ due to the MRF function using the following checks, based on equations (1-23) and (1-24).

Table 1-6: Summary table of capacity design requirements for CBF columns

Capacity design requirements	Checks	Eurocode 8 reference
Cross-section classification	No requirement	-
$M_{Ed}=M_{Ed,G}+M_{Ed,E}$	Section and member checks in bending and compression according to EC3	EN 1993-1-1, §6.3.3(4), Equation 6.61
$V_{Ed}=V_{Ed,G}+V_{Ed,E}$		EN 1993-1-1, §6.2.6(1), Equation 6.17
$N_{Ed}=N_{Ed,G}+1.1\gamma_{ov}\Omega N_{Ed,E}$		EN 1993-1-1, §6.3.3(4), Equation 6.62
Local ductility condition	No requirement	-

1.3.2.2 Beams directly connected to the rigid diaphragm

For beams that are part of concentrically braced framing systems, there is the possibility that the beam is directly connected to the rigid diaphragm that usually constitutes a concrete slab. In such a case, the CBF beam is presumed to operate as a secondary beam, where the predominant type of failure is due to bending moment with no requirement for dissipative behavior. Considering that the rigid diaphragm presents a relatively higher axial rigidity compared to the bracings, the developed axial force in the beam is insignificantly small and can be, therefore, neglected. For this reason, the main check that should be performed reflects to the most unfavourable case for the bending moment, which is ULS. Finally, unlike the bracings, no requirement for uniform distribution of ductility in height is recommended by Eurocode 8 for the CBF beams, despite the fact that they should be capacity designed as well.

Table 1-7: Summary table of capacity design requirements and checks for beams directly connected to diaphragm

Capacity design requirements	Checks	Eurocode 8 reference
Cross-section classification	No requirement	-
M_{Ed} (acquired from ULS combination)	$M_{Ed}/M_{pl,Rd} \leq 1$	EN 1993-1-1, §6.3.2.1(1), Equation 6.54
$N_{Ed} \approx 0$	-	-
Uniform distribution of ductility in height	-	-

1.3.2.3 Beams not connected to the rigid diaphragm

An alternative approach regarding the primary type of failure of a CBF beam lies on the fact that the beam is not directly connected to the rigid diaphragm. More specifically, the CBF beam is placed a few centimetres below the level of the slab, while at the same time, a secondary beam is placed right next to the CBF beam, with the responsibility to resist the vertical loads transferred from the slab. In this case, the predominant reason of failure is due to global buckling, as the diaphragm is unable to provide any lateral resistance to the CBF beam. The beam is not subjected to any vertical loads apart from its dead load, thus the possibility for bending or lateral torsional buckling is eliminated. Therefore, the most significant check corresponds to the axial resistance of the CBF beam, which should be capacity designed as well, against the most unfavourable axial force. However, no requirement for uniform distribution of ductility or classification for the cross-section of such beams are suggested, since they are not considered dissipative elements.

Table 1-8: Summary table of capacity design requirements and checks for beams not connected to diaphragm

Capacity design requirements	Checks	Eurocode 8 reference
Cross-section classification	No requirement	-
$M_{Ed,G}$ (from dead load)	Section and member checks in bending and compression according to EC3	In case interaction is considered: EN 1993-1-1, §6.3.2.1(1), Equation 6.61 EN 1993-1-1, §6.3.2.1(1), Equation 6.62
$N_{Ed}=N_{Ed,G}+1.1\gamma_{ov}\Omega N_{Ed,E}\neq 0$ (acquired from the most unfavourable seismic combination)	$N_{Ed}/N_{b,Rd}\leq 1$	EN 1993-1-1, §6.3.1.1(1), Equation 6.46

1.3.2.4 Bracings

The response of CBFs is typically dominated by the behavior of its braced members. Seismic codes rely on the limits imposed on the width-to-thickness ratios of the cross-section in order to delay or prevent local buckling. For this reason, the requirement for the classification of the bracing's cross-section to be either Class 1 or 2 has been established. In addition, seismic codes impose an upper limit on the member's slenderness in order to limit sudden dynamic loading effects, as well as the extent of the post-buckling deformations (A. Elghazouli 2009).

Table 1-9: Summary table of capacity design requirements and checks according to EN1998-1 for bracings

Capacity design requirements	Checks	Eurocode 8 reference
Cross-section classification	Class 1 or 2	EN 1998-1, §6.3.1(5), Figure 6.2 EN 1998-1, §6.5.3(2), Table 6.3
$N_{Ed}=N_{Ed,G}+N_{Ed,E}$ (for all seismic combinations)	$N_{Ed}/N_{pl,Rd}\leq 1$	EN 1998-1, §6.7.3(5)
Non-dimensional slenderness limitation	$1.3\leq\bar{\lambda}\leq 2.0$	EN 1998-1, §6.7.3(1)
Uniform distribution of ductility in height	$(\Omega_{max}-\Omega_{min})/\Omega_{min}\leq 0.25$	EN 1998-1, §6.7.3(8)
Similarity in load deflection characteristics	$\lvert A^{+}-A^{-}\rvert/(A^{+}+A^{-})\leq 0.05$	EN 1998-1, §6.7.1(3)

where

A is the area of the cross-section of the tension diagonal

α is the slope of the diagonal to the horizontal

The last requirement is determined in order to avoid significant asymmetric response effects, which means that the value of Acosα must not vary significantly between two opposite braces in the same storey. In case the compressed and the tension diagonals are identical, this requirement is satisfied.

1.4 DAMAGE LIMITATION CHECKS

1.4.1 General

As has already been indicated in the previous paragraphs, the performance requirement associated with the damage limitation state, requires the structure to support a relatively frequent earthquake without

significant damage or loss of operationality. Damage is only expected in non-structural elements and its occurrence depends on the deformation that the structure, in response to the earthquake, imposes in such elements (JRC European Commission 2012). Deformation-related criteria are particularly important in steel moment frames due to their inherent flexibility that often governs the design. There are two fundamental requirements, namely 'interstorey drifts check' and 'second-order effects' stipulated in Sections (4.4.2.2) and (4.4.3.2) of EN 1998-1 that should be satisfied in the design. The direct application of the following damage limitation checks for moment resisting frames often results in an overall lateral capacity that is significantly increased from that assumed in design (A. Elghazouli 2008). Significant levels of lateral frame overstrength can be present particularly when large q factors are used and when the spectral design acceleration is not significantly increased (A. Elghazouli 2009).

1.4.2 **Interstorey drifts check**

The interstorey drifts check is associated with the serviceability condition (SLS) as it refers to frequent seismic actions and is limited in proportion to the height h of each floor according to EN 1998-1, §4.4.3.2(1) as:

$$d_r \cdot \nu \leq \psi \cdot h \tag{1-25}$$

where

ψ is suggested as 0.005 for buildings having non-structural elements of brittle materials attached to the structure, or 0.0075 for buildings having ductile non-structural elements and 0.010 for buildings having non-structural elements fixed in a way so as not to interfere with structural deformations or without non-structural elements (EN 1998-1: 2004)

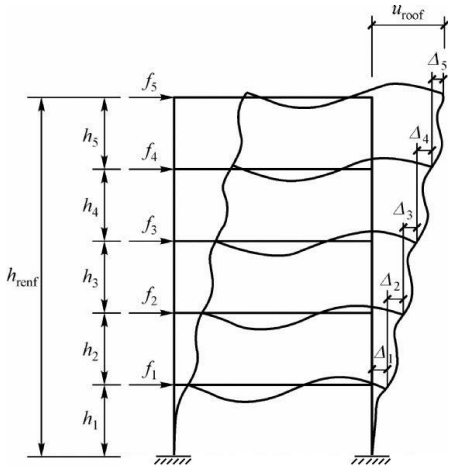

Figure 1-5: Interstorey displacements under horizontal loading

Additionally, d is the difference of the average lateral displacements d_s at the top and the bottom of the storey under consideration defined as $d_s = q \cdot d_e$, where d_e is the maximum lateral displacement provided by the elastic analysis of the structure. It is of utmost importance to define which lateral displacement is considered in equation (1-25), especially for a non-regular building in plan, where the torsional effects are significant, thus resulting in increased values of elastic displacements d_e. In order to address this issue in such a way that the interstorey drifts check does not become any more stringent, instead of

receiving the ultimate maximum displacement from the elastic analysis, there is also the alternative to calculate it in the center of rigidity. In this case, the torsional effects are almost eliminated in multi-storey buildings, thus estimating a more objective quantity for the required displacement. Obviously, in the case of regular buildings in plan, since the center of rigidity coincides with the center of mass and, therefore, no torsional effects are developed, all points across the diaphragm have the same elastic displacement.

The value of the reduction factor v depends on the importance class of the building and takes into account the lower return period of the seismic action associated with the damage limitation requirement. The recommended values of v are 0.5 for importance classes I and II and 0.4 for classes III and IV.

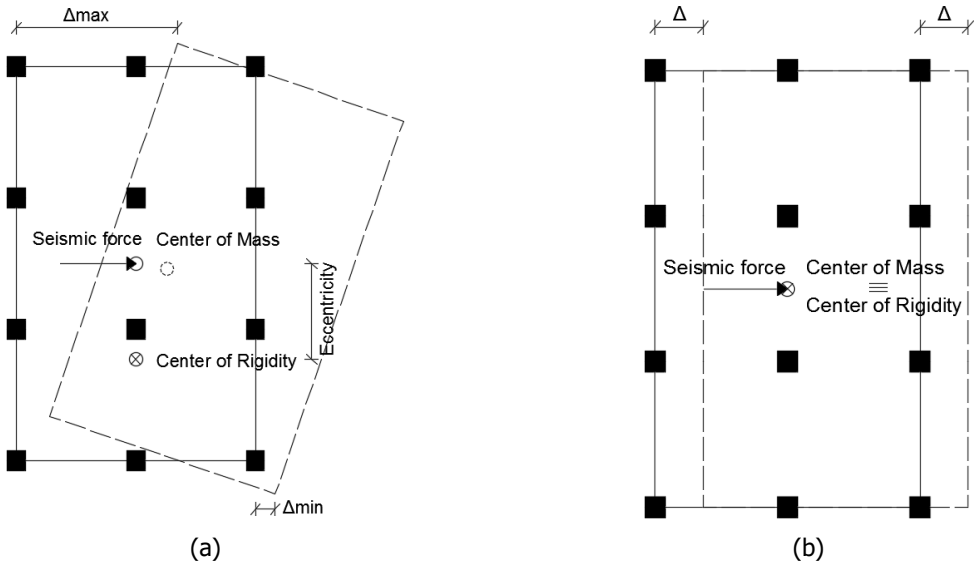

Figure 1-6: (a) Torsional effect in irregular building (b) Uniform displacement in regular building

1.4.3 **P-Δ effects**

Second-order (P-Δ) effects are of great importance especially in moment resisting frames, due to their lateral flexibility. This check refers to the Ultimate Limit State (ULS) under the seismic design situation and according to EN 1998-1, §4.4.2.2(2) the second-order effects can be estimated as:

$$\theta = \frac{P_{tot} \cdot d_r}{V_{tot} \cdot h} \tag{1-26}$$

where

d_r is the interstorey drift coefficient

P_{tot} is the total gravity load at and above the storey considered in the seismic design situation (G+0.3Q)

V_{tot} is the total seismic storey shear in the direction under investigation

If condition $\theta<0.1$ is fulfilled in all storeys, then the second-order effects need not be taken into account. If $0.1<\theta<0.2$, then they may approximately be taken into account by multiplying the relevant seismic action effects by a factor equal to $1/(1-\theta)$. For values $0.2<\theta<0.3$, a non-linear analysis of geometry should be carried out, while in no case should the interstorey drift coefficient θ exceed the value of 0.3.

2 CHAPTER 2: APPLICATION OF THE PRINCIPLES OF EC8 TO A THREE-STOREY STEEL BUILDING USING AN OPTIMUM DESIGN METHOD

2.1 DESCRIPTION OF THE PROBLEM

In this chapter, the modelling and elastic analysis of a regular multi-storey steel building that fully complies with the regulatories of Eurocodes 3 and 8 are examined. The guideline under investigation concerning the bracings is §6.7.2(2) of EN 1998-1, that explicitly stipulates that in concentrically braced frames with diagonal bracings, only the tension diagonal should be taken into account. In the following paragraphs, the effects of this specific guideline is examined in the design of a multi-storey building through possible design scenarios.

Steel concentrically braced framing systems are economic and, thus, popular forms of providing lateral resistance to multi-storey buildings. A typical CBF consists of diagonal braces attached to beams and columns using gusset plate connections (see Figure 2-1(c)). The two bracings intersect in the middle in order to reduce the compressed bracing's buckling length (see Figure 2-1 (a)).

Due to their geometric configuration, the lateral forces are resisted by developing truss action, tension and compression. This truss behavior limits the lateral drifts and low-frequency vibrations in braced buildings and, therefore, provides occupancy comfort and impedes damages in the non-structural parts. For this reason, CBFs are favoured over moment resisting frames for low return period seismic actions, although in severe earthquakes they have been proven not to perform adequately well (A. Elghazouli 2004).

Their popularity and widely applicable use render the examination of their behavior under seismic loads extremely important. Even though they have been independently investigated, it is rather important to investigate their behavior when they consist integral parts of a multi-storey structure.

(a)

(b)

(c)

Figure 2-1: (a) House of the European Union, Vienna (b) Alcoa building, San Francisco, California (c) Typical gusset plate connections of bracings to beams and columns

Consequently, in order to approach the matter of investigation under realistic conditions, the structure is re-designed in each case so as to fully comply with the Eurocodes. Therefore, for the purpose of this thesis, an optimum design methodology was developed that includes all possible requirements that Eurocodes 3 and 8 suggest. The optimum design method is suitable for any regular building in plan and elevation that constitutes of moment resisting frames and/or concentrically braced frames using the equivalent lateral force method. Ultimately, important conclusions are reached regarding the effects of capacity design and especially of the concentrically bracing systems to the design of the structure, through the investigation of multiple design scenarios.

2.2 DEFINITION OF STRUCTURAL SYSTEM

The steel building under investigation comprises of three storeys with a total height of 12 m, along with two structural systems in the two global directions of the building: MRF system with multiple bays in the X direction and a CBF system in the middle frame crosswise. The cross-section profile for the beams

is IPE, HEA or HEB for the columns, whereas for the bracings the choice is limited only to hollow sections from the SHS or RHS series. The following figures demonstrate the elementary geometry of the structure where it is obvious that the building is symmetrical along its two global axes, both in plan and elevation.

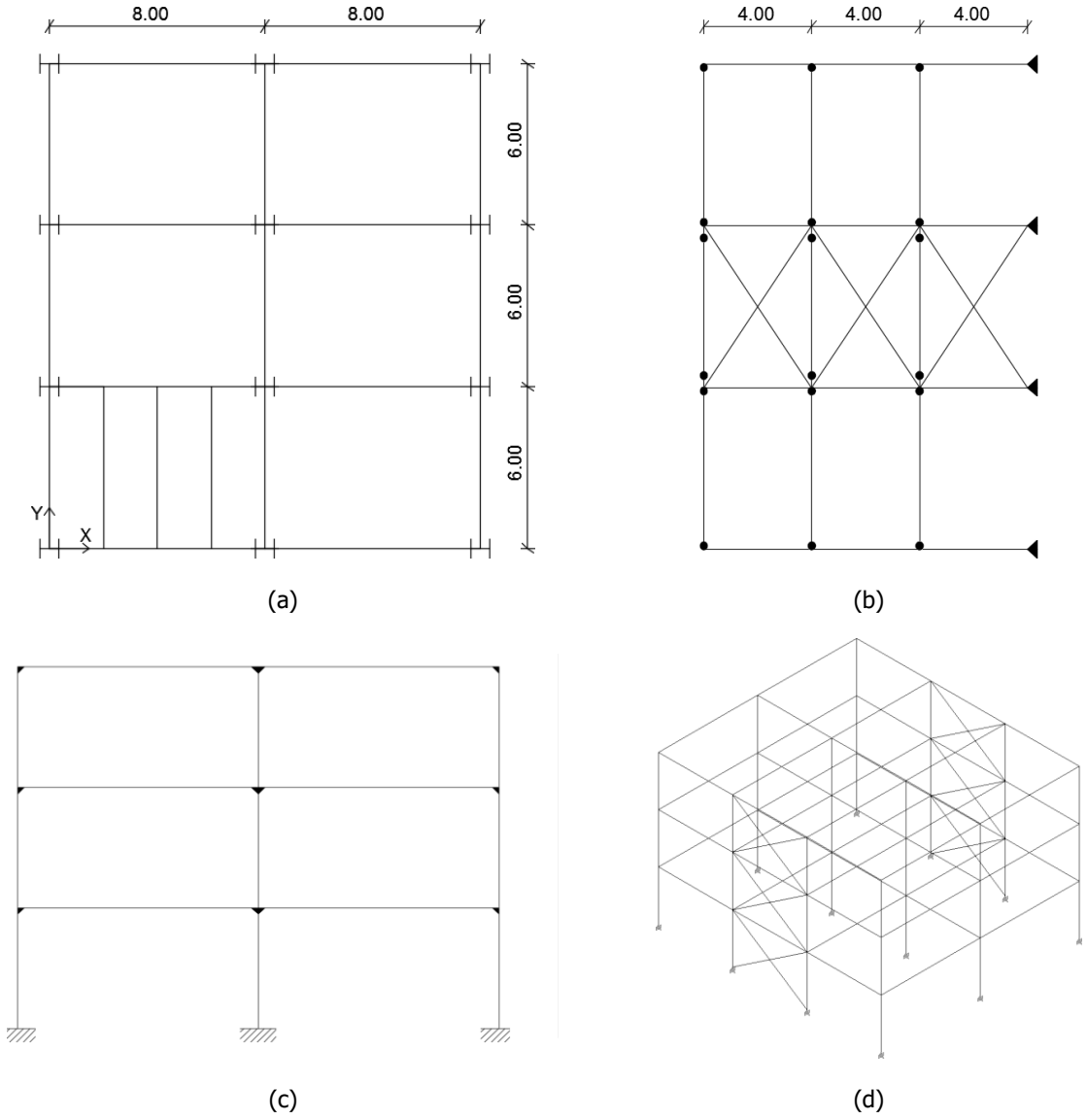

Figure 2-2: (a) Plan (b) Y elevation (c) X elevation (d) 3-dimensional demonstration of the steel building under investigation

All columns are placed in such a way that the major principal axis is activated in the MRF direction, considering that this is the primary direction for the development of bending moment in the columns. An MRF system comprises of moment connections between the beams and the columns, whereas in a CBF system, due to the existence of the bracings, all connections can be assumed to be pins. Therefore, in a structural system as the latter, only insignificant bending moments develop about the minor principal axis that gets activated for earthquakes in the Y direction. In addition, whereas an MRF system resists horizontal loads through the development of shear forces and, thus, bending moments, a CBF system relies entirely on the axial rigidity of the bracings. Finally, secondary beams are also introduced with an axial distance of 2 m, which was chosen arbitrarily. Their structural system is predefined as that of a simply supported beam with pins on both ends, directly connected to the MRF beams.

2.3 NUMERICAL SIMULATION IN ETABS

2.3.1 Definition of structural system

For the analysis of the multi-storey steel building, a three-dimensional (spatial) numerical model is created using the commercial analysis software ETABS. All elements are modelled as beam-type finite elements, whereas no eccentricity is assumed in the connections of the intersecting members. Columns are set to be fully fixed in the level of the foundations in the direction of the MRF system, whereas in the direction of the CBF system to be pins. The concrete slab of each storey is not modelled, although the equivalent vertical loads are introduced to the secondary beams, assuming a uniformly distributed load in the level of the slab. Rigid diaphragms are introduced in each storey due to the existence of the concrete slab, meaning that the behavior of the slab is approached through a solid disc with the ability to develop deformations due to bending moments, although not axially. The design of the members is primarily executed manually in order to acquire more trustworthy results. Therefore, the choice of the automatic modelling as well as the checks that the commercial software integrates, are not used at all throughout the modelling of the structure. The selected type of finite elements for the modelled members is beam-type finite elements, while the concrete slab is not modelled at all.

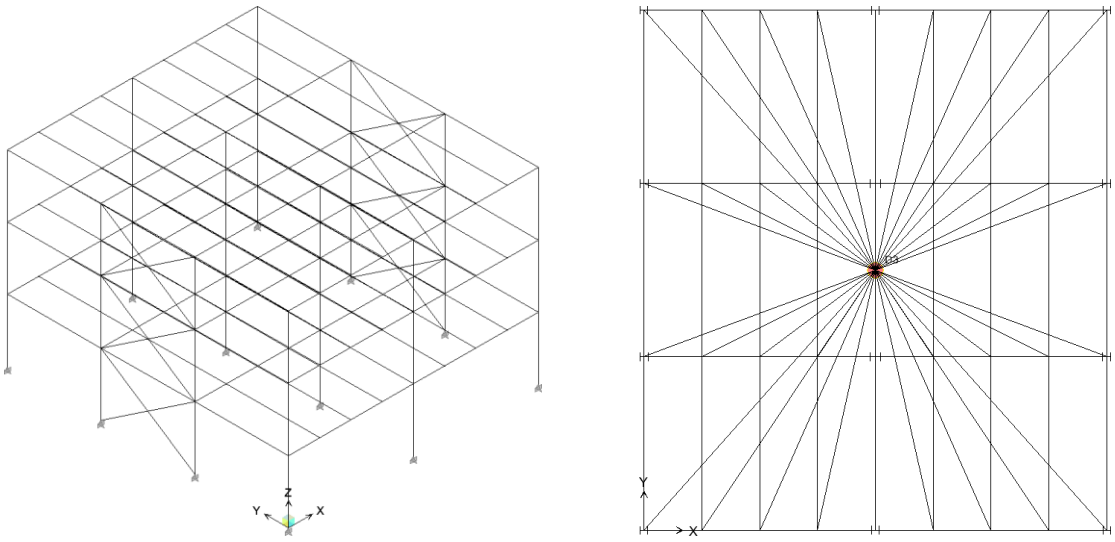

(a) (b)

Figure 2-3: (a) Definition of structural model in ETABS (b) Definition of storey's rigid diaphragm in plan

2.3.2 Definition of material

The material is defined for all members as hot rolled steel of S355 grade. This assumption is mainly made considering the demanding seismic requirements in terms of member sections. Taking into account that ETABS is used only for the static analysis of the structure (internal forces and displacements), the software assumes an infinitely linear behavior of the material and, therefore, no yielding strength is required to be introduced. The grade of the steel is irrelevant to the developed internal forces, as it only determines the ultimate strength of the members which is checked manually in each case.

2.3.3 **Definition of vertical loads**

In a seismic design situation, the vertical loads (permanent and variable loads) should be taken into account as they define the mass that determines the period of vibration and, ultimately, the imposed seismic loads. The vertical loads imposed in the structure under investigation comprise of:

- dead load of the steel members as well as a uniform one from the concrete slab in each storey distributed to the elements with regard to their influence area
- superimposed dead load in the perimeter of the building due to masonry
- variable load uniformly distributed in the level of the slab

The following figures demonstrate the distribution of the vertical as well as the seismic loads in the software. All of the aforementioned loads are repeatedly imposed in each storey of the building.

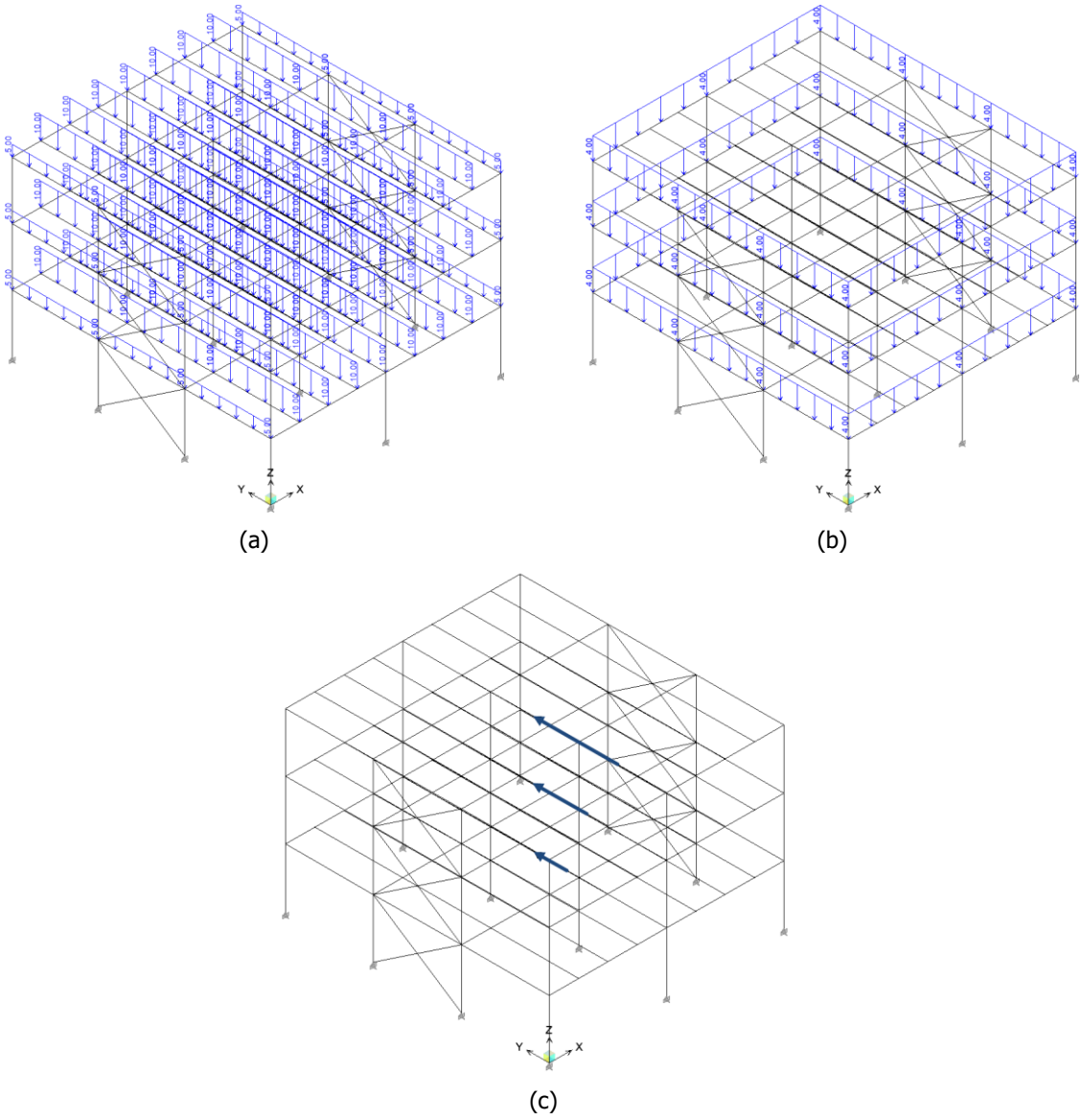

(a) (b)

(c)

Figure 2-4: (a) Distribution of equivalent dead and variable loads from the slab directly applied to secondary beams (b) Distribution of masonry loads in the perimeter (c) Typical distribution of imposed seismic loads

2.3.4 **Design loads combinations**

The multi-storey building under investigation should demonstrate an ability to resist the vertical and horizontal imposed loads in the most unfavourable combination in the seismic situation. The seismic design combination prescribed in EN 1998-1: 2004, §6.4.3.4 where $\psi_{2,i}=0.30$ for residential areas, is:

$$\sum_{j\geq 1} G_{k,j} + \sum_{i\geq 1} \psi_{2,i} \cdot Q_{k,i} + A_{Ed} \tag{2-1}$$

$$E_{Ed,X} + 0.30E_{Ed,Y} \;\&\; E_{Ed,Y} + 0.30E_{Ed,X} \tag{2-2}$$

Eccentricity is taken into account along both axes and, therefore, the following 18 possible combinations should be taken into account in the design of the structural elements of the building.

Table 2-1: Summary table of the design loads combinations
(G=element dead load, G'=slab's dead load, G"=masonry's dead load, Q=variable load)

Name	Combinations
ULS	1.35G+1.35G'+1.35G"+1.50Q
SLS	G+G'+G"+Q
SEISM1	G+G'+G"+0.3Q+(EX+ECCY)+0.3(EY+ECCX)
SEISM2	G+G'+G"+0.3Q+(EX+ECCY)+0.3(EY − ECCX)
SEISM3	G+G'+G"+0.3Q+(EX − ECCY)+0.3(EY+ECCX)
SEISM4	G+G'+G"+0.3Q+(EX − ECCY)+0.3(EY − ECCX)
SEISM5	G+G'+G"+0.3Q − (EX+ECCY)+0.3(EY+ECCX)
SEISM6	G+G'+G"+0.3Q − (EX+ECCY)+0.3(EY − ECCX)
SEISM7	G+G'+G"+0.3Q − (EX − ECCY)+0.3(EY+ECCX)
SEISM8	G+G'+G"+0.3Q − (EX-ECCY)+0.3(EY − ECCX)
SEISM9	G+G'+G"+0.3Q+(EY+ECCX)+0.3(EX+ECCY)
SEISM10	G+G'+G"+0.3Q+(EY+ECCX)+0.3(EX − ECCY)
SEISM11	G+G'+G"+0.3Q+(EY − ECCX)+0.3(EX+ECCY)
SEISM12	G+G'+G"+0.3Q+(EY − ECCX)+0.3(EX − ECCY)
SEISM13	G+G'+G"+0.3Q+(EY+ECCX) − 0.3(EX+ECCY)
SEISM14	G+G'+G"+0.3Q+(EY+ECCX) − 0.3(EX − ECCY)
SEISM15	G+G'+G"+0.3Q+(EY − ECCX) − 0.3(EX+ECCY)
SEISM16	G+G'+G"+0.3Q+(EY − ECCX) − 0.3(EX − ECCY)

2.4 OPTIMUM DESIGN METHOD

The modelling of a multi-storey steel building that fully complies with all regulatories of Eurocodes 3 and 8 described in previous paragraphs, can be a time-consuming procedure that may not always result in the most economic design solution. It is crucial, therefore, in terms of time and financial sources, to combine all assumptions and checks required by Eurocodes in a single algorithm. This algorithm integrates all the essential steps during the design process in an explicit order that leads to a balanced solution between analysis effort as well as material economy. It should be mentioned that the flow chart is created in order to demonstrate the procedure schematically and in no case does it abide by strict mathematic or programming rules.

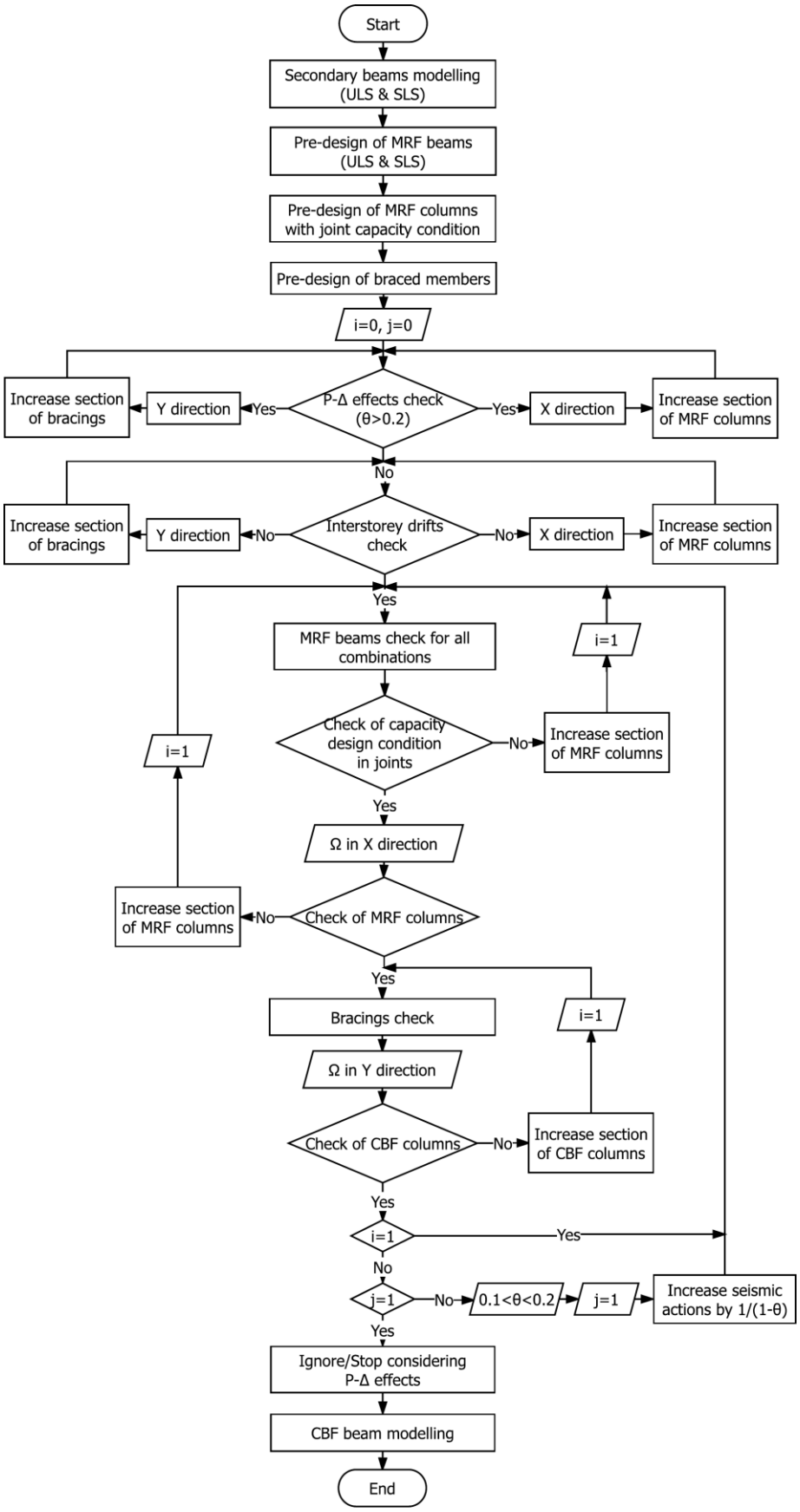

Figure 2-5: Flow chart of optimum design method for regular steel buildings (developed using online software Lucidchart)

The sequence of orders presented in the flow chart is determined so as to minimize the number of the required analyses. The main concept behind the optimum method lies on the fact that the value of the seismic loads ultimately depends on the rigidity in the direction of the earthquake, when the total mass can be assumed to be approximately constant. Therefore, considering that the vertical loads have a constant value, it is crucial to define the sections of the members that primarily resist the seismic loads. In particular, these members can be assumed to be the columns in the MRF system in the X direction, while in the case of the CBF system, the bracings. Small cross-sections lead to reduced rigidity and, thus, increased period of vibration which results in small seismic loads. However, the structure should not only be able to resist the design loads according to the combinations in Table 2-1, but it should also comply with the stringent limitations regarding the deformation as well as the developed P-Δ effects.

2.5 DESIGN IGNORING COMPRESSED BRACING: SCENARIO 1

2.5.1 General

In order to investigate the effects of the post-buckling and yielding behavior of the diagonals in the seismic load-bearing capacity of the structure, possible elastic scenarios that account for the different approaches of guideline EN 1998-1, §6.7.2(2) are introduced. The speculation on whether or not to include the compressed bracing in the elastic analysis, does not have an immediate and conclusive answer and is examined through a number of possible scenarios. Another approach, however, suggests that the seismic actions are calculated for the design earthquake, where the buckling of the compressed bracing has already taken place. In Scenario 1, the structure is modelled by taking into account only the tension diagonal in the structural configuration, thus completely ignoring the contribution of the compressed bracing in the lateral rigidity of the structure during the static analysis.

Before proceeding to the design methodology for this scenario, the seismic design components introduced in Chapter 1, should be defined. Consequently, the ductility class of the building is arbitrarily determined as DCM, as no further information concerning the seismicity of the area or the importance of the building are known. Furthermore, the ductility class along with the lateral force resisting system, determine the behavior factor of the building in each direction. Therefore, according to Table 1-2, for DCM and moment resisting frames, the maximum value of the behavior factor is suggested as q=4 in the X direction, whereas for DCM and concentric bracings with diagonals the recommended value is q=4 in the Y direction as well. Finally, the three-storey steel building under investigation can be categorized as regular in elevation, considering it includes cross-sections and loads that are similar for all storeys in conjunction with the absence of setbacks. Furthermore, since it complies with all the aforementioned criteria regarding regularity in plan, the structure is rendered regular in general.

2.5.2 Detailed application of optimum design method

The following figures demonstrate the fundamental principles for the design of columns and bracings. Apart from the resistance capacity checks for the members, the capacity design requirements play an extremely important and definitive role in the final design of members, such as columns or bracings, which are assumed to be the primary members that provide lateral resistance under seismic loading.

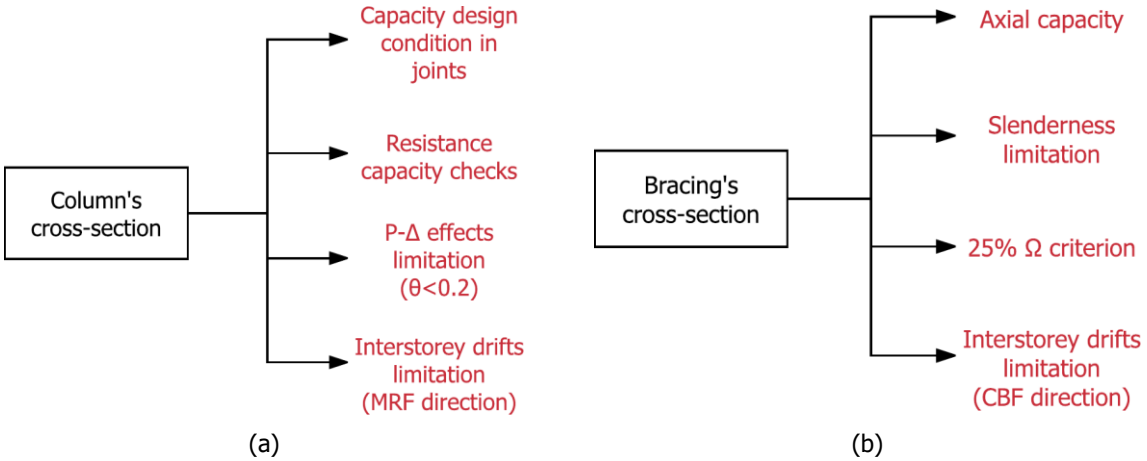

Figure 2-6: Schematic representation of general design requirements for (a) columns (b) bracings

2.5.2.1 Secondary beams modelling

The design of the secondary beams constitutes the first step, considering that they are pinned on both ends and are, therefore, not affected at all by the seismic loads due to the existence of the rigid diaphragm. With regard to the fact that their structural system is statically determined, they also do not affect the imposed vertical loads in the MRF beams. The secondary beams are ultimately designed based on the required strength in the Ultimate Limit State (ULS), as well as the deflection limitation provided by the Serviceability Limit State (SLS). Considering that the influence area of the beams is 2 m for the interior beams and 1m for the beams in the perimeter in addition to the masonry load, the design loads for the two cases are defined as:

$$b_{eff}=2m \begin{cases} q_d=1.35(b_{eff}\cdot g)+1.50(b_{eff}\cdot q)=1.35\cdot 2\cdot 5+1.5\cdot 2\cdot 3=22.5\,kN/m & (2\text{-}3) \\ q_s=1.00(b_{eff}\cdot g)+1.00(b_{eff}\cdot q)=1.00\cdot 2\cdot 5+1.00\cdot 2\cdot 3=16.0\,kN/m & (2\text{-}4) \end{cases}$$

$$b_{eff}=1m \begin{cases} q_d=1.35(b_{eff}\cdot g+g^*)+1.50(b_{eff}\cdot q)=1.35(1\cdot 5+4)+1.5\cdot 1\cdot 3=15.15\,kN/m & (2\text{-}5) \\ q_s=1.00(b_{eff}\cdot g+g^*)+1.00(b_{eff}\cdot q)=1.00(1\cdot 5+4)+1.00\cdot 1\cdot 3=12.0\,kN/m & (2\text{-}6) \end{cases}$$

where g=5 kN/m and q=3 kN/m are the uniformly distributed dead load and variable load respectively in the level of the slab, while g^*=4 kN/m is the load in the perimeter due to the existence of masonry.

The assumptions that the dead load is ignored, as well as that the section class is either 1 or 2 are made, in order to acquire the bending moment and, thus, the cross-section in the pre-design as follows:

$$b_{eff}=2m \qquad M_{Ed}=q_d l^2/8=101.25\,kN/m \le M_{pl,Rd}=W_{pl,y}f_y \rightarrow W_{pl,y} \ge 285.2\ cm^3 \rightarrow IPE240 \qquad (2\text{-}7)$$

$$b_{eff}=1m \qquad M_{Ed}=q_d l^2/8=68.18\,kN/m \le M_{pl,Rd}=W_{pl,y}f_y \rightarrow W_{pl,y} \ge 285.2\ cm^3 \rightarrow IPE240 \qquad (2\text{-}8)$$

The determined IPE240 does not fulfill the deflection requirement, as an IPE270 is rendered sufficient according to the following serviceability conditions for floors.

G+Q (b_{eff}=2m) $$\delta = 5q_s l^4/(384EI_y) \le \delta_{max} = L/250 = 2.4 \text{ cm} \rightarrow I_y \ge 5357 \text{ cm}^4 \rightarrow \text{IPE270} \quad (2\text{-}9)$$

G+Q (b_{eff}=1m) $$\delta = 5q_s l^4/(384EI_y) \le \delta_{max} = L/250 = 2.4 \text{ cm} \rightarrow I_y \ge 4017 \text{ cm}^4 \rightarrow \text{IPE270} \quad (2\text{-}10)$$

Q (b_{eff}=2m) $$\delta = 5ql^4/(384EI_y) \le \delta_2 = L/300 = 2 \text{ cm} \rightarrow I_y \ge 2411 \text{ cm}^4 \text{ (satisfied)} \quad (2\text{-}11)$$

Final check of moment resistance as well as deflection limits for IPE270 section, considering the dead load of the beam.

$$g = A\gamma_s = 0.36 \text{ kN/m} \rightarrow M_{Ed} = 101.25 + (1.35g)l^2/8 = 103.44 \text{ kNm} \le M_{pl,Rd} = W_{pl,y} f_y = 171.82 \text{ kNm} \quad (2\text{-}12)$$

The most unfavourable state in terms of deflection is in the case of the dead and the variable load (G+Q) and for the influence are of 2m.

$$\delta = 5q_s l^4/(384EI_y) = 2.3 \text{ cm} \le \delta_{max} = 2.4 \text{ cm} \quad (2\text{-}13)$$

The class of the cross-section should be checked to be either 1 or 2, otherwise the bending moment resistance is estimated using the elastic quantities.

Flange: $$c/t_f = (b - t_w - 2r)/(2t_f) = 4.8 < 9\varepsilon = 7.29 \rightarrow \text{Class 1} \quad (2\text{-}14)$$

Web: $$c/t_w = (h - 2c)/t_w = 33.2 < 72\varepsilon = 58.3 \rightarrow \text{Class 1} \quad (2\text{-}15)$$

Therefore, the secondary beams are classified as Class 1 and they are able to develop their full plastic resistance. Finally, the ability of the selected beams to resist shear force is also checked as:

$$V_{Ed} = q_d l/2 = 69 \text{ kN} \le V_{pl,Rd} = A_v(f_y/\sqrt{3}) = 17.1(35.5/\sqrt{3}) = 351 \text{ kN} \quad (2\text{-}16)$$

Ultimately, all secondary beams are selected as IPE270, as illustrated in Figure 2-7.

2.5.2.2 Pre-design of MRF beams

The next step after the modelling of the secondary beams is the preliminary design of the beams that are part of the moment resisting frame (MRF) system. The reason why this step precedes the design of other members, is that the moment rigidity of the beams in the beam-column joints mainly defines the buckling length and, thus, the cross-section of the columns in an MRF system. It should be mentioned that the MRF beams should be able to resist the developed bending moment and the respective shear forces for all combinations of Table 2-1, although they should not be checked for axial capacity, due to the existence of the rigid diaphragm. The MRF beams are pre-designed based on the ULS and SLS only and after a preliminary design of the columns is executed, their moment and shear capacity is checked in all seismic design combinations. In parallel to the secondary beams, the MRF beams are designed with regard to an influence area, which is 3m for the beams in the perimeter and 6m for the internal ones, same as their axial distance. The design loads for the two cases are defined as:

$$b_{eff}=6m \begin{cases} q_d=1.35(b_{eff}\cdot g)+1.50(b_{eff}\cdot q)=1.35\cdot(6\cdot5)+1.5\cdot(6\cdot3)=67.5\ kN/m & (2\text{-}17) \\ q_s=1.00(b_{eff}\cdot g)+1.00(b_{eff}\cdot q)=1.00\cdot(6\cdot5)+1.0\cdot(6\cdot3)=48\ kN/m & (2\text{-}18) \end{cases}$$

$$b_{eff}=3m \begin{cases} q_d=1.35(b_{eff}\cdot g+g^*)+1.50(b_{eff}\cdot q)=1.35\cdot(3\cdot5+4)+1.5\cdot3\cdot3=39.15\ kN/m & (2\text{-}19) \\ q_s=1.00(b_{eff}\cdot g+g^*)+1.00(b_{eff}\cdot q)=1.00\cdot(3\cdot5+4)+1.0\cdot3\cdot3=28\ kN/m & (2\text{-}20) \end{cases}$$

where g=5 kN/m and q=3 kN/m are the uniformly distributed dead load and variable load respectively in the level of the slab, while g^*=4 kN/m is the load in the perimeter due to the existence of masonry.

The assumptions that the dead load is ignored, as well as that the section class is either 1 or 2 are also made for the pre-design of the MRF beams in the non-seismic situation. A significant assumption made for the pre-design of the MRF beams refers to their structural system. Considering that in the X direction the structure is statically undetermined, the sections of the members indirectly determine the developed internal forces. Therefore, in order to eliminate the parameter of the columns' section in the preliminary design of the beams, their structural system is assumed to be fixed on both ends and the maximum developed moments are defined as:

b_{eff}=6m $$M_{Ed}=q_d l^2/12=360\ kN/m \le M_{pl,Rd}=W_{pl,y}f_y \rightarrow W_{pl,y}\ge1014\ cm^3 \rightarrow IPE400 \quad (2\text{-}21)$$

b_{eff}=3m $$M_{Ed}=q_d l^2/12=208.8\ kN/m \le M_{pl,Rd}=W_{pl,y}f_y \rightarrow W_{pl,y}\ge588\ cm^3 \rightarrow IPE300 \quad (2\text{-}22)$$

The determined MRF beams sections fulfill the deflection requirements, according to the following serviceability conditions for floors.

G+Q (b_{eff}=6m) $$\delta=q_s l^4/(384EI_y) \le \delta_{max}=L/250=3.2\ cm \rightarrow I_y \ge 7619\ cm^4 \rightarrow IPE300 \quad (2\text{-}23)$$

G+Q (b_{eff}=3m) $$\delta=q_s l^4/(384EI_y) \le \delta_{max}=L/250=3.2\ cm \rightarrow I_y \ge 4444\ cm^4 \rightarrow IPE270 \quad (2\text{-}24)$$

Q (b_{eff}=6m) $$\delta=q l^4/(384EI_y) \le \delta_2=L/300=2.67\ cm \rightarrow I_y \ge 3424\ cm^4 \text{ (satisfied)} \quad (2\text{-}25)$$

Q (b_{eff}=3m) $$\delta=q l^4/(384EI_y) \le \delta_2=L/300=2.67\ cm \rightarrow I_y \ge 1712\ cm^4 \text{ (satisfied)} \quad (2\text{-}26)$$

Final check of moment resistance as well as deflection limits for IPE270 section, considering the dead load of the beam in the cases when b_{eff}=6m:

$$g=A\gamma_s=0.66\ kN/m \rightarrow M_{Ed}=360+(1.35g)l^2/8=367.13\ kNm \le M_{pl,Rd}=W_{pl,y}f_y=464\ kNm \quad (2\text{-}27)$$

as well as when b_{eff}=3m:

$$g=A\gamma_s=0.42\,kN/m \rightarrow M_{Ed}=208.8+(1.35g)l^2/8=213.34\ kNm \leq M_{pl,y,Rd}=W_{pl,y}f_y=222.94\ kNm \quad (2\text{-}28)$$

However, when the dead load is included, $M_{Ed}/M_{pl,y,Rd}=0.96$ and, therefore, the beam is increased to IPE330 where $M_{Ed}/M_{pl,y,Rd}=0.75$. The class of both cross-sections IPE330 and IPE400 is checked:

Flange $b_{eff}=6m$
$$c/t_f=(b-t_w-2r)/(2t_f)=4.8<9\varepsilon=7.29 \rightarrow \text{Class 1} \quad (2\text{-}29)$$

Web $b_{eff}=6m$
$$c/t_w=(h-2c)/t_w=38.5<72\varepsilon=58.3 \rightarrow \text{Class 1} \quad (2\text{-}30)$$

Flange $b_{eff}=3m$
$$c/t_f=(b-t_w-2r)/(2t_f)=5.4<9\varepsilon=7.29 \rightarrow \text{Class 1} \quad (2\text{-}31)$$

Web $b_{eff}=3m$
$$c/t_w=(h-2c)/t_w=36.1<72\varepsilon=58.3 \rightarrow \text{Class 1} \quad (2\text{-}32)$$

Therefore, both MRF beams are classified as Class 1 in bending and they are able to develop their full plastic resistance. Finally, the ability of the selected MRF beams to resist shear force is also checked as:

$b_{eff}=6m$
$$V_{Ed}=q_d l/2=273.6\ kN \leq V_{pl,Rd}=A_v(f_y/\sqrt{3})=33.2(35.5/\sqrt{3})=680\ kN \quad (2\text{-}33)$$

$b_{eff}=3m$
$$V_{Ed}=q_d l/2=158.9\ kN \leq V_{pl,Rd}=A_v(f_y/\sqrt{3})=23.9(35.5/\sqrt{3})=490\ kN \quad (2\text{-}34)$$

Ultimately, the internal MRF beams are selected in the pre-design phase as IPE400, whereas the beams in the perimeter as IPE330.

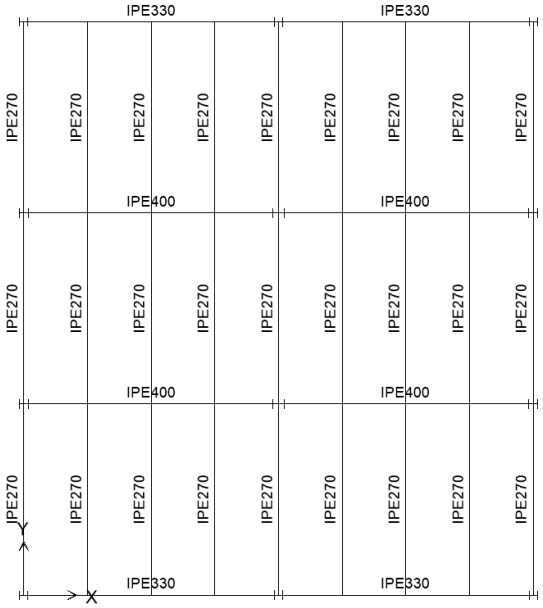

Figure 2-7: Demonstration of the preliminary design of the secondary and the main beams

2.5.2.3 Pre-design of MRF columns

The preliminary design of the columns is mainly based on the capacity design condition for joints or:

$$\sum MR_c \geq 1.3 \sum MR_b \tag{2-35}$$

This specific check is extremely definitive for the design of the columns and does not require the estimation of seismic loads. The pre-designed MRF beams are used to form the quantity $\sum MR_b$ and with the assumption that a full plastic hinge is formed in the joint, the acquired sections are determined as:

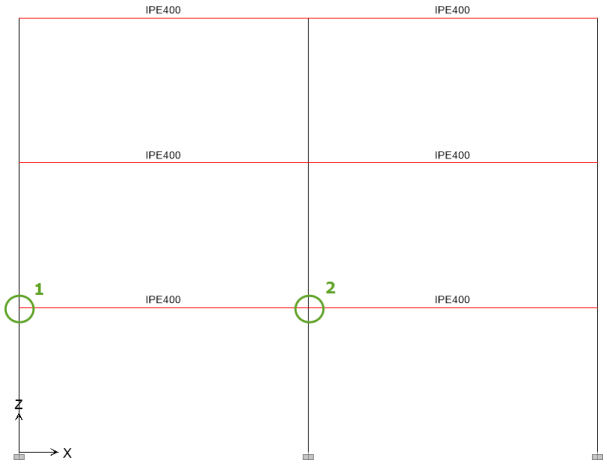

Figure 2-8: Capacity design condition in the joints of the internal MRF framing system

Joint 1

$$\sum MR_b = W_{pl}^{IPE400} \cdot f_y = 1307 \cdot 35.5/100 = 464 \text{ kNm} \tag{2-36}$$

$$\sum MR_c = 2 \cdot W_{pl,y,c} \cdot f_y \geq 1.3 \sum MR_b \rightarrow W_{pl,y,c} \geq 850 \text{ cm}^3 \rightarrow \text{HEB240 } (W_{pl,y} = 1053 \text{ cm}^3) \tag{2-37}$$

Joint 2

$$\sum MR_b = 2 \cdot W_{pl}^{IPE400} \cdot f_y = 2 \cdot 1307 \cdot 35.5/100 = 928 \text{ kNm} \tag{2-38}$$

$$\sum MR_c = 2 \cdot W_{pl,y,c} \cdot f_y \geq 1.3 \sum MR_b \rightarrow W_{pl,y,c} \geq 1700 \text{ cm}^3 \rightarrow \text{HEB300 } (W_{pl,y} = 1869 \text{ cm}^3) \tag{2-39}$$

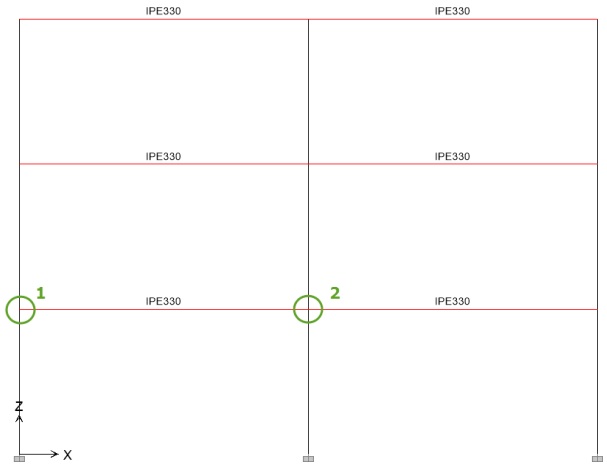

Figure 2-9: Capacity design condition in the joints of the external framing system

Joint 1

$$\sum MR_b = W_{pl}^{IPE330} \cdot f_y = 804 \cdot 35.5/100 = 285.78 \text{ kNm} \quad (2\text{-}40)$$

$$\sum MR_c = 2 \cdot W_{pl,y,c} \cdot f_y \geq 1.3 \sum MR_b \rightarrow W_{pl,y,c} \geq 523 \text{ cm}^3 \rightarrow \text{HEB200 } (W_{pl,y} = 643 \text{ cm}^3) \quad (2\text{-}41)$$

Joint 2

$$\sum MR_b = 2 \cdot W_{pl}^{IPE330} \cdot f_y = 2 \cdot 804 \cdot 35.5/100 = 571.56 \text{ kNm} \quad (2\text{-}42)$$

$$\sum MR_c = 2 \cdot W_{pl,y,c} \cdot f_y \geq 1.3 \sum MR_b \rightarrow W_{pl,y,c} \geq 1047 \text{ cm}^3 \rightarrow \text{HEB260 } (W_{pl,y} = 1283 \text{ cm}^3) \quad (2\text{-}43)$$

2.5.2.4 Pre-design of braced members

The modelling of the braced members is primarily dominated by the seismic loads in the direction of the CBF system. However, considering that a 30% of the X direction is included, the rigidity of the columns and, thus, the imposed seismic loads increase the design forces of the braced members. Hollow sections are only selected due to their comparatively smaller mass and, therefore, cost. The requirements stipulated by Eurocode 8 for CBF diagonals were introduced in Table 1-9, but are also presented in the following table as they provide the basis for their final design.

Table 2-2: Summary table of capacity design requirements and checks according to EN1998-1 for braced members

Capacity design requirements	**Checks**	**Eurocode 8 reference**
Cross-section classification	Class 1 or 2	EN 1998-1, §6.3.1(5), Figure 6.2 EN 1998-1, §6.5.3(2), Table 6.3
$N_{Ed}=N_{Ed,G}+N_{Ed,E}$ (for all seismic combinations)	$N_{Ed}/N_{pl,Rd} \leq 1$	EN 1998-1, §6.7.3(5)
Non-dimensional slenderness limitation	$1.3 \leq \bar{\lambda} \leq 2.0$	EN 1998-1, §6.7.3(1)
Uniform distribution of ductility in height	$(\Omega_{max}-\Omega_{min})/\Omega_{min} \leq 0.25$	EN 1998-1, §6.7.3(8)

The first criterion taken into account refers to the non-dimensional slenderness limitation, as it does not require to calculate the values of the seismic loads. The class is assumed to be 1 or 2 and is checked at the end of the final design. The non-dimensional slenderness is defined as:

$$\bar{\lambda_y} = \frac{L_{cr,y}}{\lambda_1 \cdot i_y} \quad \text{and} \quad \bar{\lambda_z} = \frac{L_{cr,z}}{\lambda_1 \cdot i_z} \quad (2\text{-}44)$$

which can be inversed in order to acquire the minimum and maximum radius of gyration for the upper and the lower limit of the slenderness respectively as:

$$i_{y,min} = \frac{L_{cr,y}}{\lambda_1 \cdot 2} = 2.37 \text{ cm} \quad \text{and} \quad i_{y,max} = \frac{L_{cr,y}}{\lambda_1 \cdot 1.5} = 3.65 \text{ cm} \quad (2\text{-}45)$$

$$i_{z,min} = \frac{L_{cr,z}}{\lambda_1 \cdot 2} = 2.37 \text{ cm} \quad \text{and} \quad i_{z,max} = \frac{L_{cr,z}}{\lambda_1 \cdot 1.5} = 3.65 \text{ cm} \quad (2\text{-}46)$$

where $L_{cr,y} = L_{cr,z} = 0.5L = 0.5\sqrt{6^2+4^2} = 3.6$ m and $\lambda_1 = 93.9 \cdot \varepsilon = 93.9 \cdot 0.81 = 76.1$.

Secondly, the design axial force for each bracing is received from the most unfavourable seismic combination, as the contribution of the vertical loads to the bracings is negligible and the ULS and SLS are ignored.

$$A_{min} = N_{Ed,i}/f_y \quad (2\text{-}47)$$

In order to calculate the imposed seismic loads, sections for all members of the building should be defined. The sections acquired from the capacity design conditions for the joints are set for the columns. Since the axial capacity criterion in equation (2-47) depends on the developed axial forces in the bracings which ultimately rely on the imposed seismic loads and, thus, cross-sections, only the first requirement is met for the first analysis. Furthermore, for material economy reasons, the minimum possible section in terms of mass and, thus, cost is selected from tables Table 2-5) and/or Table 2-6) for the upper bracings, whereas the sections increase gradually downwards. Finally, after the first definition of cross-sections, a static analysis for the horizontal as well as the vertical loads in each combination is carried out in order to receive the values of the developed axial forces. The dead load of the bracings as well as the vertical loads from the slab are also included.

Table 2-3: Preliminary design forces for the bracings

Storey	Section	SEISM1	SEISM2	SEISM3	SEISM4	SEISM5	SEISM6	SEISM7	SEISM8
1	SHS80X4	88.49	98.90	97.98	87.57	98.90	88.49	97.98	97.98
2	SHS70X4	74.22	84.15	83.86	73.93	84.15	74.22	83.86	83.86
3	SHS70X3	46.68	52.61	52.55	46.63	52.61	46.68	52.55	52.55

Storey	Section	SEISM9	SEISM10	SEISM11	SEISM12	SEISM13	SEISM14	SEISM15	SEISM16
1	SHS80X4	269.20	278.94	279.22	269.47	279.22	269.47	269.20	278.94
2	SHS70X4	223.38	232.67	232.76	223.47	232.76	223.47	223.38	232.67
3	SHS70X3	140.79	146.33	146.35	140.81	146.35	140.81	140.79	146.33

The most unfavourable (maximum) seismic forces according to the seismic combinations of Table (2-4) are summarized in the following table for each bracing:

Table 2-4: Axial capacity and radius of gyration requirements for the bracings

Storey	$i_{z,min}$ (cm)	$i_{z,max}$ (cm)	$N_{Ed,i}$ (kN)	$A_{req,i}$ (cm^2)	$A_{exist,i}$ (cm^2)	$\Omega_i = N_{pl,Rd,i}/N_{Ed,i}$
1	2.37	3.65	279.22	7.87	12	1.53
2	2.37	3.65	232.76	6.56	10.4	1.59
3	2.37	3.65	146.35	4.12	7.94	1.93

The slenderness criterion is obviously the most unfavourable and definitive one, since it leads to the selection of increased sections. However, the last criterion concerning the uniform distribution of ductility in height across the bracings is not satisfied as $(\Omega_{max}-\Omega_{min})/\Omega_{min}$ =26.2% > 25%. Therefore, a different approach is made, where both SHS and RHS series are included in order to take advantage of the reduced inertial characteristics of the RHS sections. In particular, the RHS series offer a smaller radius of gyration about the minor principal axis for the same area as an SHS section.

Table 2-5: Available SHS cross-sections and acceptable limits due to design requirements for bracings

SHS Sections					
B (mm)	**T (cm)**	**A (cm^2)**	**M (kg/m)**	**I (cm^4)**	**i (cm)**
60	3	6.74	5.29	36.2	2.32
	4	8.79	6.90	45.4	2.27
	5	10.7	8.42	53.3	2.23
70	3	7.94	6.24	59	2.73
	4	10.4	8.15	74.7	2.68
	5	12.7	9.99	88.5	2.64
80	4	12	9.41	114	3.09
	5	14.7	11.6	137	3.05
	6.3	18.1	14.2	156	2.99
90	4	13.6	10.7	166	3.50
	5	16.7	13.1	200	3.45
	6.3	20.7	16.2	238	3.40
100	4	15.2	11.9	232	3.91
	5	18.7	14.7	279	3.86
	6.3	23.2	18.2	336	3.80

Table 2-6: Available RHS cross-sections and acceptable limits due to design requirements for bracings

RHS Sections							
B (mm)	**T (cm)**	**A (cm^2)**	**M (kg/m)**	**I_y (cm^4)**	**i_y (cm)**	**I_z (cm^4)**	**i_z (cm)**
100X50	4	11.2	8.78	140	3.53	46.2	2.03
	5	13.7	10.8	167	3.48	54.3	1.99
	6.3	16.9	13.3	197	3.42	63	1.93
100x60	4	12	9.41	158	3.63	70.5	2.43
	5	14.7	11.6	189	3.58	83.6	2.38
	6.3	18.1	14.2	225	3.52	98.1	2.33
120x60	4	13.6	10.7	249	4.28	83.1	2.47
	5	16.7	13.1	299	4.23	98.8	2.43
	6.3	20.7	16.2	358	4.16	116	2.37
120x80	4	15.2	11.9	303	4.46	161	3.25
	5	18.7	14.7	365	4.42	193	3.21
	6.3	23.2	18.2	440	4.36	230	3.15
140x80	4	16.8	13.2	441	5.12	184	3.31
	5	20.7	16.3	534	5.08	222	3.27
	6.3	25.7	20.2	646	5.01	265	3.21
150X100	6.3	29.5	23.1	898	5.52	474	4.01
	8	36.8	28.9	1087	5.44	569	3.94
	10	44.9	35.3	1282	5.34	665	3.85

Table 2-7: Review of the design for cross-sections in the bracings

Storey	Cross-section	Class
1	RHS100X60X5	1
2	RHS100X60X4	1
3	SHS70X3	1

The reviewed cross-sections in the bracings are introduced in the structure and, afterwards, the axial forces in the bracings are calculated and presented in the following tables. It should be stated that the sections of the bracings are not finalized yet, since this step includes only their pre-design phase.

Table 2-8: New design forces for the bracings

Storey	Section	SEISM1	SEISM2	SEISM3	SEISM4	SEISM5	SEISM6	SEISM7	SEISM8
1	RHS100X60X5	103.39	25.15	65.78	12.94	64.70	14.02	24.06	24.06
2	RHS100X60X4	85.49	21.82	52.50	11.55	52.22	11.83	21.54	21.54
3	SHS70X3	51.25	11.63	33.96	5.91	33.91	5.96	11.59	11.59

Storey	Section	SEISM9	SEISM10	SEISM11	SEISM12	SEISM13	SEISM14	SEISM15	SEISM16
1	RHS100X60X5	285.97	274.68	25.15	13.86	274.36	285.64	13.54	24.82
2	RHS100X60X4	234.05	224.15	21.82	11.92	224.07	233.96	11.84	21.74
3	SHS70X3	143.68	138.50	11.63	6.45	138.48	143.67	6.43	11.62

The most unfavourable (maximum) seismic force according to the seismic combinations of Table (2-9) is received for each bracing and summarized in the following table:

Table 2-9: Axial capacity and radius of gyration requirements for the bracings

Storey	$i_{z,min}$ (cm)	$i_{z,max}$ (cm)	$N_{Ed,i}$(kN)	$A_{req,i}$(cm^2)	$A_{exist,i}$(cm^2)	$\Omega_i = N_{pl,Rd,i}/N_{Ed,i}$
1	2.37	3.65	285.97	8.06	14.7	1.82
2	2.37	3.65	234.05	6.59	12	1.82
3	2.37	3.65	143.68	4.05	7.94	1.96

The requirement regarding the uniform distribution of ductility in the bracings is finally satisfied $(\Omega_{max}-\Omega_{min})/\Omega_{min} = 7.6\% < 25\%$ and, consequently, the preliminary design for the bracings results in the following sections. The class of the section is also checked in order to ensure sufficient ductile behavior and they are all classified as Class 1 in compression.

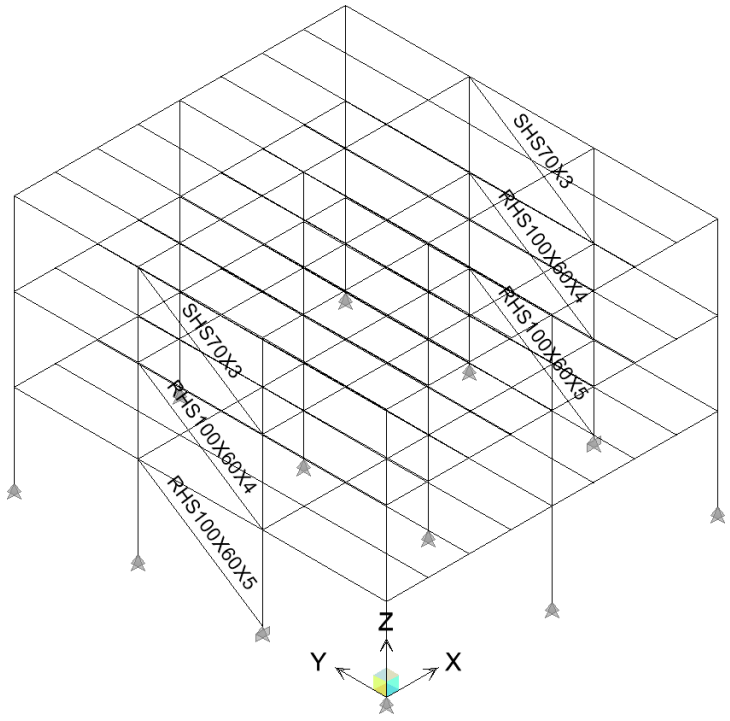

Figure 2-10: Preliminary design of the bracings

2.5.2.5 P-Δ effects check

According to the developed methodology, the next step after the preliminary design of the columns and bracings, is to make a first estimation regarding the magnitude of the P-Δ effects. The damage limitation checks are very stringent and play a significant role in the design of the lateral force resisting systems, which in this case consist of the bracings and the MRF columns. In order to avoid any possibility for non-linear analysis, the value of coefficient θ is limited below 0.2 by increasing either the section of the MRF columns or the bracings, depending on the direction that does not abide by this rule.

According to the following table, the condition of θ<0.2 is not met in the direction of the MRF system, whereas in the direction of the CBF system the checks are all satisfied. This clearly demonstrates the effectiveness of a CBF system in terms of lateral displacements compared to an MRF system. The sections of the MRF columns are repeatedly increased until the aforementioned condition is met. Taking into consideration that the columns in the four edges are the least rigid as they are connected only to a single MRF beam, it is expected that their cross-section will significantly increase during the iterative process due to its lower lateral rigidity.

Table 2-10: Calculation of the P-Δ effects coefficients – condition θ<0.2 is not met

Storey	**P_{tot} (kN)**	**h (m)**	**$V_{tot,X}$ (kN)**	**$V_{tot,Y}$ (kN)**	**dX (m)**	**dY (m)**	**θ_X**	**X Check**	**θ_Y**	**Y Check**
1	2102.35	4	177.94	250.23	0.0427	0.0401	0.126	✓	0.084	✓
2	4205.16	4	297.70	418.64	0.0650	0.0435	0.230	X	0.109	✓
3	6308.30	4	357.59	502.86	0.0523	0.0412	0.231	X	0.129	✓

The sections of the MRF columns are gradually increased, until the condition θ<0.2 is marginally met. The quantities in Table 2-10 are not yet multiplied by the factor 1/(1-θ) as they are checked at the end of the procedure according to the flow chart, when the design of all members is finalized.

Table 2-11: Calculation of the P-Δ effects coefficients – condition θ<0.2 is ultimately met

Storey	**P_{tot} (kN)**	**h (m)**	**$V_{tot,X}$ (kN)**	**$V_{tot,Y}$ (kN)**	**dX (m)**	**dY (m)**	**θ_X**	**X Check**	**θ_Y**	**Y Check**
1	2110.96	4	194.91	251.65	0.0426	0.0398	0.115	✓	0.083	✓
2	4222.39	4	326.36	421.36	0.0613	0.0430	0.198	✓	0.108	✓
3	6334.13	4	392.10	506.23	0.0453	0.0408	0.183	✓	0.127	✓

2.5.2.6 Interstorey drifts check

In conjunction with the P-Δ effects check, the next step is to satisfy the displacement requirements. Despite the fact that the stringent condition of θ<0.2 is satisfied, the interstorey drifts limitation is marginally not met and another attempt is made where the sections of the columns are slightly increased. The following tables represent the values of the interstorey drifts in both principal directions of the building and for each floor in the two cases. The conclusion stated in §1.4.1, that the direct application of the damage limitation checks for moment resisting frames often results in an overall lateral capacity that is significantly increased from that assumed in design, is verified.

Table 2-12: Calculation of the interstorey drifts – condition θ<0.2 is met/drift limit is not met

Storey	dX (m)	dY (m)	$d_{r,X}$ (m)	$d_{r,Y}$ (kN)	v	h (m)	$d_{r,X}$·v	$d_{r,Y}$·v	α	X Check	Y Check
1	0.0426	0.0398	0.0107	0.0099	0.5	4	0.0053	0.0050	0.0075	0.71 ✓	0.66 ✓
2	0.0613	0.0430	0.0153	0.0107	0.5	4	0.0077	0.0054	0.0075	1.02 X	0.72 ✓
3	0.0453	0.0408	0.0113	0.0102	0.5	4	0.0057	0.0051	0.0075	0.75 ✓	0.68 ✓

It should be pointed out that the software does not automatically multiply the elastic displacements with the respective behavior factor q in each direction, as it only calculates the elastic displacements that correspond to the design seismic loads. Consequently, the extracted maximum displacements at each storey and direction are multiplied by q=4 in order to acquire the maximum seismic displacement.

Table 2-13: Calculation of the interstorey drifts – condition θ<0.2 is met/drift limit is also met

Storey	dX (m)	dY (m)	$d_{r,X}$ (m)	$d_{r,Y}$ (kN)	v	h (m)	$d_{r,X}$·v	$d_{r,Y}$·v	α	X Check	Y Check
1	0.0418	0.0394	0.0105	0.0098	0.5	4	0.0052	0.0049	0.0075	0.70 ✓	0.66 ✓
2	0.0599	0.0426	0.0150	0.0107	0.5	4	0.00749	0.0053	0.0075	0.998 ✓	0.71 ✓
3	0.0439	0.0406	0.0110	0.0101	0.5	4	0.0055	0.0051	0.0075	0.73 ✓	0.68 ✓

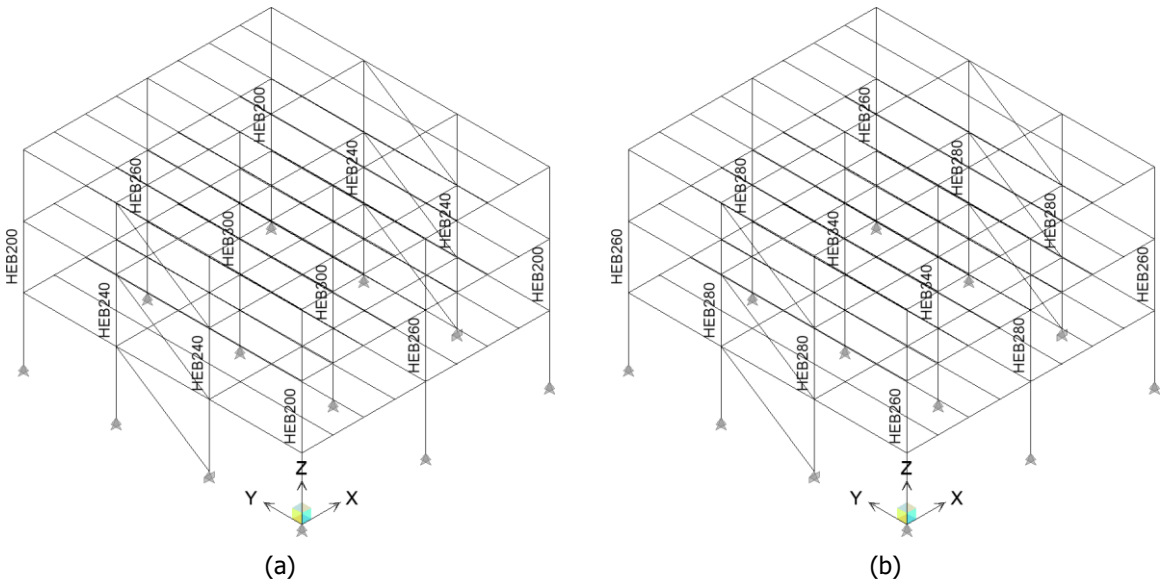

(a) (b)

Figure 2-11: Design of columns due to (a) capacity design condition in the joints (b) damage limitation checks

2.5.2.7 MRF beam checks

Despite the fact that the MRF beams do not contribute directly to the definition of the seismic loads, they determine the buckling length of the columns. The pre-design of the MRF beams was based on the Ultimate Limit as well as the Serviceability Limit States (ULS & SLS), while the seismic loads were completely ignored. Taking into account that the structural system in the X direction is statically undetermined, the sections of both beams, as well as columns, contribute to the definition of the internal forces.

Consequently, both internal forces should be checked in each beam individually in the non-seismic combinations, while the maximum deflections are re-checked in the SLS. According to the static analysis carried out using ETABS, the maximum vertical deflections are:

$$\delta_{max}=1.88 \text{ cm} < \delta_{max,req}=3.2 \text{ cm} \ \& \ \delta_2=0.67 \text{ cm} < \delta_{2,req}=2.67 \text{ cm}$$

Table 2-14, §1.3.1.2: Summary table of capacity design requirements and checks for MRF columns

Capacity design requirements	**Checks**	**Eurocode 8 reference**
Cross-section classification	Class 1 or 2	EN 1998-1, §6.3.1(5), Figure 6.1 EN 1998-1, §6.5.3(2), Table 6.3
$M_{Ed}=M_{Ed,G}+1.1\gamma_{ov}\Omega M_{Ed,E}$	Section and member checks in bending and compression according to EC3	EN 1993-1-1, §6.3.3(4), Equation 6.61
$N_{Ed}=N_{Ed,G}+1.1\gamma_{ov}\Omega N_{Ed,E}$		EN 1993-1-1, §6.3.3(4), Equation 6.62
$V_{Ed}=V_{Ed,G}+1.1\gamma_{ov}\Omega V_{Ed,E}$		EN 1993-1-1, §6.2.6(1), Equation 6.17

The seismic bending moment demands for the MRF beams at each end are illustrated in Figure 2-12 (a) and (b) for a typical seismic combination, such as SEISM1. The following table represents the bending moments only for the first elevation of the MRF system, whereas in the following elevations the values are almost twice due to the existence of secondary beams on both sides. More specifically, all beams are checked for all 16 seismic combinations, while the portrayed Ω is received as the minimum value for both ends and seismic combinations.

Table 2-15: Typical bending moment demands for MRF beams in the seismic design combination SEISM1

Left end				**Right end**				**Ω_i**
G+0.3Q (kNm)	**E (kNm)**	**M_{Ed} (kNm)**	**$M_{Ed}/M_{pl,Rd}$**	**G+0.3Q (kNm)**	**E (kNm)**	**M_{Ed} (kNm)**	**$M_{Ed}/M_{pl,Rd}$**	
-97.38	-19.23	-116.61	0.409	-123.49	18.30	-105.19	0.369	1.564
-123.49	-18.30	-141.79	0.497	-97.38	19.23	-78.15	0.274	
-105.21	-16.73	-121.94	0.427	-119.37	16.16	-103.21	0.362	
-119.37	16.16	-103.21	0.362	-105.21	16.73	-88.48	0.310	
-85.01	-9.82	-94.83	0.332	-129.15	9.11	-120.04	0.421	
-129.15	-9.11	-138.26	0.484	-85.01	9.82	-75.19	0.263	

Table 2-16: Typical shear force demands for MRF beams in the seismic design situation

Left end				**Right end**			
G+0.3Q (kNm)	**E (kNm)**	**V_{Ed} (kNm)**	**$V_{Ed}/(0.5V_{pl,Rd})$**	**G+0.3Q (kNm)**	**E (kNm)**	**V_{Ed} (kNm)**	**$V_{Ed}/(0.5V_{pl,Rd})$**
-69.42	-71.36	-140.78	0.575 ✓	75.95	71.36	147.31	0.601 ✓
-75.95	-71.36	-147.31	0.601 ✓	69.42	71.36	140.78	0.575 ✓
-70.92	-71.36	-142.28	0.581 ✓	74.46	71.36	145.82	0.595 ✓
-74.46	-71.36	-145.82	0.595 ✓	70.92	71.36	142.28	0.581 ✓
-67.17	-71.36	-138.53	0.566 ✓	78.21	71.36	149.57	0.611 ✓
-78.21	-71.36	-149.57	0.611 ✓	67.17	71.36	138.53	0.566 ✓

Table 2-16 demonstrates the shear force demands for the respective MRF system, where $V_{Ed}=V_{Ed,G}+V_{Ed,M}$. In particular, $V_{Ed,G}$ is the design value of the shear force due to the non-seismic actions in the seismic design situation (G+0.3Q), whereas $V_{Ed,M}$ is the design value of the shear force due to the application of the plastic moments i at both ends and is defined as $V_{Ed,M}=\left(M_{pl,Rd,A}+M_{pl,Rd,B}\right)/L$. The shear forces should be checked for all seismic combinations according to the requirements of Table 1-4. In case $V_{Ed}/V_{pl,Rd}\leq 0.5$, no reduction of the plastic moment resistance is needed due to the existence of shear force.

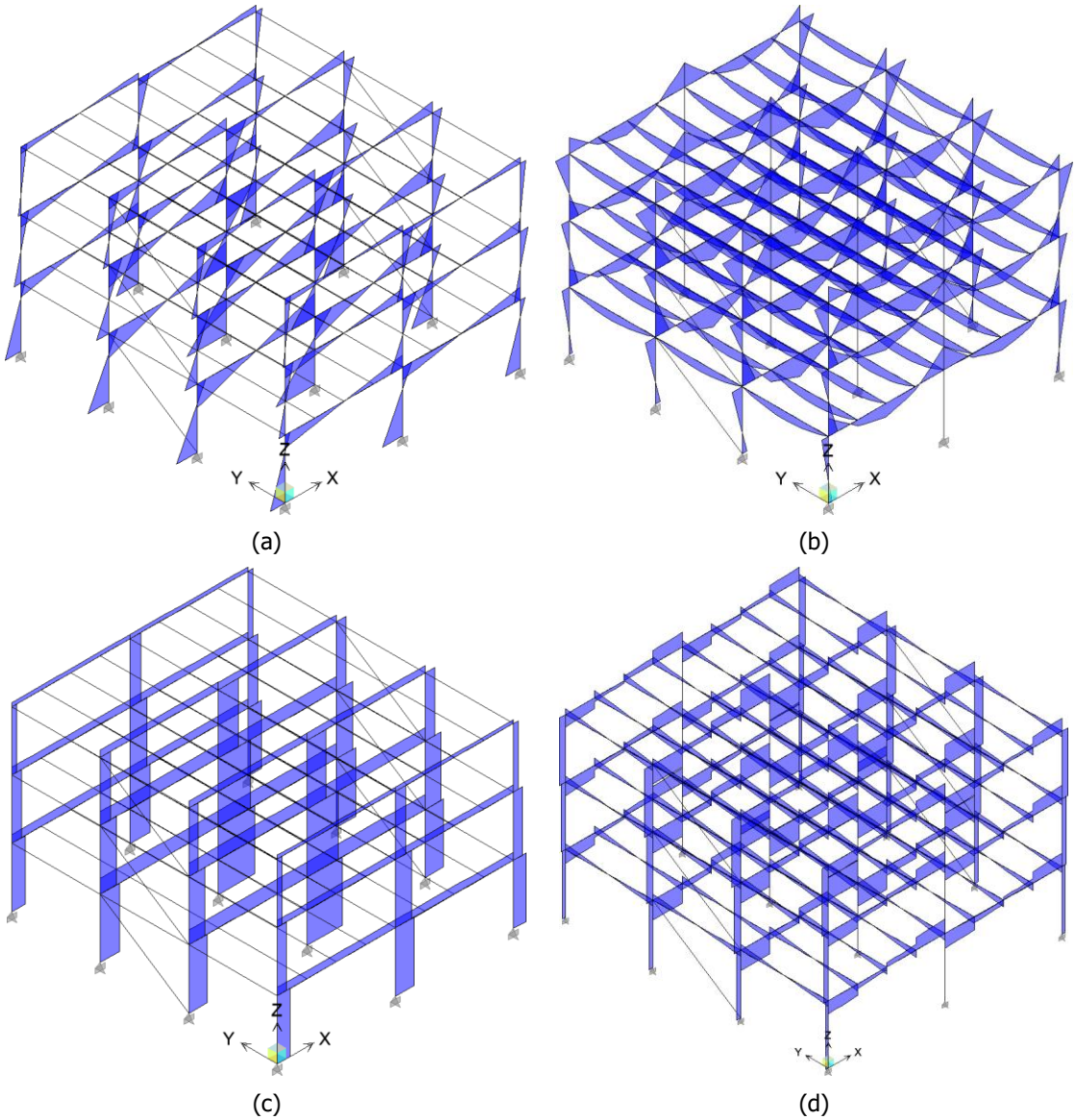

Figure 2-12: (a) Bending moment diagram in seismic combination SEISM1 (b) bending moment diagram for the gravity loads in the seismic design situation (G+0.3Q) (c) shear force diagram only for the seismic loads (E) in combination SEISM1 (d) shear force diagram for the gravity loads (G+0.3Q)

2.5.2.8 Capacity design condition in joints

The capacity design condition in the joints of the MRF system $\sum MR_c \geq 1.3 \sum MR_b$ does not need to be re-checked, since the damage limitation requirements increased the sections in the columns, rendering this specific check more favorable.

2.5.2.9 MRF columns check

According to the previous steps, the design of the columns is primarily dominated by the damage limitation requirements in the direction of the MRF system, whereas their preliminary design is based on the capacity design condition in the joints. However, the final sections of the columns are defined from the following table. In case the demand of these checks leads to increased sections, the rigidity and, therefore, the seismic loads are also increased and the checks in the MRF beams, as well as the value of Ω should be estimated from the beginning. The following tables include the maximum values of internal forces in the base of the MRF columns illustrated in Figure 2-13(a) and (b) for the non-seismic as well as the seismic combinations respectively. According to EN 1998-1: 2004 ,§6.6.3 the design forces should be obtained using the following combination:

$$E_d = E_{d,G+0.3Q} + 1.1\gamma_{ov}\Omega E_{d,E} \quad (2\text{-}48)$$

where the material overstrength factor is $\gamma_{ov}=1.25$, whereas the multiplicative factor is $\Omega_X=1.564$.

The column design combination is $E_d = E_{d,G+0.3Q} + 1.1 \cdot 1.25 \cdot 1.564 \cdot E_{d,E} = E_{d,G+0.3Q} + 2.15E_{d,E}$. The checks should be performed according to the following expressions:

$$\frac{N_{Ed}}{\chi_y N_{Rk}} + k_{yy}\frac{M_{y,Ed}}{\chi_{LT} M_{y,Rk}} \leq 1 \quad (2\text{-}49)$$

$$\frac{N_{Ed}}{\chi_z N_{Rk}} + k_{zy}\frac{M_{y,Ed}}{\chi_{LT} M_{y,Rk}} \leq 1 \quad (2\text{-}50)$$

Table 2-17: Internal forces in the MRF columns in the non-seismic combinations

Combinations	**$N_{Ed}=N_{Ed,G}$ (kN)**	**V_{Ed} (kN)**	**M_{Ed} (kNm)**
ULS	533.04	27.74	75.97
SLS	383.30	19.87	54.41

Table 2-18: Internal forces in the MRF columns in the seismic combinations

Combinations	**$N_{Ed}=N_{Ed,G}+1.1\gamma_{ov}\Omega N_{Ed,E}$**	**$V_{Ed}=V_{Ed,G}+1.1\gamma_{ov}\Omega V_{Ed,E}$**	**$M_{Ed}=M_{Ed,G}+1.1\gamma_{ov}\Omega M_{Ed,E}$**
SEISM1	250.44	29.51	116.11
SEISM2	234.03	41.64	152.88
SEISM3	243.03	35.91	134.30
SEISM4	226.62	48.04	171.07
SEISM5	368.16	58.55	149.36
SEISM6	351.74	46.42	112.59
SEISM7	359.15	52.82	130.78
SEISM8	359.15	52.82	130.78
SEISM9	288.74	1.20	30.33
SEISM10	286.51	3.12	35.79
SEISM11	234.03	41.64	152.88
SEISM12	231.81	43.56	158.33
SEISM13	324.05	25.22	49.31

Combinations	$N_{Ed}=N_{Ed,G}+1.1\gamma_{ov}\Omega N_{Ed,E}$	$V_{Ed}=V_{Ed,G}+1.1\gamma_{ov}\Omega V_{Ed,E}$	$M_{Ed}=M_{Ed,G}+1.1\gamma_{ov}\Omega M_{Ed,E}$
SEISM14	326.27	27.14	54.76
SEISM15	269.34	15.22	73.24
SEISM16	271.57	13.30	67.78

Due to the existence of the CBF system, neither shear force nor bending moment are developed in the columns. According to equations (2-49) and (2-50), all existing columns can adequately resist the internal forces.

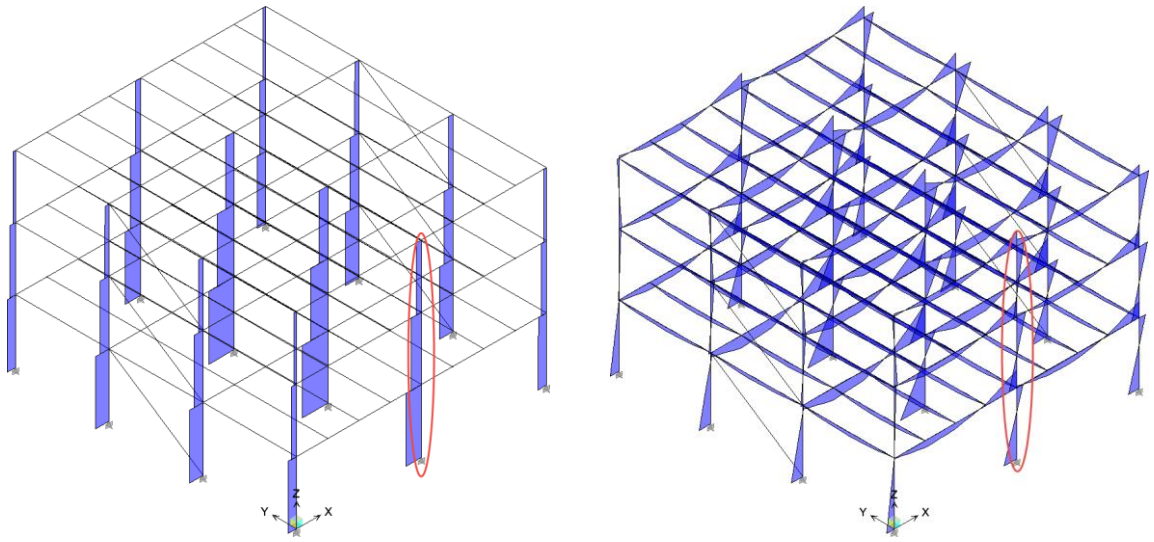

(a) (b)

Figure 2-13: (a) Axial force diagram in Ultimate Limit State (b) bending moment diagram in combination SEISM1

In addition, the columns in the edges of the building develop a small axial force due to the 30% of seismic force in the X direction. In Figure 2-13(b) the vertical loads are ignored in order to acquire a better understanding of the truss function of the CBF system and, in particular, the role of the bracing's vertical component to the axial force of the CBF columns.

2.5.2.10 Bracings check

After the extensive check of the columns in the direction of the MRF system, the check in the crosswise direction of the CBF system follows. However, the columns should be capacity designed in this direction as well and, therefore, the multiplicative factor Ω in Y direction is obtained. It should be pointed out that the axial forces in the bracings should be calculated from scratch, since the sections of the columns are increased due to the damage limitation requirements and, consequently, the seismic loads are relatively higher compared to the pre-design phase.

Table 2-19: New design forces for the bracings after the final design of the columns

Storey	Section	SEISM1	SEISM2	SEISM3	SEISM4	SEISM5	SEISM6	SEISM7	SEISM8
1	RHS100X60X5	105.49	118.41	117.14	104.22	118.41	105.49	117.14	116.32
2	RHS100X60X4	87.64	99.71	99.41	87.34	99.71	87.64	99.41	97.50
3	SHS70X3	46.68	59.03	59.00	52.67	59.03	52.71	59.00	57.64

Storey	Section	SEISM9	SEISM10	SEISM11	SEISM12	SEISM13	SEISM14	SEISM15	SEISM16
1	RHS100X60X5	322.73	334.26	334.64	323.11	334.64	323.11	322.73	334.26
2	RHS100X60X4	266.13	276.90	276.99	266.22	276.99	266.22	266.13	276.90
3	SHS70X3	161.55	167.90	167.20	161.56	167.20	161.56	161.55	167.20

Table 2-20: Axial capacity and radius of gyration requirements for the bracings

Storey	$i_{z,min}$ (cm)	$i_{z,max}$ (cm)	$N_{Ed,i}$ (kN)	$A_{req,i}$ (cm^2)	$A_{exist,i}$ (cm^2)	$\Omega_i = N_{pl,Rd,i}/N_{Ed,i}$
1	2.37	3.65	334.64	9.42	12	1.56 ✓
2	2.37	3.65	276.99	7.80	10.4	1.54 ✓
3	2.37	3.65	167.20	4.71	7.94	1.69 ✓

2.5.2.11 CBF columns check

Since the minimum value of Ω in the direction of the CBF system is calculated, the capacity design checks for the CBF columns can now be carried out. According to §1.3.2.1, the columns directly connected to the bracings should be capacity designed using the following equation:

$$N_{b,Rd}(M_{Ed}) \geq N_{Ed,G} + 1.1\gamma_{ov}\Omega N_{Ed,E} \quad (2\text{-}51)$$

where the material overstrength factor is $\gamma_{ov}=1.25$, whereas the multiplicative factor is $\Omega_X=1.54$.

The column design combination is $N_{b,Rd}=N_{Ed,G}+1.1\gamma_{ov}\Omega N_{Ed,E}=N_{Ed,G}+2.12N_{Ed,E}$. The checks should be performed according to equations (2-49) and (2-50), when the values of axial force are increased due to capacity design, but the bending moment about the major principal axis remains the same.

Table 2-21, §1.3.2.1: Summary table of capacity design requirements and checks according to EN1998-1

Capacity design requirements	Checks	Eurocode 8 reference
Cross-section classification	No requirement	-
$M_{Ed}=M_{Ed,G}+M_{Ed,E}$	Section and member checks in bending and compression according to EC3	EN 1993-1-1, §6.3.3(4), Equation 6.61
$V_{Ed}=V_{Ed,G}+V_{Ed,E}$		EN 1993-1-1, §6.2.6(1), Equation 6.17
$N_{Ed}=N_{Ed,G}+1.1\gamma_{ov}\Omega N_{Ed,E}$		EN 1993-1-1, §6.3.3(4), Equation 6.62

The following tables include the maximum values of internal forces in the base of the CBF columns illustrated in Figure 2-14(a) and (b) for the non-seismic as well as the seismic combinations respectively. The bending moment in the seismic combinations is owed to the 30% seismic force in the X direction as well as the vertical loads in the seismic design situation. The existing CBF columns can adequately resist the capacity designed forces for all seismic and non-seismic combinations.

Table 2-22: Internal forces in the CBF columns in the non-seismic combinations

Combinations	$N_{Ed}=N_{Ed,G}$ (kN)	V_{Ed} (kN)	M_{Ed} (kNm)
ULS	912.74	43.22	118.79
SLS	653.36	30.77	84.59

Table 2-23: Internal forces in the CBF columns in the seismic combinations

Combinations	$N_{Ed}=N_{Ed,G}+N_{Ed,E}$	$N_{Ed}=N_{Ed,G}+1.1\gamma_{ov}\Omega N_{Ed,E}$	V_{Ed}	M_{Ed}
SEISM1	591.90	680.89	9.61	548.80
SEISM2	474.01	434.80	19.59	795.90
SEISM3	542.47	577.71	8.16	514.85
SEISM4	424.59	331.63	18.13	761.95
SEISM5	647.36	796.68	55.87	1066.98
SEISM6	529.48	550.59	45.89	819.89
SEISM7	578.91	653.77	44.43	785.94
SEISM8	578.91	653.77	44.43	785.94
SEISM9	866.96	1255.08	13.67	27.76
SEISM10	852.13	1224.13	14.11	37.94
SEISM11	474.01	434.80	19.59	795.90
SEISM12	459.18	1224.13	19.15	785.72
SEISM13	883.60	434.80	33.31	512.49
SEISM14	898.43	403.85	32.88	502.31
SEISM15	490.65	1289.82	0.05	313.08
SEISM16	505.48	1320.77	0.38	321.35

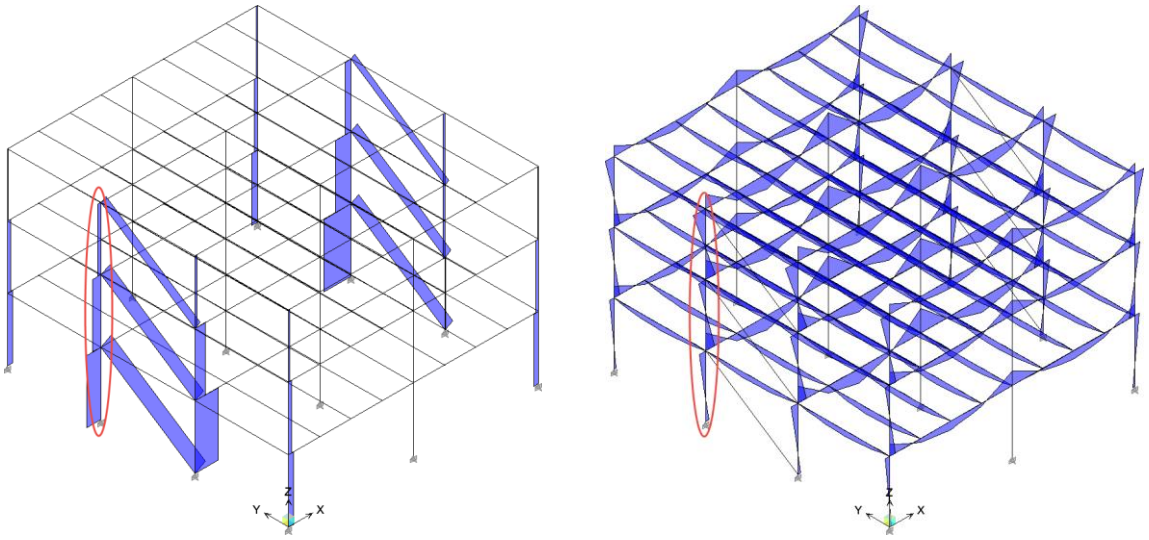

(a) (b)

Figure 2-14: (a) Axial force diagram increased due to capacity design in combination SEISM1 (b) bending moment diagram due to 30% seismic force in X direction

2.5.2.12 Final P-Δ effects check

After the final design of the columns and the beams, the developed P-Δ effects should be checked form the beginning in order to determine whether or not to increase the internal forces. Assuming that the columns were designed so as to fulfill the limitation of θ<0.2 in both directions, there is no possibility

for this condition not to be met. Since the sections of the columns were slightly increased in order to satisfy the interstorey drifts check, the values of the P-Δ effects are the following:

Table 2-24: Calculation of the final P-Δ effects

Storey	P_{tot} (kN)	h (m)	$V_{tot,X}$ (kN)	$V_{tot,Y}$ (kN)	dX (m)	dY (m)	θ_X	X Check	θ_Y	Y Check
1	2112.37	4	200.50	252.77	0.0418	0.0394	0.110	✓	0.082	✓
2	4225.21	4	335.76	423.29	0.0599	0.0426	0.188	✓	0.106	✓
3	6338.37	4	403.40	508.57	0.0439	0.0406	0.173	✓	0.126	✓

According to Table 2-24, the internal seismic forces should be increased by a factor of 1/(1-θ)=1.23. Therefore, all structural members such as MRF beams, bracings, MRF and CBF columns should be rechecked from the beginning for the increased internal forces, which, in this case, all members can adequately resist.

Another important part of the methodology lies on counters i and j that do not play an apparent role in the modelling procedure. In particular, quantity j is defined in order to stipulate that once the P-Δ effects are taken into account and the internal forces are increased by the factor 1/(1-θ), no further increase should be taken into account, thus stopping a meaningless iterative procedure (j=1). However, the only exception is made in case the section of the columns is increased either due to the capacity design condition in the joints or during the MRF and CBF checks (i=i+1). For this reason, quantity i is introduced in order to take into account the increased rigidity and, thus, seismic loads which ultimately obliges the designer to check from the beginning the capacity of all structural members. It should be clearly stated that in case the sections of the columns are increased, the P-Δ effects should be calculated again in parallel with the incremental factor 1/(1-θ). In addition, due to the increased values of internal forces, the value of Ω is reduced, rendering the capacity design checks for the members more favorable.

2.5.2.13 CBF beam directly connected to rigid diaphragm

The CBF beams are structural members that do not contribute in any way in the lateral rigidity of the structure and, therefore, they are modelled at the end of the design procedure. In the case where the CBF beam is directly connected to the rigid diaphragm, the main check that should be performed lies on the most unfavourable case for the bending moment, which is the Ultimate Limit State (ULS) according to Table 1-7. In this case, the CBF beam is assumed to operate as a secondary beam with no requirement for dissipative behavior similar to the secondary beams located in the perimeter

2.5.2.14 CBF beam not connected to rigid diaphragm

In this case, no lateral resistance is provided by the diaphragm and the CBF beam operates as a single beam under significant compression due to seismic loading. The most significant check that should be performed corresponds to the axial resistance of the CBF beam against the most unfavourable axial force. The axial force is developed in conjunction with an insignificant value of bending moment due to the dead load of the beam, which can be neglected. Any interaction between the axial force and the bending moment due to the extremely small value of the latter can also be ignored. The following table, also presented in §1.3.2.3, summarizes the design requirements for CBF beams.

Table 2-25, §1.3.2.3: Summary table of capacity design requirements and checks for beams not connected to rigid diaphragm

Capacity design requirements	**Checks**	**Eurocode 8 reference**
Cross-section classification	No requirement	-
$M_{Ed,G}$ (from dead load)	Section and member checks in bending and compression according to EC3	In case interaction is considered: EN 1993-1-1, §6.3.2.1(1), Equation 6.61 EN 1993-1-1, §6.3.2.1(1), Equation 6.62
$N_{Ed}=N_{Ed,G}+1.1\gamma_{ov}\Omega N_{Ed,E}\neq 0$ (acquired from the most unfavourable seismic combination)	$N_{Ed}/N_{b,Rd} \leq 1$	EN 1993-1-1, §6.3.1.1(1), Equation 6.46
Uniform distribution of ductility in height	-	-

Taking into account that the axial force decreases in height, the sections of the CBF beams are reduced as well. Unlike the bracings, no requirement for uniform distribution of ductility in height is recommended by Eurocode 8 for the CBF beams, despite the fact that they should be capacity designed as well. The axial force demands are estimated for each seismic combination and storey in the following table by calculating manually the horizontal component of the tension bracing's axial force (component Ncosφ) due to the untrustworthy results received by the software in case the rigid diaphragm function is disabled. It should be clarified that the CBF beams that are not connected to the diaphragm are only activated due to seismic loading ($N_{Ed,G}=0$).

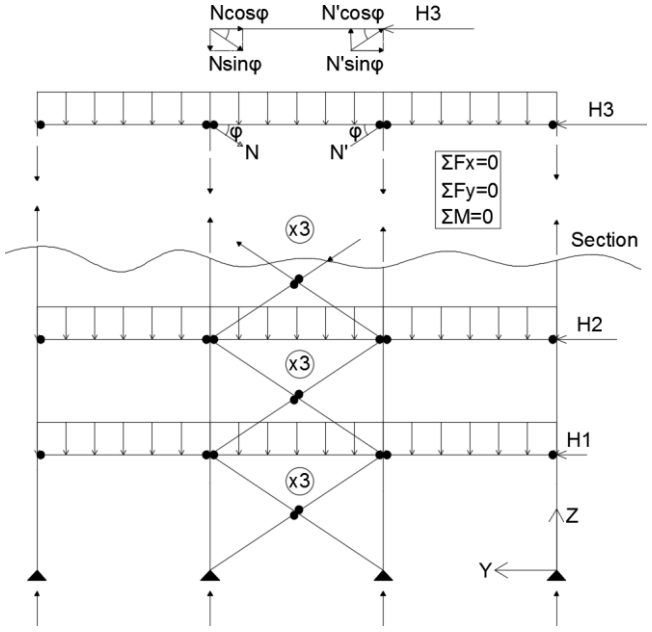

Figure 2-15: Representation of the truss action in the CBF system

An alternative approach is to create a 2-dimensional model that would include half the horizontal loads due to symmetry, the uniformly distributed loads due to masonry as well as the vertical reactions from the MRF and the secondary beams, since they affect indirectly the value of the vertical component of the bracing according to the condition $\sum M=0$. A static analysis in this simplified model, using for example the software BEAM2D, would return the requested axial force for each CBF beam in height, although

the static analysis should be repeated for every seismic combination.

The effective buckling length of the CBF beam is 6m, considering that they are pinned on both ends. Since it is a member under compression, the axial capacity of the section is reduced by a factor of χ due to global buckling. It should be mentioned that there is no requirement for the classification of the beam's cross-section. The reductive factor χ is assumed as 0.7 and will be checked after the selection of the cross-section. The following table includes the axial force before and after the capacity requirement only for the CBF beam of the 1st storey.

Table 2-26: Axial force in the CBF beam of the first storey in the seismic combinations

Combinations	**N (tension bracing)**	$\mathbf{N_{Ed}=1.1\gamma_{ov}\Omega N_{Ed,E}\cos\varphi}$
SEISM1	105.49	185.86
SEISM2	118.41	208.62
SEISM3	117.14	206.39
SEISM4	104.22	183.62
SEISM5	118.41	208.62
SEISM6	105.49	185.86
SEISM7	117.14	206.39
SEISM8	116.32	204.94
SEISM9	322.73	568.61
SEISM10	334.26	588.92
SEISM11	334.64	589.59
SEISM12	323.11	569.28
SEISM13	334.64	589.59
SEISM14	323.11	569.28
SEISM15	322.73	568.61
SEISM16	334.26	588.92

The buckling resistance of each CBF beam is estimated according to the regulatories of Eurocode 3 for members under compression. In particular, the sections are assumed to be either Class 1 or 2, which is checked after the final selection of the cross-section in Table 2-28.

Table 2-27: Design internal forces and characteristics of final CBF beams

Storey	$\mathbf{\chi_0}$	$\mathbf{N_{Ed,i}}$ **(kN)**	$\mathbf{A_{req,i}}$ **(cm^2)**	**L (cm)**	$\mathbf{A_i}$ **(cm^2)**	$\mathbf{i_z}$ **(cm)**	$\mathbf{\bar{\lambda}_z}$	$\mathbf{\chi_{real}}$	$\mathbf{N_{b,Rd}}$ **(kN)**	$\mathbf{N_{Ed}/N_{b,Rd}}$
1	0.7	589.6	23.7	600	38.3	6.26	1.26	0.49	671	0.88 ✓
2		488.0	19.6	600	35.8	5.85	1.35	0.44	564	0.86 ✓
3		295.8	11.9	600	26.7	5.50	1.43	0.40	381	0.78 ✓

Table 2-28: Final selection of CBF beams and classification under compression

Storey	Cross-section	Class (compression)
1	SHS160X6.3	1 ✓
2	SHS150X6.3	1 ✓
3	SHS140X5	2 ✓

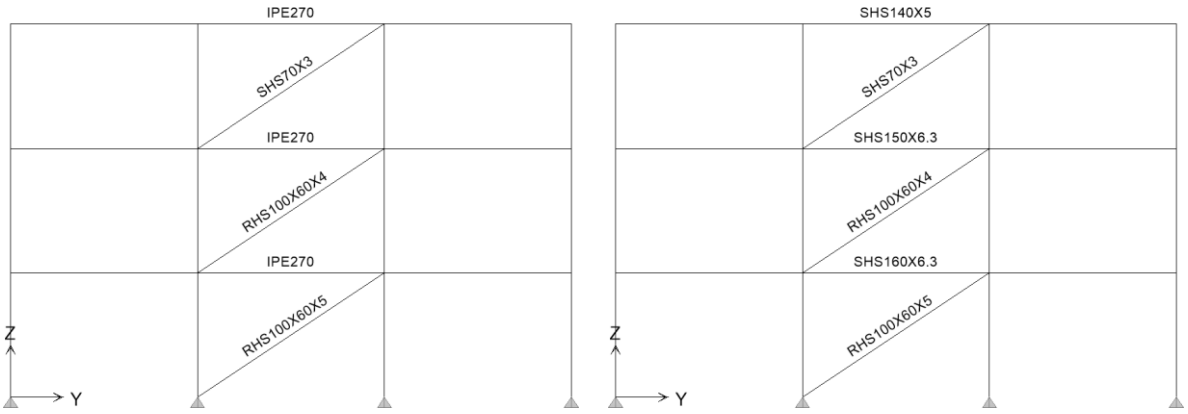

(a) (b)

Figure 2-16: Comparison of the CBF beam modelling when the beam is (a) directly connected to diaphragm (b) not connected to diaphragm

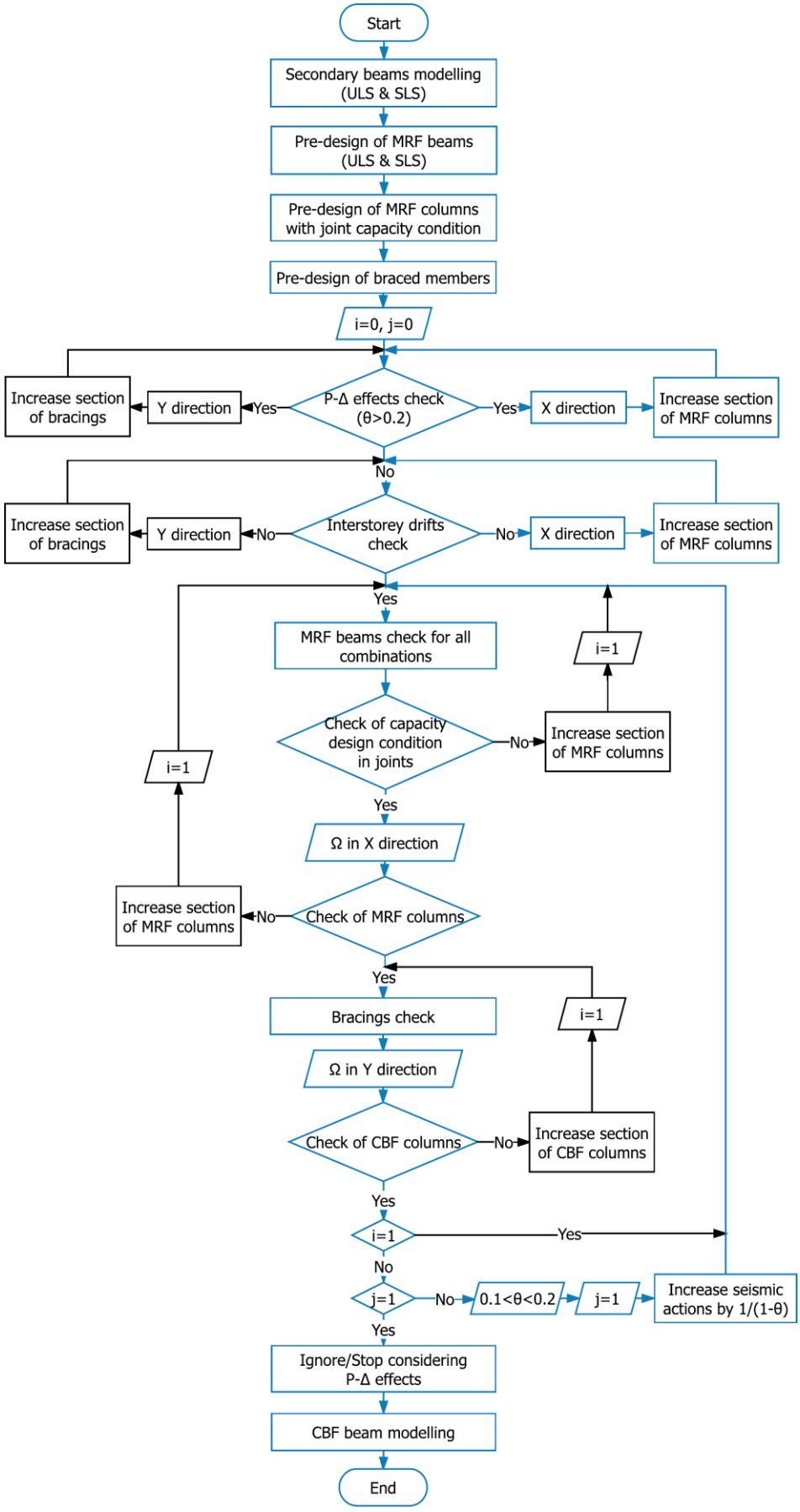

Figure 2-17: Procedure followed for the design of the building in Scenario 1 according to the design method

2.5.2.15 Modal analysis

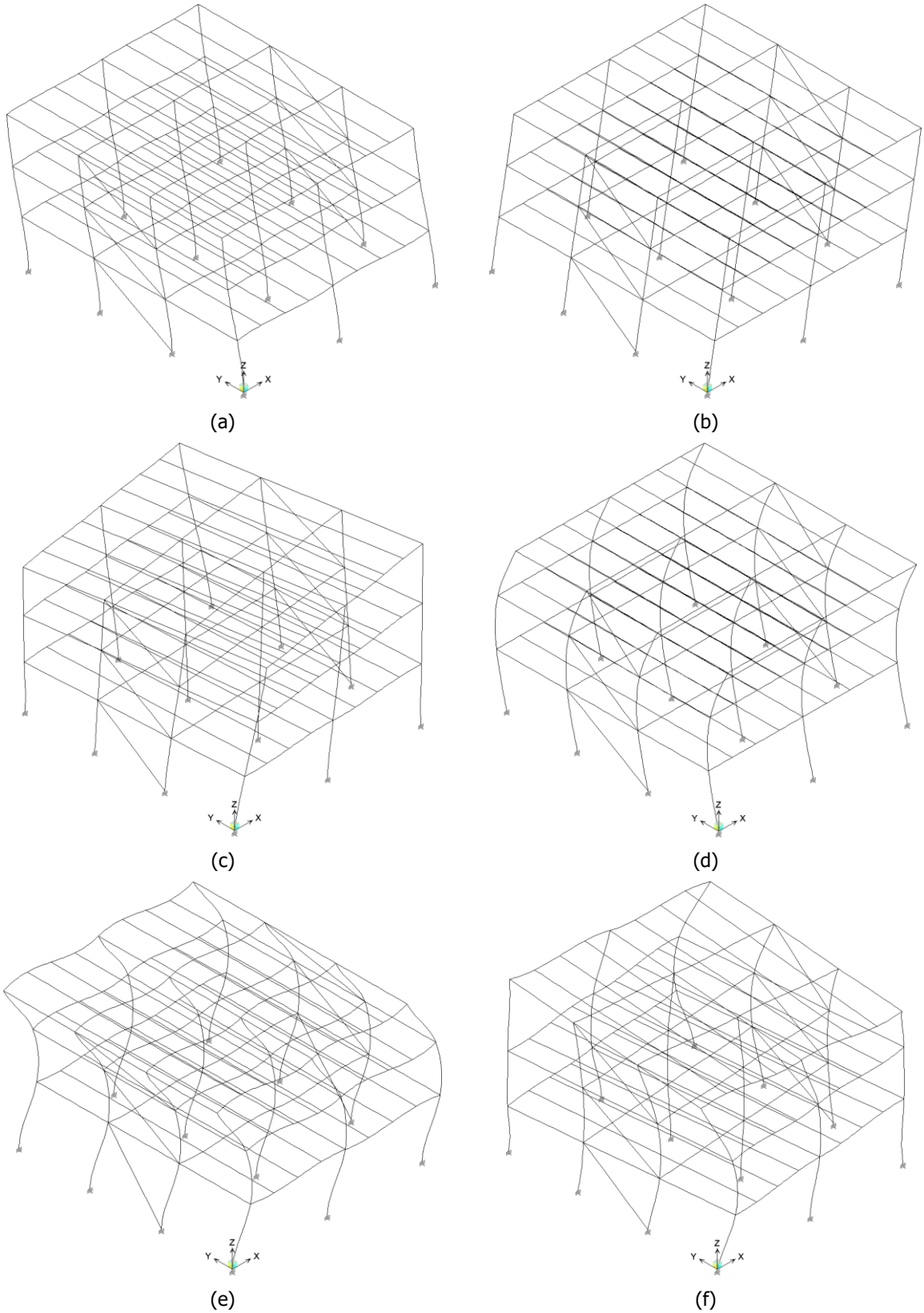

Figure 2-18: Modes of vibration (a) X direction $T_{1,X}$=1.12 sec (b) Y direction $T_{2,Y}$=0.95 sec (c) around Z axis $T_{3,Z}$=0.80 sec (d) T_4=0.357 sec (e) T_5=0.356 sec (f) T_6=0.28 sec

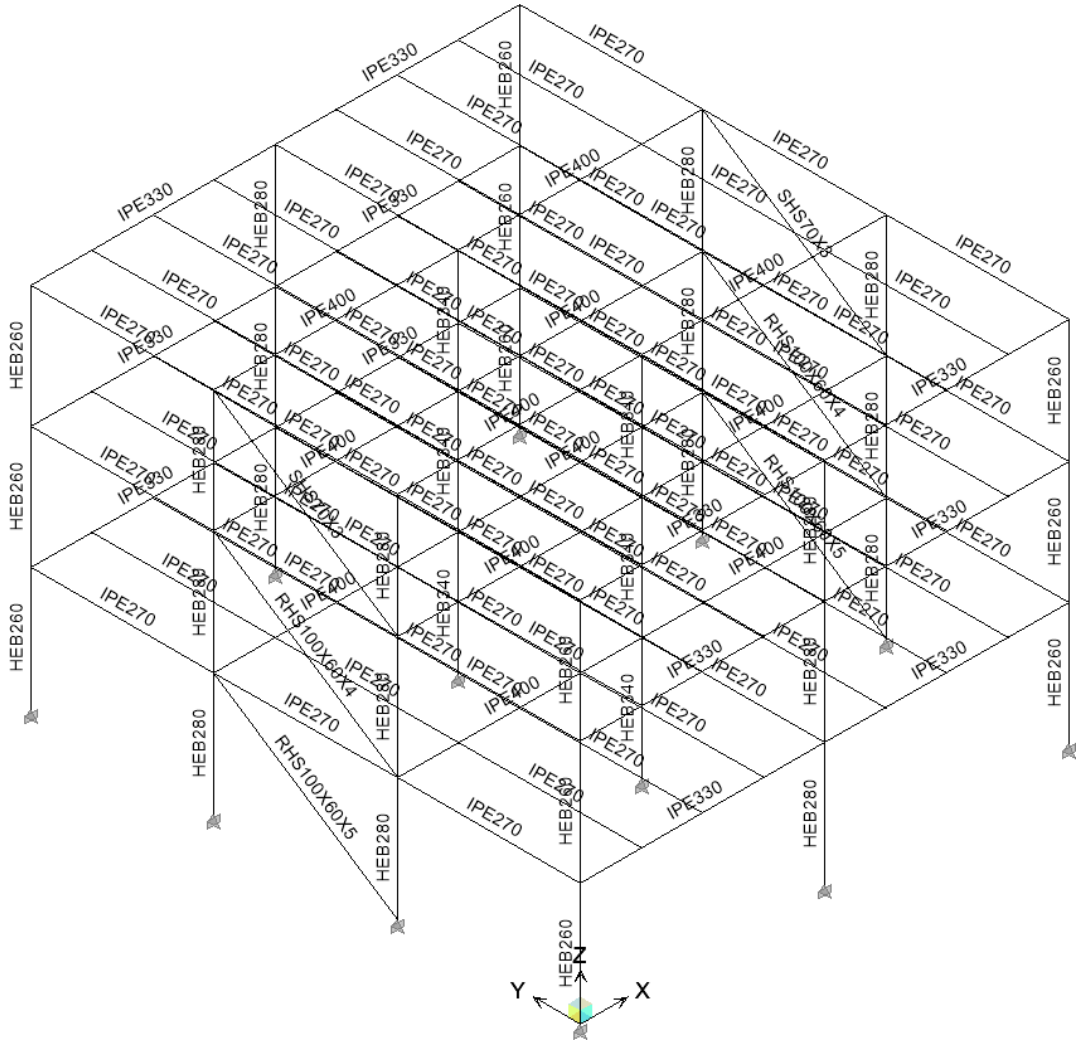

Figure 2-19: Final design of the building under investigation in Scenario 1

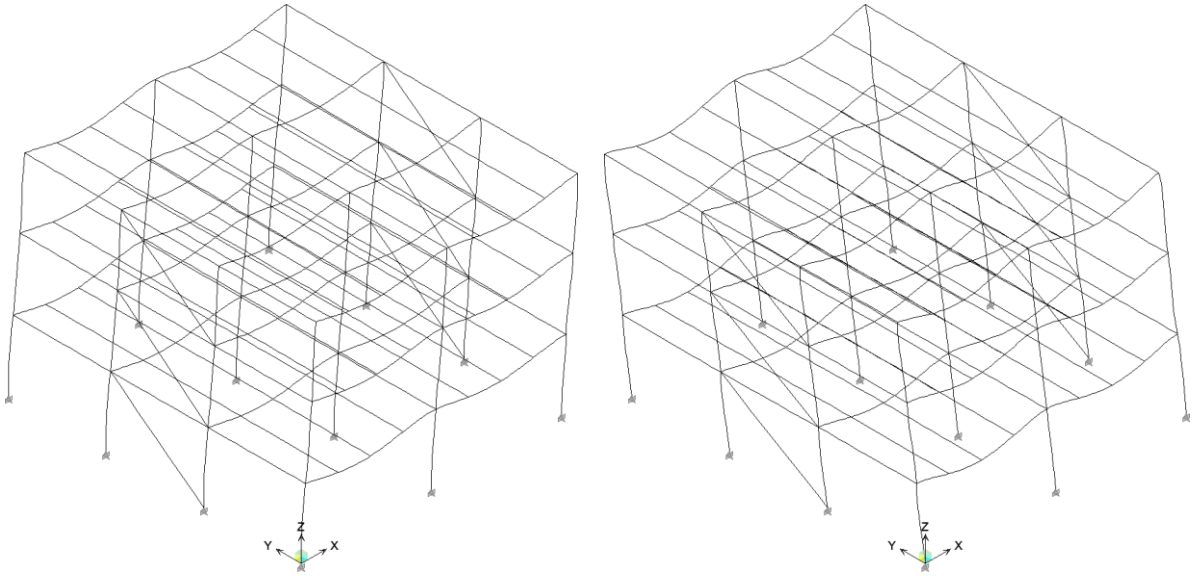

(a) (b)

Figure 2-20: Deformed shape of the structure under vertical seismic loads and (a) X earthquake (b) Y earthquake with no eccentricity

2.6 DESIGN IGNORING COMPRESSED BRACING – ELASTIC ANALYSIS WITH BOTH BRACINGS: SCENARIO 2

When taking into account the tension bracing only, the rigidity of the structure, thus the period of vibration which defines the seismic loads, is almost $\sqrt{2}$ times higher than if both braced members contributed in the total rigidity of the structure. This is demonstrated in expression (2-52), where the effect of the different rigidity in the period of vibration in Scenarios 1 and 2 is presented, assuming that the total mass of the structure remains almost constant, despite the introduction of the second braced member. Different fundamental periods of vibration account for different spectral accelerations and, therefore, seismic actions, although the structural configuration changes the distribution of internal forces along the members of the structure.

$$T_1=2\pi\sqrt{\frac{m}{k_1}} \;\&\; T_2=2\pi\sqrt{\frac{m}{k_2}} \;\text{ where } k_2=2k_1 \rightarrow T_2=\sqrt{2}T_1 \tag{2-52}$$

This scenario is simply an extension of Scenario 1, as the sections selected in the first scenario are maintained, while both braced members, which are designed ignoring the compressed one, are included in the elastic analysis. Attention should be paid in the developed axial force in the direction of the CBF system as well as the bending moments in the MRF, since they define the predominant type of failure in each direction. The following figure depicts the comparison between the introduction of 1 and 2 bracings in the structural configuration in terms of axial forces, along with a typical distribution of seismic loads in the case where no eccentricity is taken into account. Therefore, according to Figure 2-21 (c) and (d), lower axial forces are developed in the CBF columns due to the vertical component of the bracing in Scenario 2, which is a more favorable situation compared to the respective forces in Scenario 1. However, the developed axial forces in the tension bracings are increased, although they are not checked for axial capacity since this scenario is created only for the comparison of internal forces. It is definitely not considered a realistic situation, since it would consist an uneconomic designing solution. Obviously, the introduction of both bracings eliminates further the displacements across the CBF system.

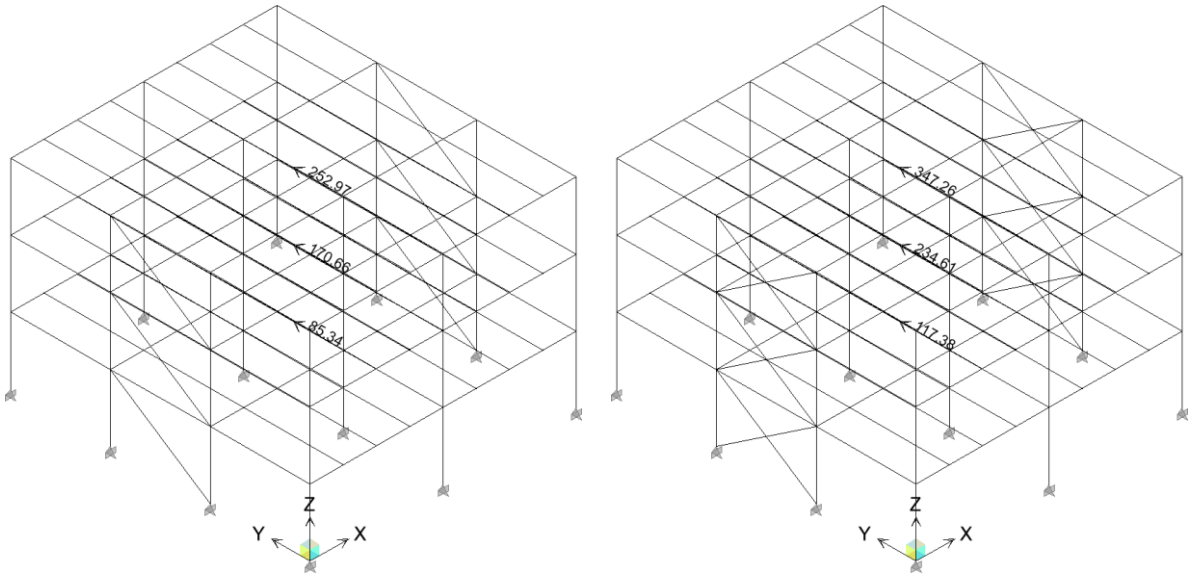

(a) (b)

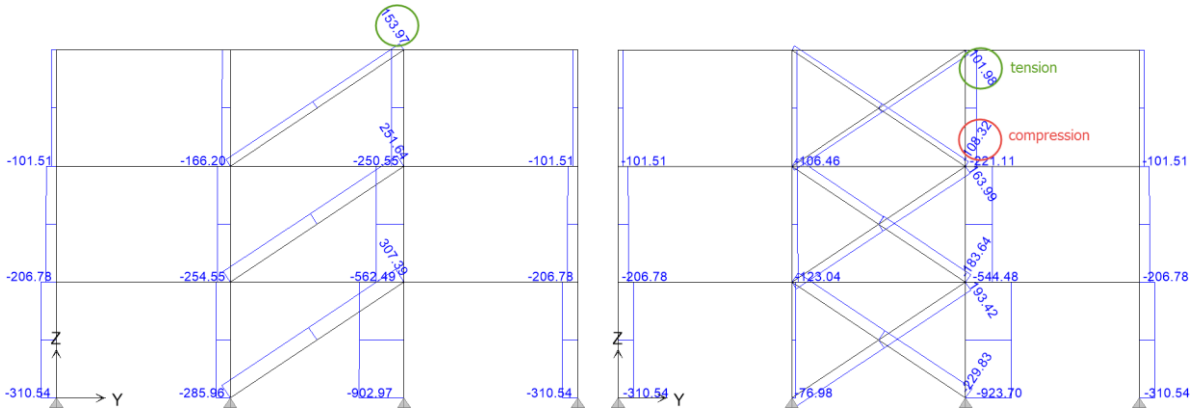

(c) (d)

Figure 2-21: Comparative figures in terms of (a) imposed seismic loads in Scenario 1 (b) imposed seismic loads in Scenario 2 (c) axial forces in the CBF system for Scenario 1, only tension bracing (d) axial forces in the CBF system for Scenario 2, both bracings

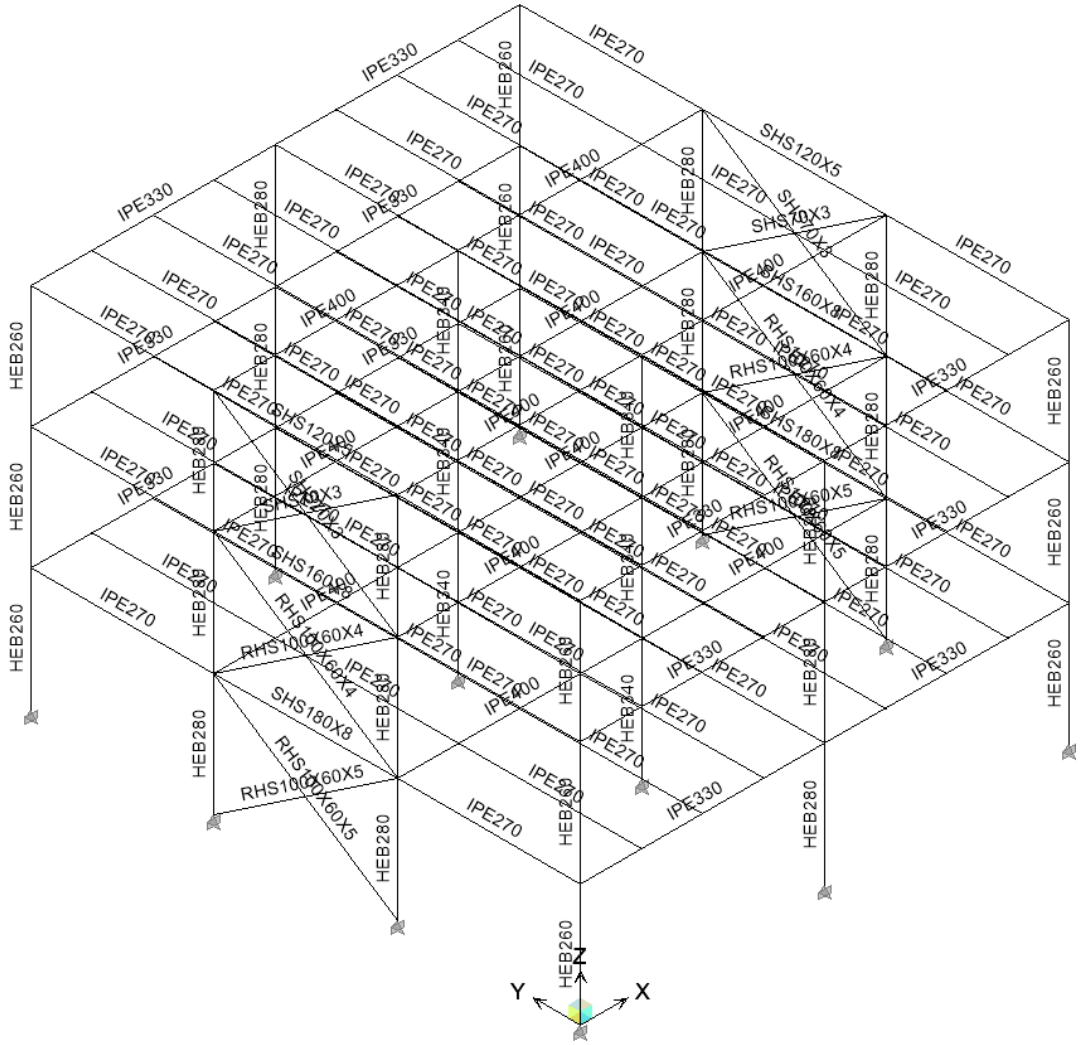

Figure 2-22: Building under investigation in Scenario 2, both bracings for the elastic analysis

2.7 DESIGN CONSIDERING COMPRESSED BRACING: SCENARIO 3

2.7.1 General

The scenario approaches the modelling of the structure by considering both bracings, not only in the elastic analysis, but also during the design. The building is re-designed according to the developed methodology which was extensively analyzed in §2.5.2. This scenario is considered to be a rather realistic approach concerning the participation of the compressed bracing in the final design of the building. According to Scenario 1, the conclusion that the slenderness criterion ($1.3 \leq \bar{\lambda} \leq 2.0$) is the most unfavourable and definitive for the design of the bracings, was reached. Consequently, in order to investigate the effect of the non-dimensional slenderness limitation in the load bearing capacity of the structure using non-linear analyses, the bracings are modelled for the following indents; in the first case the aforementioned criterion is satisfied, whereas in the second it is not. Finally, it should be noted that the vertical loads retain the same value in all elastic scenarios, while the seismic loads vary due to the different rigidity. For this reason, the first steps of the methodology regarding the pre-design of the beams and the columns are identical to Scenario 1, since the value of seismic loads does not play any role during the preliminary design. The damage limitation requirements are not presented extensively, since a procedure similar to Scenario 1 is followed. For ease of reference, only the final results regarding internal forces and displacements are presented.

2.7.2 Slenderness limitation requirement satisfied

The 3 requirements regarding the preliminary design of braced members, also stated in §2.5.2.4, are the following. For the final design of the bracings the other 2 requirements regarding the classification of the cross-section as well as the uniform distribution of ductility in height are also examined.

$$i_{min} = \frac{L_{cr}}{\lambda_1 \cdot 2} = 2.37 \text{ cm} \tag{2-53}$$

$$i_{max} = \frac{L_{cr}}{\lambda_1 \cdot 1.5} = 3.65 \text{ cm} \tag{2-54}$$

$$A_{min} = N_{Ed,i} / f_y \tag{2-55}$$

Consequently, the primary selection of sections is based only on the slenderness limitation, while due to economy, the first attempt includes the same sections for all bracings.

Table 2-29: Axial capacity and radius of gyration requirements for the bracings

Storey	Section	$i_{z,min}$ (cm)	$i_{z,max}$ (cm)	$N_{Ed,i}$ (kN)	$A_{req,i}$ (cm^2)	$A_{exist,i}$ (cm^2)	$\Omega_i = N_{pl,Rd,i}/N_{Ed,i}$
1	SHS60X4	2.37	3.65	182.58	5.14	8.79	2.33
2	SHS60X4	2.37	3.65	153.90	4.34	8.79	2.40
3	SHS60X4	2.37	3.65	95.43	2.69	8.79	2.95

In this scenario where both bracings are taken into account, the slenderness limitation is extremely unfavorable in comparison to the requirement for axial resistance, as the extremely high values of Ω indicate. However, the criterion concerning the uniform distribution of ductility in height across the

bracings is not satisfied as $(\Omega_{max}-\Omega_{min})/\Omega_{min}$ =26.6% > 25%. Finally, after readjusting the selected sections in order to satisfy the aforementioned requirement, the final design of the bracings as well as the developed axial forces are summarized in the following table. At this point, it should be mentioned, that the axial forces are increased due to the P-Δ effects by a factor of 1/(1-θ)=1.24.

According to the following table, the values of the multiplicative factor Ω for the capacity design of the non-dissipative members are still increased, even during the final design of the bracings. Therefore, the conclusion assumed in the beginning, that the slenderness limitation criterion is very definitive for the bracings, is ultimately verified.

Table 2-30: Axial capacity and radius of gyration requirements for the bracings – P-Δ effects included

Storey	Section	$i_{z,min}$ (cm)	$i_{z,max}$ (cm)	$N_{Ed,i}$ (kN)	$A_{req,i}$ (cm^2)	$A_{exist,i}$ (cm^2)	$\Omega_i = N_{pl,Rd,i}/N_{Ed,i}$
1	SHS80X5	2.37	3.65	252.34	7.11	14.7	2.07
2	SHS70X4	2.37	3.65	214.56	6.04	10.4	1.72
3	SHS70X3	2.37	3.65	133.51	3.76	7.94	2.11

The criterion concerning the uniform distribution of ductility in height across the bracings is ultimately satisfied as $(\Omega_{max}-\Omega_{min})/\Omega_{min}$ =22.7% < 25%.

2.7.2.1 Damage limitation requirements

The damage limitation checks are satisfied in both directions, as Table 2-31 and Table 2-32 represent.

Table 2-31: Calculation of the interstorey drifts

Storey	dX (m)	dY (m)	$d_{r,X}$ (m)	$d_{r,Y}$ (kN)	v	h (m)	$d_{r,X}\cdot v$	$d_{r,Y}\cdot v$	α	X Check	Y Check
1	0.0424	0.0295	0.0106	0.0074	0.5	4	0.0053	0.0037	0.0075	0.71 ✓	0.49 ✓
2	0.0600	0.0337	0.0150	0.0084	0.5	4	0.0075	0.0042	0.0075	0.99 ✓	0.56 ✓
3	0.0443	0.0269	0.0111	0.0067	0.5	4	0.0055	0.0034	0.0075	0.74 ✓	0.45 ✓

Table 2-32: Calculation of the P-Δ effects

Storey	P_{tot} (kN)	h (m)	$V_{tot,X}$ (kN)	$V_{tot,Y}$ (kN)	dX (m)	dY (m)	θ_X	X Check	θ_Y	Y Check
1	2112.63	4	196.83	336.79	0.0424	0.0295	0.114	✓	0.046	✓
2	4228.59	4	329.75	564.22	0.0600	0.0337	0.192	✓	0.063	✓
3	6346.17	4	396.26	678.02	0.0443	0.0269	0.178	✓	0.063	✓

Finally, the classification of the selected bracings' cross-sections should be checked in order to ensure ductile behavior in the tension diagonals that operate as dissipative zones.

Table 2-33: Classification of the bracing's cross-sections

Storey	Section	Class (compression
1	SHS80X5	1
2	SHS70X4	1
3	SHS70X3	1

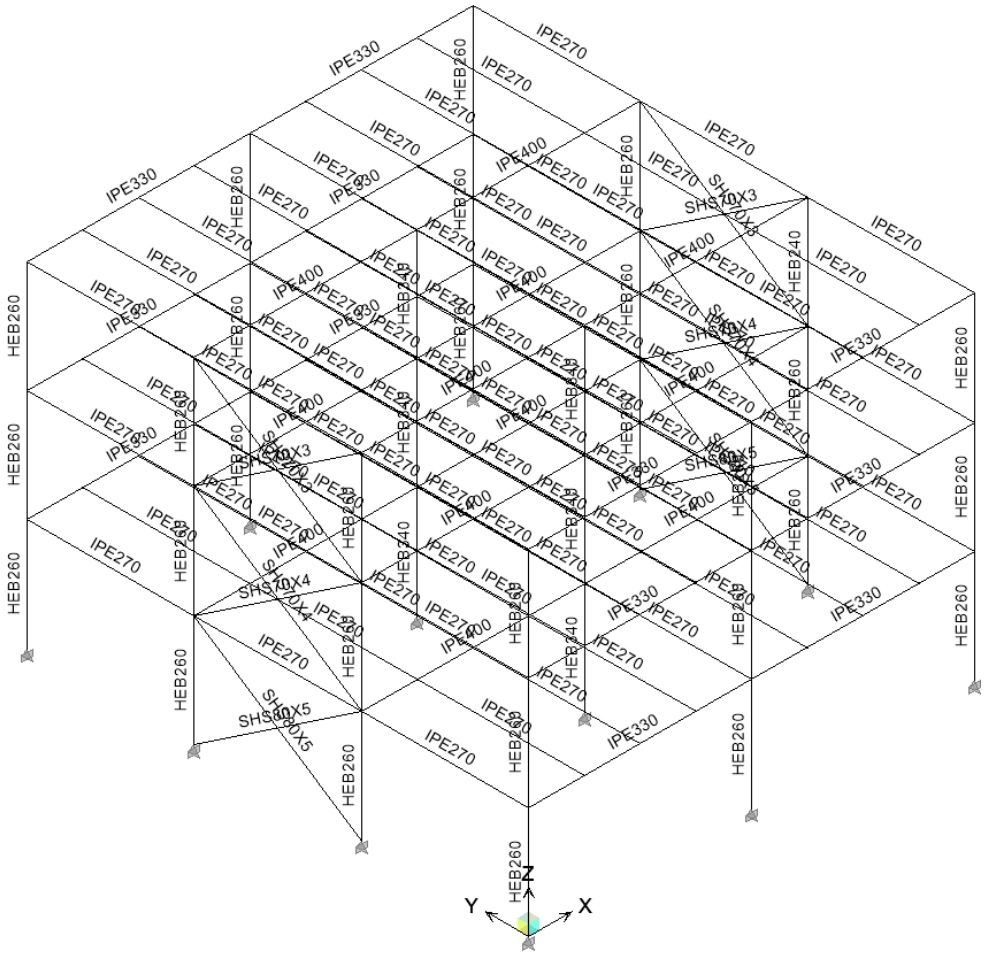

Figure 2-23: Final design of the building under investigation in Scenario 3 – slenderness limitation satisfied

2.7.3 **Slenderness limitation requirement not satisfied**

In this case, the radius of gyration requirements that reflect the limitation in the member's slenderness, is ignored and the primary section of the bracing is based entirely on the axial capacity requirement.

Table 2-34: Axial capacity requirements for the bracings

Storey	**Section**	$N_{Ed,i}$ **(kN)**	$A_{req,i}$ **(cm²)**	$A_{exist,i}$ **(cm²)**	$\Omega_i = N_{pl,Rd,i}/N_{Ed,i}$
1	SHS50X3	146.79	4.13	5.54	1.34
2	SHS50X3	125.80	3.54	5.54	1.22
3	SHS40X3	77.07	2.17	4.34	2.00

The criterion concerning the uniform distribution of ductility in height across the bracings is not satisfied as $(\Omega_{max}-\Omega_{min})/\Omega_{min} = 63.2\% < 25\%$. According to Table 2-34, the 3rd storey presents a much higher value of Ω compared to the other two storeys, which means that the smallest possible section from the SHS series is not suitable in this case and, therefore, a section with smaller area is required. The CHS series offers the required smaller section and, for the sake of uniformity, all bracings are selected from the CHS series, even though the SHS series could be maintained in the first two storeys.

Table 2-35: Calculation of the interstorey drifts

Storey	dX (m)	dY (m)	$d_{r,X}$ (m)	$d_{r,Y}$ (kN)	v	h (m)	$d_{r,X}$·v	$d_{r,Y}$·v	α	X Check	Y Check
1	0.0439	0.0442	0.0110	0.0111	0.5	4	0.0055	0.0055	0.0075	0.73 ✓	0.74 ✓
2	0.0614	0.0418	0.0153	0.0105	0.5	4	0.0077	0.0052	0.0075	0.99 ✓	0.70 ✓
3	0.0460	0.0444	0.0115	0.0111	0.5	4	0.0057	0.0056	0.0075	0.77 ✓	0.74 ✓

Table 2-36: Calculation of the P-Δ effects

Storey	P_{tot} (kN)	h (m)	$V_{tot,X}$ (kN)	$V_{tot,Y}$ (kN)	dX (m)	dY (m)	θ_X	X Check	θ_Y	Y Check
1	2112.85	4	196.94	229.82	0.0439	0.0442	0.118	✓	0.102	✓
2	4226.61	4	326.37	384.76	0.0614	0.0418	0.199	✓	0.115	✓
3	6340.42	4	392.10	462.25	0.0460	0.0444	0.186	✓	0.152	✓

Table 2-37: Axial capacity requirements for the bracings

Storey	Section	$N_{Ed,i}$ (kN)	$A_{req,i}$ (cm^2)	$A_{exist,i}$ (cm^2)	$\Omega_i = N_{pl,Rd,i}/N_{Ed,i}$
1	CHS60.3X3.2	142.34	4.01	5.74	1.43
2	CHS48.3X4	124.91	3.52	5.57	1.58
3	CHS33.7X3.2	72.12	2.03	3.07	1.51

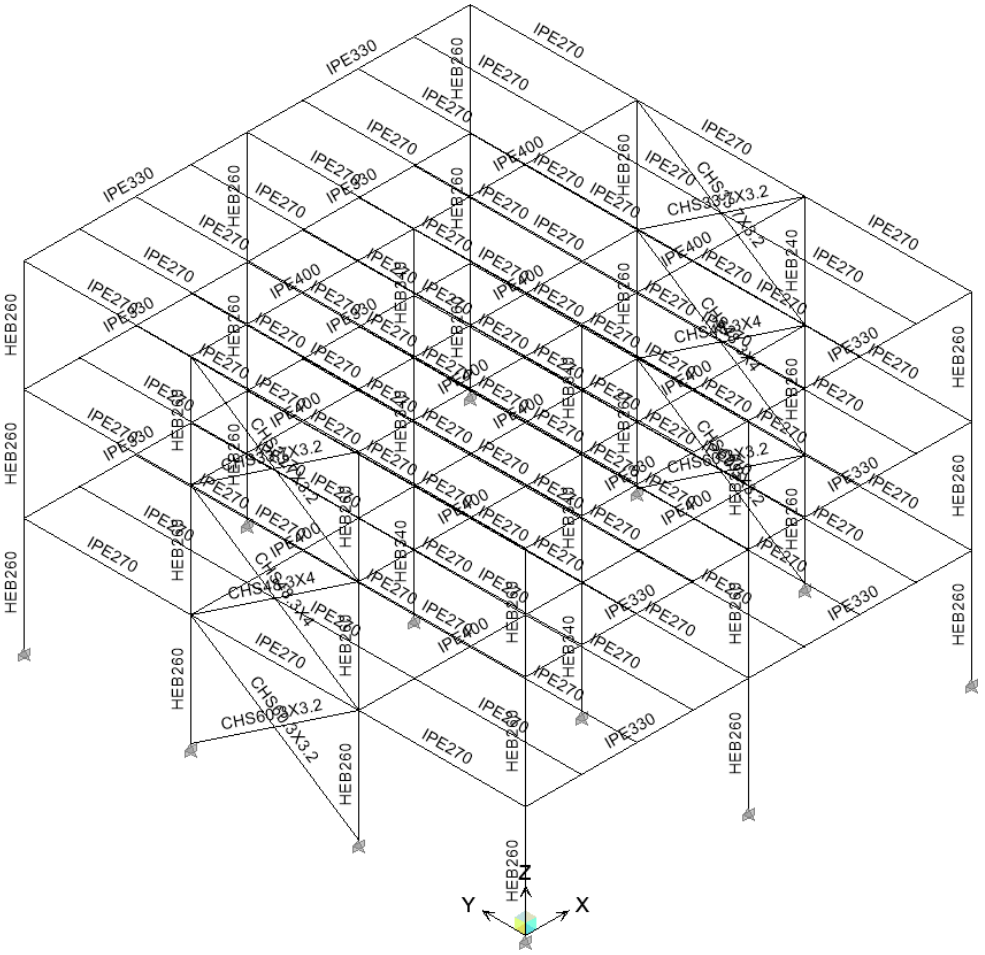

Figure 2-24: Final design of the building under investigation in Scenario 4 – slenderness limitation not satisfied

2.8 DESIGN ASSUMING HALF AREA AND TWICE TENSION AXIAL FORCE: SCENARIO 4

A different solution concerning the consideration of the compressed bracing in the modelling of the structure is to include it in the structural configuration, although the area of both bracings is assumed to be half the initial one, while twice the tension axial force is received for the design of the bracings. This assumption is made in order to approach the guideline that stipulates that only the tension diagonal should be considered in the elastic analysis. The modelling procedure according to the developed optimum methodology is followed in this scenario as well, and the final design of the three-storey building results in the same outcome as Scenario 3. All seismic actions developed in the structure are calculated with the full area of the cross-sections and, thus, axial rigidity of the bracings.

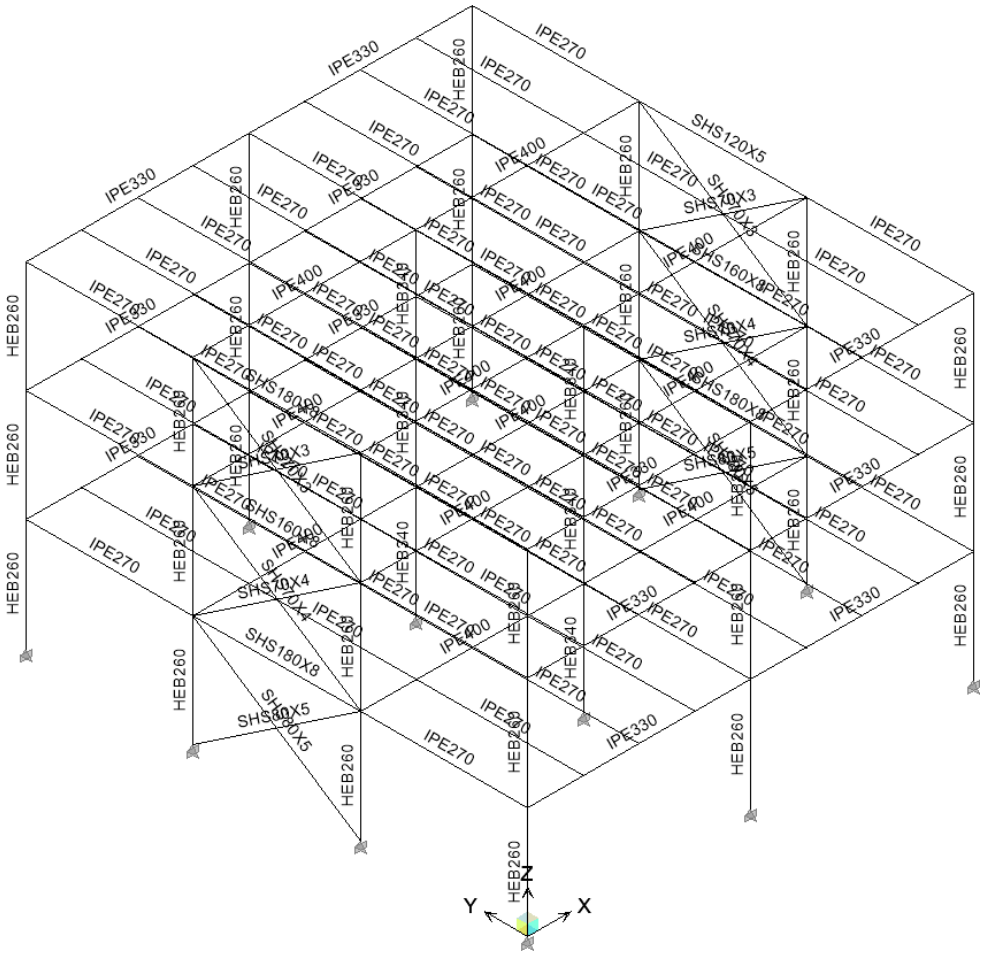

Figure 2-25: Final design of the building under investigation in Scenario 4

2.9 DESIGN IGNORING SEISMIC CODES: SCENARIO 5

In this approach, the modelling of the structure under investigation is based entirely on the capacity of the members in terms of internal forces, while the regulatories of Eurocode 8 are completely ignored. This approach aims to highlight the necessity, as well as the effect of the application of seismic codes in the load-bearing capacity of the structure. The bracings were designed only for the tension diagonal

and the case where both bracings contribute was not examined. The damage limitation checks as well as the slenderness criterion which are the most stringent and, therefore, definitive requirements for the design of the columns and the bracings respectively, are clearly not fulfilled in this Scenario. It should be stated, though, that even though the seismic codes are consciously ignored, all seismic combinations defined in Table 2-1 are taken into account. In the following paragraphs, the resistance requirements according to Eurocode 3 are summarized for each structural member and with the sequence followed for their design. Finally, no requirement for cross-section classification is mandatory to be fulfilled.

2.9.1 **Beams**

The modelling of the secondary beams is identical to §2.5.2.1, as they are not considered to be seismic members. On the other hand, the main beams or MRF beams should present adequate resistance to the most unfavourable bending moment among the Ultimate Limit State (ULS) and the defined seismic combinations. Furthermore, all main beams should comply with deformation limits in the Serviceability Limit State (SLS). Finally, they are re-checked for all seismic combinations again, after the final design of the columns.

2.9.2 **Columns**

After the pre-design of the main beams, the question whether or not the modelling of the columns or the bracings should precede is made. Since a 30% of the crosswise direction is considered in the direction under investigation, it is not definitive whether the bracings or the columns are modelled first in order.

The columns should be able to resist adequately the most unfavourable combination of axial force and bending moment about the major principal axis only according to the following expressions, stipulated in §6.3.3(4), Eq. (6.61) and (6.62).

$$\frac{N_{Ed}}{\chi_y N_{Rk}} + k_{yy}\frac{M_{y,Ed}}{\chi_{LT} M_{y,Rk}} \leq 1 \tag{2-56}$$

$$\frac{N_{Ed}}{\chi_z N_{Rk}} + k_{zy}\frac{M_{y,Ed}}{\chi_{LT} M_{y,Rk}} \leq 1 \tag{2-57}$$

where N_{Ed} and $M_{y,Ed}$ are not increased due to capacity design, while $M_{z,Ed}=0$.

In addition, for doubly symmetrical I-sections or other flanges sections, allowance need not be made for the effect of the axial force on the plastic resistance moment about the y-y axis, when both the following criteria, stipulated in §6.2.9.1(4), Eq. (6.33) and (6.34) are satisfied.

$$N_{Ed} \leq 0.25 N_{pl,Rd} \tag{2-58}$$

In case interaction between the axial force and the bending moment should be considered, the plastic resistance moment is decreased according to the following expression:

$$M_{N,y,Rd} = M_{pl,y,Rd}\,(1-n)/(1-0.5a) \tag{2-59}$$

where $n = N_{Ed}/N_{pl,Rd}$ and $a = (A-2bt_f)/A \leq 0.5$

Finally, the columns should present adequate shear resistance in the X principal direction, as:

$$V_{Ed}/V_{pl,Rd} \leq 1 \quad (2\text{-}60)$$

2.9.3 **Bracings**

The bracings are designed for the maximum developed tension axial force according to all seismic combinations. It is important to mention that for the modelling of the bracings only the tension diagonal was considered in the structural system. However, in the non-linear analyses investigated in §3.7, both bracings are considered. After the final design of the bracings and the columns, an attempt to decrease their sections is made. However, the initially selected sections were the minimum required ones and are presented in the following table.

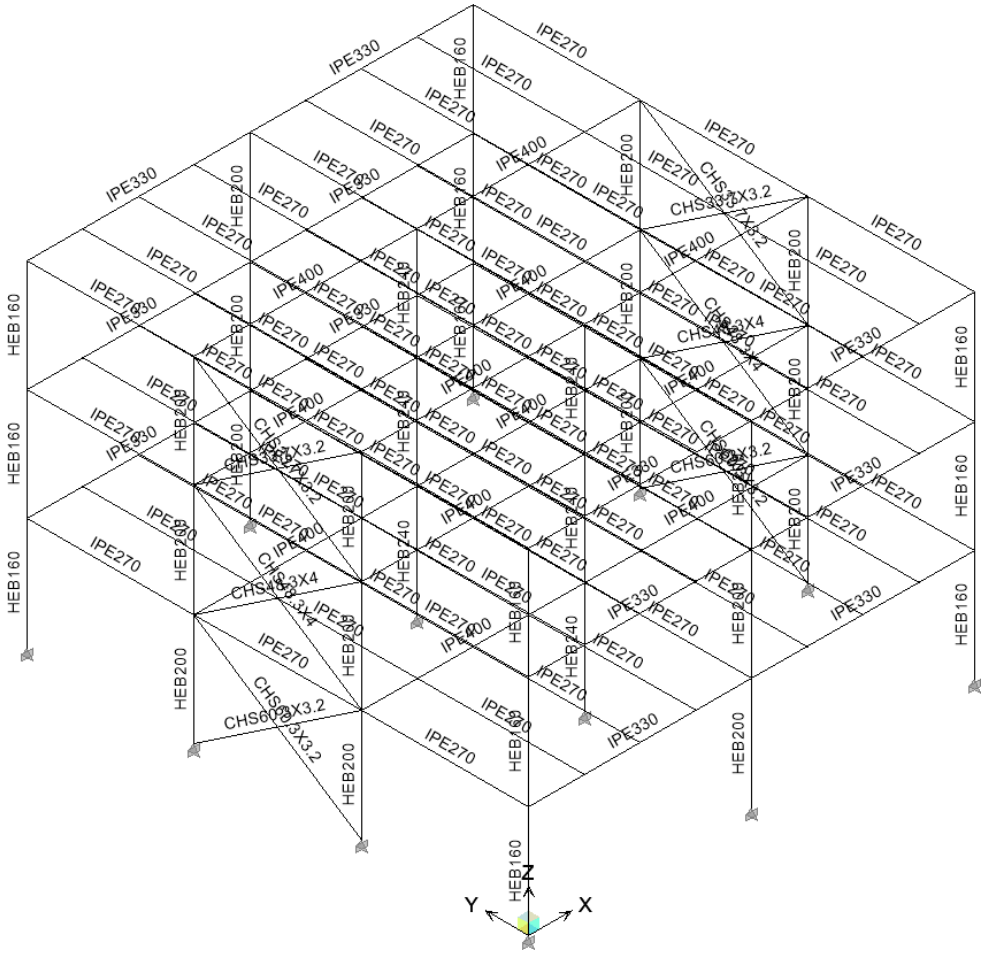

Figure 2-26: Final design of the building under investigation in Scenario 5 - no seismic codes

2.9.4 **Damage limitation checks**

The interstorey drifts checks are marginally met in the direction of the bracings, while in the direction of the MRF system they are clearly not met. Concerning the P-Δ effects the maximum value of 0.3 suggested by Eurocode 8 is exceeded in the last two storeys. The following quantities are only presented for reasons of completeness, since the requirements of Eurocode 8 in conjunction with the damage limitation checks are ignored in this scenario.

Table 2-38: Calculation of the interstorey drifts

Storey	dX (m)	dY (m)	$d_{r,X}$ (m)	$d_{r,Y}$ (kN)	ν	h (m)	$d_{r,X}$·ν	$d_{r,Y}$·ν	α	X Check	Y Check
1	0.0485	0.0543z	0.0121	0.0136	0.5	4	0.0061	0.0068	0.0075	0.81 ✓	0.90 ✓
2	0.0769	0.0519	0.0192	0.0130	0.5	4	0.0096	0.0065	0.0075	0.99 ✓	0.87 ✓
3	0.0708	0.0535	0.0177	0.0134	0.5	4	0.0089	0.0067	0.0075	1.18 X	0.89 ✓

Table 2-39: Calculation of the P-Δ effects

Storey	P_{tot} (kN)	h (m)	$V_{tot,X}$ (kN)	$V_{tot,Y}$ (kN)	dX (m)	dY (m)	θ_X	X Check	θ_Y	Y Check
1	2094.21	4	196.74	336.79	0.0485	0.0543	0.178	✓	0.144	✓
2	4188.82	4	238.26	328.79	0.0769	0.0519	0.338	XX	0.165	✓
3	6283.54	4	286.11	394.82	0.0708	0.0535	0.389	XX	0.213	✓

2.10 CONCLUSIONS

In this chapter, the fundamental principles of Eurocode 8 that were extensively presented in Chapter 1, are directly applied in a regular three-storey steel building. More specifically, 4 possible design scenarios are created that aim to address the concern regarding the consideration of the compressed bracing in the structural configuration according to §6.7.2(2) of Eurocode 8. Another approach, however, suggests that the seismic actions are calculated for the design earthquake, where the buckling of the compressed bracing has already taken place. When taking into account the tension bracing only, the rigidity of the structure, thus the period of vibration which defines the seismic loads, is almost $\sqrt{2}$ times higher than if both braced members contributed in the total rigidity of the structure. Different fundamental periods of vibration account for different spectral accelerations and, therefore, seismic actions, although the structural configuration changes the distribution of internal forces along the members of the structure.

However, a conclusive answer can only be provided through the assessment of the load-bearing capacity using non-linear analyses to approach the 'actual' behavior of the structure more accurately. Therefore, in order to provide a realistic basis for the upcoming non-linear investigation, all scenarios are designed from the beginning. The necessity to optimize this iterative procedure is significant and, for the purpose of this diploma thesis, a methodology for the optimum design of regular multi-storey steel buildings that integrates all requirements of Eurocodes 3 and 8 was developed. Each scenario constitutes a different approach concerning the contribution or not of the compressed bracing in the structural system.

In Scenario 1, the structure was designed when only the tension diagonal was considered in the structural configuration, while in Scenario 2 the modelling was based only on the tension bracing according to the first case, although both bracings were taken into account during the elastic analysis. Scenario 3, on the other hand, approaches the matter under investigation by considering both diagonals in the modelling procedure and results in slightly different cross-sections compared to Scenario 1. The last possible case is Scenario 4, which assumes half the area of the bracings' cross-sections while twice the value of the tension axial force is received. This scenario results in the same cross-sections for all members as Scenario 3 and is, therefore, not worth further investigation.

A fifth design scenario is introduced, namely Scenario 5, where the structure under investigation is designed based on the resistance checks, while the requirements of the seismic code are completely ignored. This approach aims to highlight the necessity of capacity design in the case where the nominal values of either the seismic actions or the resistance of the members differ compared to the design.

Concerning the modelling of the bracings, the most definitive requirement was the non-dimensional slenderness limitation in conjunction with the 25% Ω criterion that aims to achieve uniform ductility in height. The requirement for axial resistance is more favorable compared to the slenderness criterion and, as a result, the cross-sections of the bracings are increased significantly. The design of the columns is dominated by the damage limitation checks in the direction of the moment resisting frames, where the displacements and the secondary effects are important, due to the large lateral flexibility of these framing systems. However, the design of the main, as well as the secondary beams, is based on the Ultimate and the Serviceability Limit states which are rendered more unfavorable compared to the seismic situations.

3 CHAPTER 3: INVESTIGATION OF THE THREE STOREY STEEL BUILDING'S BEHAVIOR THROUGH NON-LINEAR ANALYSES

3.1 GENERAL

This chapter focuses on the investigation of the seismic response of a regular steel building by bypassing the limits of elastic analysis. It proceeds to develop a more comprehensive picture regarding its actual response, which is primarily dominated by the behavior of the braced members. In the following paragraphs, the compressed bracing's contribution to the resistance of seismic loads is taken into account using different scenarios of elastic analysis along with their possible structural systems. Considering both braced members, though, requires non-linear analyses in order to approach the post-buckling behavior of the compressed bracing and, thus, evaluate the seismic capacity of the entire structure.

Subsequently, comparative results between the different scenarios and elastic analyses are also presented. The effect of the rather definitive non-dimensional slenderness criterion to the design of the bracings is investigated in terms of load-bearing capacity and displacements, which inspired the need to highlight the necessity of the entire concept of capacity design. Finally, the best design scenario is suggested as a simplified attempt to approach the contribution of the compressed bracing, without being necessary to proceed to any time-consuming non-linear analyses of the entire structure.

3.2 NUMERICAL SIMULATION IN ADINA

The simulation of the structure for the required non-linear analyses is carried out with the finite element analysis software ADINA. It should be reminded that Eurocode 8 limits the cross-section classification

for braced members to Class 1 or 2, as in frames with concentric diagonal bracings the dissipative zones are located in the tension diagonals only. This limitation eliminates the possibility of local buckling in the compressed braced members. For this reason, they are simulated with beam-type finite elements, as the only possible form of buckling is the global. Regarding the simulation of the columns, Eurocode 8 limits the cross-section classification to Class 1 or 2 as well, capacity design was applied to both X and Y directions and the entire structure complies with the damage limitations and secondary effects checks. Taking all this into consideration, beam-type finite elements are also introduced for the simulation of the columns as any form of buckling is prevented due to the aforementioned reasons.

The mesh density was selected to 20 number of subdivisions per member as an attempt to balance an acceptable precision in the bracing member's global buckling and the required computational effort.

3.2.1 **Definition of geometry**

The design based on the elastic analysis in ETABS according to Eurocodes 3 and 8, are now introduced in the non-linear model under investigation. In order to reduce the computational effort, the secondary beams were not included in the non-linear model. Instead, their loads along with their dead loads, were replaced with concentrated loads which are applied directly into the main beams. In the following figures, the typical geometry of the structure with the tension bracings only as well as with both bracings is illustrated.

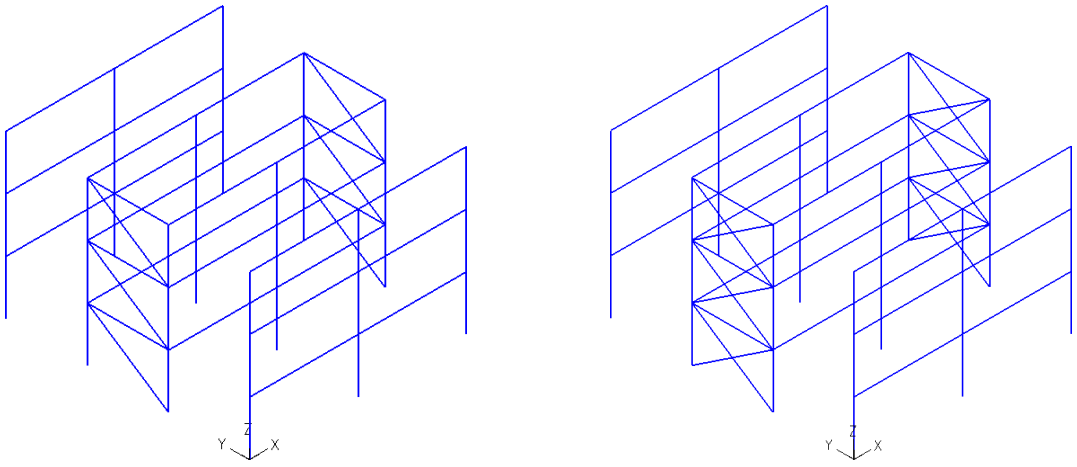

(a) (b)

Figure 3-1: Demonstration of geometry in the non-linear model with (a) the tension diagonal only (b) both diagonals

3.2.2 **Definition of material**

The actual behaviour of the structure is largely affected by material non-linearity, as load-bearing capacity in the Y direction depends on both braced members. While, on one hand, geometric non-linearity is crucial for the development of the compressed bracing's global buckling, on the other hand the tension bracing's main type of failure depends on yielding. Therefore, a bilinear elastic-plastic material is introduced in the non-linear model, with a realistic maximum allowable effective plastic strain of 20% and a strain hardening modulus of 750.000 GPa, so as the ultimate tensile strength reaches the value of 490 MPa as stipulated in EN1993-1-1: 2005, §3.2.3 Table 3.1.

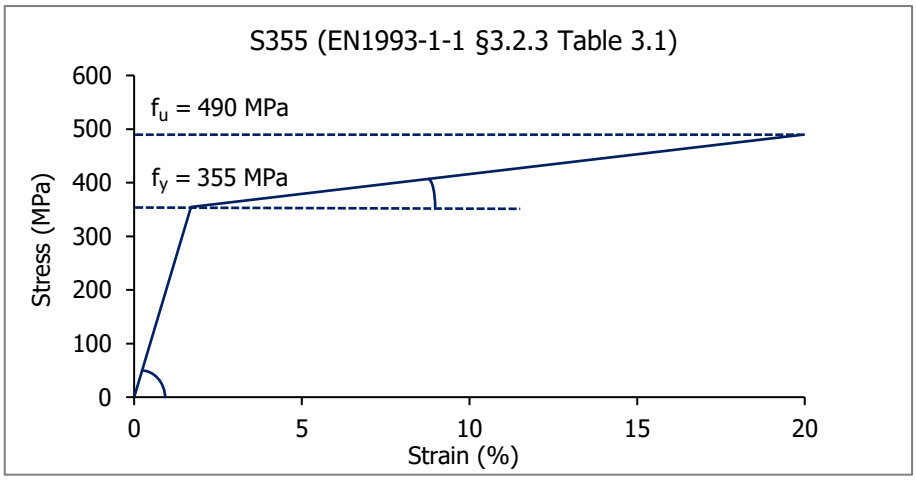

Figure 3-2: Stress – strain nominal diagram for hot rolled structural steel of S355 grade

3.2.3 **Definition of rigid diaphragm**

In order to ensure a homogeneous horizontal displacement for each storey due to the existence of a concrete slab, rigid links are introduced to each storey. In each level, all in plane points' relative displacements are restrained in the X and Y direction, while a master node is set in the centre of mass of each diaphragm, where the seismic actions are applied. The following figure demonstrates the rigid diaphragms in the case of the tension diagonal, but the exact same configuration applies in the case of both braced members as well.

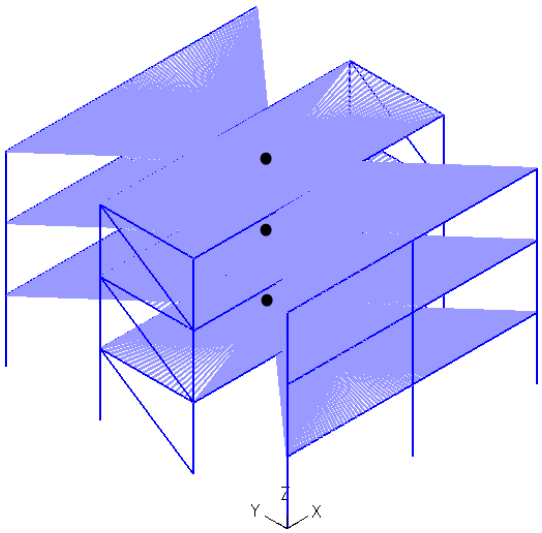

Figure 3-3: Demonstration of rigid diaphragms and master nodes at each level

3.2.4 **Definition of end-releases**

The non-linear model should fully comply in terms of mass, loads, cross-sections, boundary conditions and end-releases with the linear model. As a matter of fact, end-releases in braced members, whether in or out of plane, define the member's buckling length and ultimately its buckling axial resistance. Therefore, in and out of plane moment end-releases were introduced to each bracing system, rendering the effective buckling lengths identical in both directions and equal to the member's initial length.

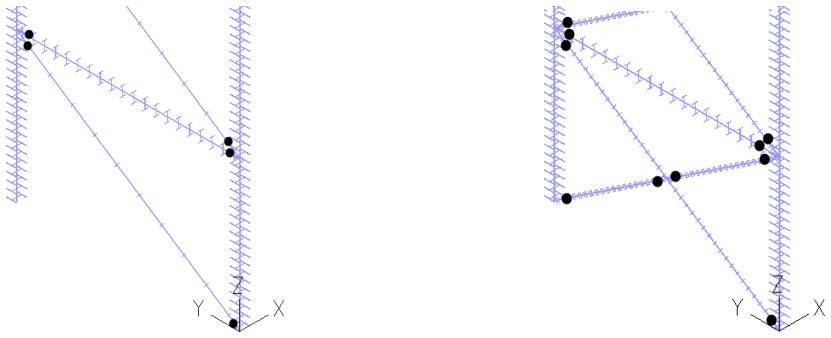

(a) (b)

Figure 3-4: Demonstration of bracing's moment end-releases with (a) the tension bracing only (b) both bracings

3.2.5 **Definition of seismic loads**

The vertical loads applied in the non-linear model are designated by the seismic combination (G+0.3Q), while horizontal loads are defined by the lateral force method. A modal response spectrum analysis was not carried out in the non-linear analysis, as its basic assumption is material non-linearity, which contradicts the theoretical assumption of the elastic material in the modal response spectrum analysis method. The following figure illustrates the load distribution for the seismic combination in the case of the non-linear model where the compressed bracings have been intentionally ignored. Nevertheless, the vertical loads retain the same values in the case of the structural configuration with both braced members, except from the horizontal loads' values which are different due to the increased rigidity.

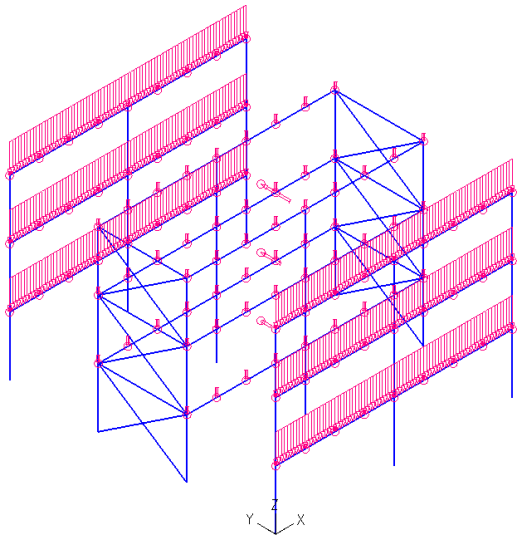

Figure 3-5: Demonstration of vertical and horizontal loads for the seismic combination in the non-linear model

3.3 INVESTIGATION OF SCENARIO 1

The first scenario under investigation was designed in §2.5, abides by all regulatories of Eurocodes 3 and 8 and includes only the tension bracing during the modelling by intentionally ignoring the existence of the compressed bracing in the structural configuration. It should be clarified that the behavior of the

three-storey steel building through non-linear analyses is investigated in the following paragraphs only in the case where the CBF beams operate as secondary beams and are, therefore, laterally resisted by the rigid diaphragm. Consequently, the only members under compression that are expected to present failure due to global buckling are the compressed bracings.

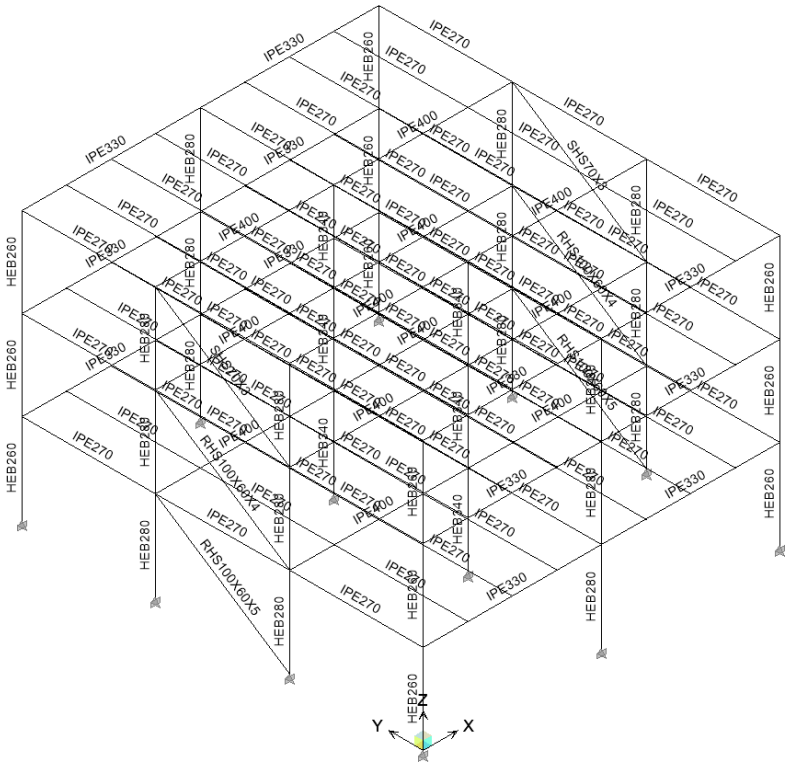

Figure 3-6: Design based on elastic analysis for Scenario 1 according to Eurocodes 3 and 8

Moreover, in order to evaluate the results from the elastic analysis, the braced members under compression should be included in the non-linear model. This is to approach a more realistic behaviour of the structure, as well as the influence of the post-buckling behavior to the ultimate response of the structure.

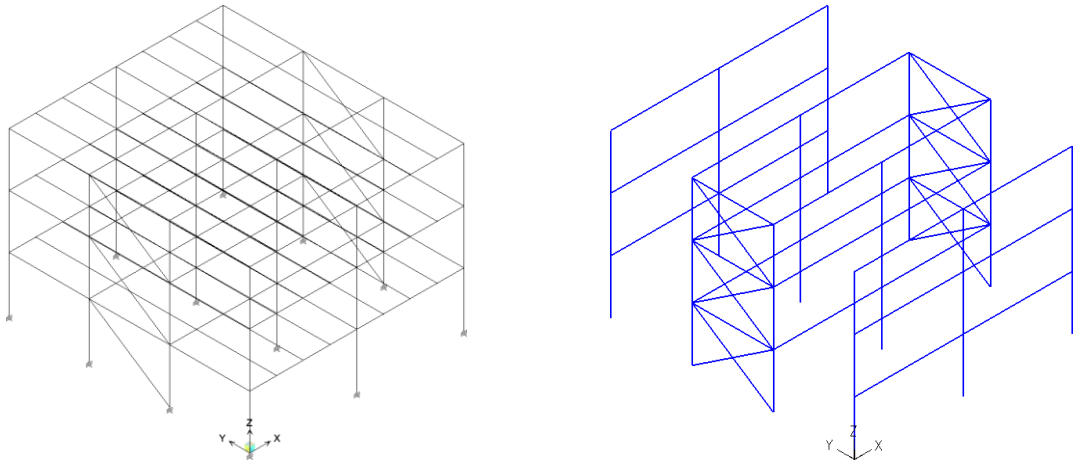

(a) (b)

Figure 3-7: Definition of model in (a) elastic analysis with ETABS (b) non-linear analysis with ADINA

Before proceeding to the non-linear analysis, an accumulative table is presented with the most significant characteristics of the structure's braced members under compression, such as cross-section, effective buckling length, major and minor principal axis non-dimensional slenderness, reduction factor, design buckling resistance and elastic critical force. The buckling axial resistance of the RHS members relies entirely on their out of plane resistance.

Table 3-1: Summary table of useful quantities about the compressed bracings

Storey	Cross-section	A (cm^2)	$N_{pl,Rd}$ (kN)	i_y (cm)	$\bar{\lambda}_y$
1	RHS100X60X5	14.7	522	3.58	1.33
2	RHS100X60X4	12	426	3.63	1.31
3	SHS70X3	7.94	282	2.73	1.74

Storey	Cross-section	i_z (cm)	$\bar{\lambda}_z$	χ	$N_{b,Rd}$ (kN)	N_{cr} (kN)
1	RHS100X60X5	2.38	1.99	0.22	117	133
2	RHS100X60X4	2.43	1.95	0.23	99	112
3	SHS70X3	2.73	1.74	0.29	81	94

3.3.1 Non-linear model verification

First and foremost, it is crucial to verify the non-linear model of the structure. It is based on the comparison of internal forces and storey displacements between the linear model in ETABS and the non-linear model in ADINA for seismic loads applied in the Y direction without any accidental eccentricity.

In the following figures the results between the non-linear model in ADINA and the linear model in ETABS are presented and compared for each possible scenario. In both models, axial forces do not develop in the main beams, due to the existence of the rigid diaphragm and the assumption of infinite axial rigidity in the XY plane.

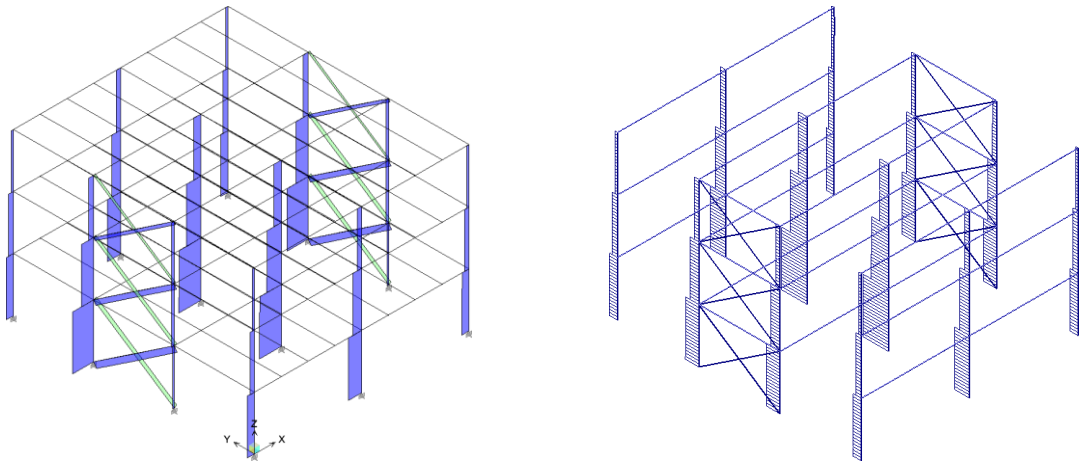

(a) (b)

Figure 3-8: Bending moment diagram for (a) linear model in ETABS (b) non-linear model in ADINA

The distribution of axial forces illustrated in the figure above is developed due to both vertical and horizontal forces for the seismic combination without accidental eccentricity. The only columns that get additionally activated due to the horizontal loads are the ones directly connected to the bracing systems.

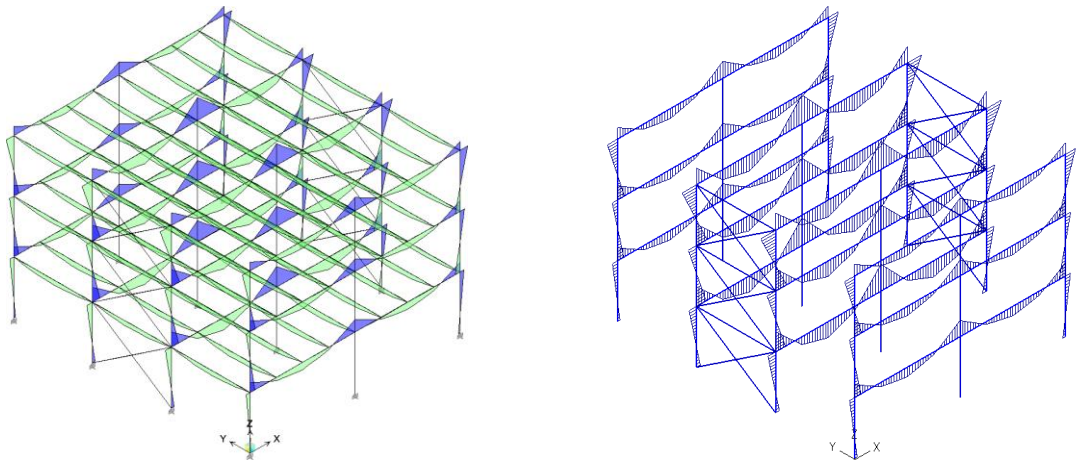

(a) (b)

Figure 3-9: Bending moment diagram for (a) linear model in ETABS (b) non-linear model in ADINA

Table 3-2: Comparative table of internal forces and displacements for the two different models

Model	**Maximum axial force in bracings (kN)**	**Maximum axial force in columns (kN)**	**Maximum bending moment (kNm)**	**Maximum upper storey Y displacement (m)**
ETABS	229.8	959.2	219.5	0.0199
ADINA	229.4	959.4	225.9	0.0199

As demonstrated in the comparative table above, the non-linear model comes to almost absolute agreement in terms of internal forces and displacements with the linear and, afterwards, an attempt to reduce the computational effort to the minimum required is made. The exterior moment-resisting frames that are not directly connected to the bracing systems and do not contribute in the rigidity of the structure in the Y direction, are removed from the non-linear model as shown in the following figure 1-10. Furthermore, both bracing systems are included in the model, as it would be inaccurate to proceed only with its symmetric half, since any form of symmetry is eliminated during a non-linear analysis.

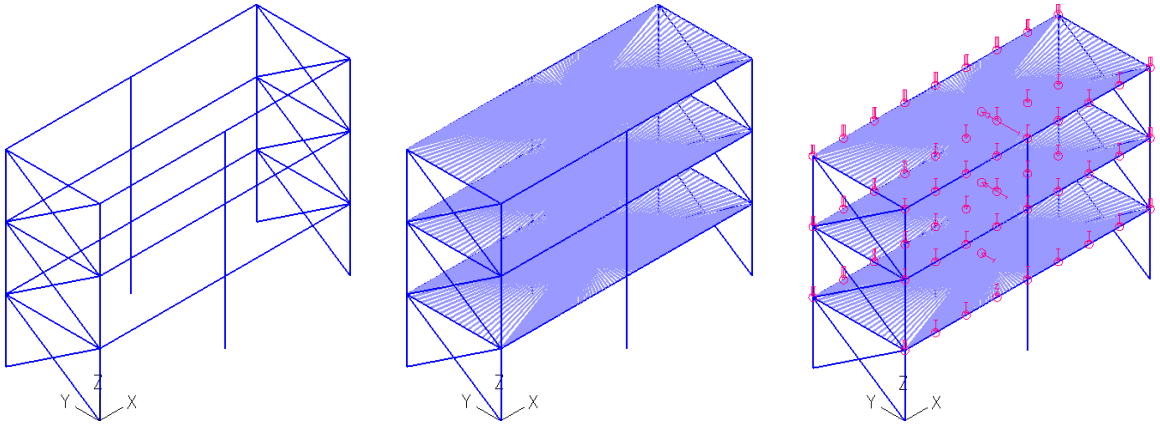

(a) (b) (c)

Figure 3-10: Simplified non-linear model (a) definition of geometry (b) definition of rigid diaphragm (c) definition of loading for the seismic combination

3.3.2 **Non-linear analysis of material**

This type of analysis aims to simulate the response of the structure in case only the tension diagonal is taken into consideration, as stipulated by Eurocode's 8 guideline in §6.7.2.(2). The main purpose of executing a non-linear analysis of material, is that it accounts for a static pushover analysis. The purpose of the pushover analysis is to evaluate the expected performance of a structural system by estimating its strength and deformation demands in design earthquakes by means of a static inelastic analysis. The results from the non-linear analysis are verified and compared to a typical pushover curve extracted by a commercial analysis software, such as ETABS.

3.3.2.1 Non-linear analysis of material using ADINA

In the case where the existence of the compressed bracing member is neglected and all columns under compression are capacity designed, the possibility of failure related to global buckling is limited. Additionally, since the main beams in the X direction are not affected by the seismic loads in the Y direction, the only possible type of failure that could turn the structure into a sway mechanism, is the yielding of the tension diagonals. Therefore, when only the tension diagonal is taken into account in the non-linear model, the only type of non-linearity which is expected to be crucial for the structure's response, is the material non-linearity.

3.3.2.2 Pushover analysis using a commercial software

More often than not, commercial design softwares integrate useful tools that are commonly used by engineers for a typical non-linear analysis, such as static pushover curves. It should be noted that the main topic of interest in this thesis is the evaluation of the load-bearing capacity of the structure and thus, the curve calculated by the software will not be used for the evaluation of the structure in terms of target displacements. The following diagram demonstrates the comparison between a non-linear analysis of material and a pushover curve where only the tension diagonal is considered. Finally, $V_{b,1}$ accounts for the developed base shear when only the tension diagonal in considered. It should also be pointed out that all elastic base shears are calculated based on the inelastic spectral acceleration.

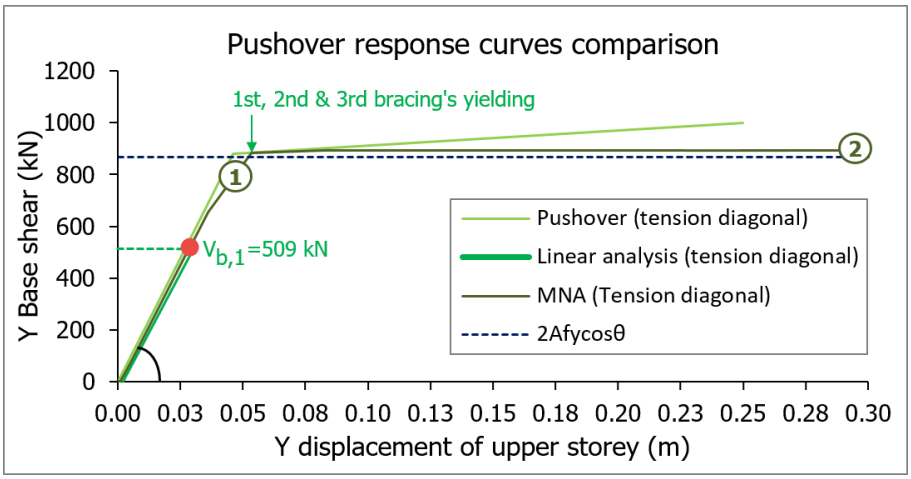

Figure 3-11: Comparison between a typical pushover curve and non-linear analysis of material (MNA)

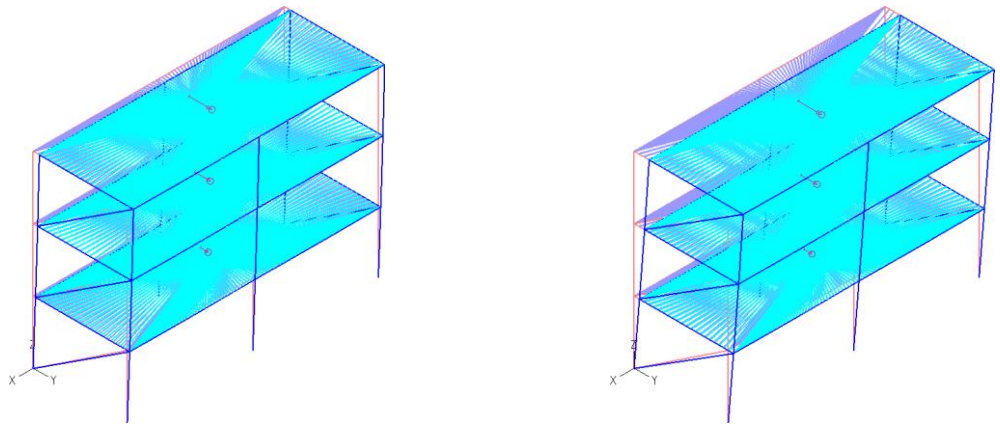

(a) (b)

Figure 3-12: Deformed shape of the structure in (a) Point 1 and (b) Point 2 in MNA curve

The comparative Figure 3-11 describes the structure's response in the Y direction, when non-linearity completely relies on the material. The typical pushover curve from the commercial software comes to an agreement in terms of load-bearing capacity, as in both curves the tangent becomes almost zero for a base shear value of 900 kN. Since the bracings are designed in an optimum way, it is expected that their yielding takes place almost for all three at the same time, which is actually the case.

Nevertheless, the structure seems to retain its load-bearing capacity to 900 kN in the case of the MNA with a tangent close to zero, due to the hardening of the material. Unfortunately, the commercial software is not capable of taking into account the material's hardening. This may lead to less accurate results that do not come to absolute agreement with those represented by the MNA, especially after the structure reaches its ultimate load.

Moreover, a simplified way to verify the maximum load, is the assumption that the base shear is resisted by the horizontal component of the 1st storey braced members' axial forces. Considering that each bracing has a plastic yielding strength of $N_{pl,Rd} = Af_y = 522$ kN, the total resisting base shear can reach the value of $2N_{pl,Rd}\cos\theta = 868$ kN. This result comes to an agreement with the maximum base shear developed, when the axial contribution of the columns is taken into account. Additionally, the two curves seem to demonstrate almost the same elastic rigidity.

Another important conclusion can be reached regarding the different values between the horizontal load-bearing capacity and the design earthquake's base shear. The design of the braced members was based on the 3 criteria mentioned in §6.7.3(1), one of which is that of axial resistance. However, the limit of the member's non-dimensional slenderness $1.3 \leq \bar{\lambda} \leq 2.0$ in conjunction with the 25% criteria for Ω, leads to higher demand for cross-sections, thus resulting in increased load-bearing capacity compared to the design earthquake's base shear.

3.3.3 **Non-linear analysis of geometry and material with initial imperfections**

3.3.3.1 Linearized buckling analysis

The main purpose of a linearized buckling analysis is to extract buckling modes in order to introduce initial imperfections in the non-linear model. It should be noted that a linearized buckling analysis

increases both vertical and horizontal loads at the same time, thus becoming an insecure method for the evaluation of buckling loads. The following figures demonstrate the buckling modes that were selected and introduced as initial imperfections.

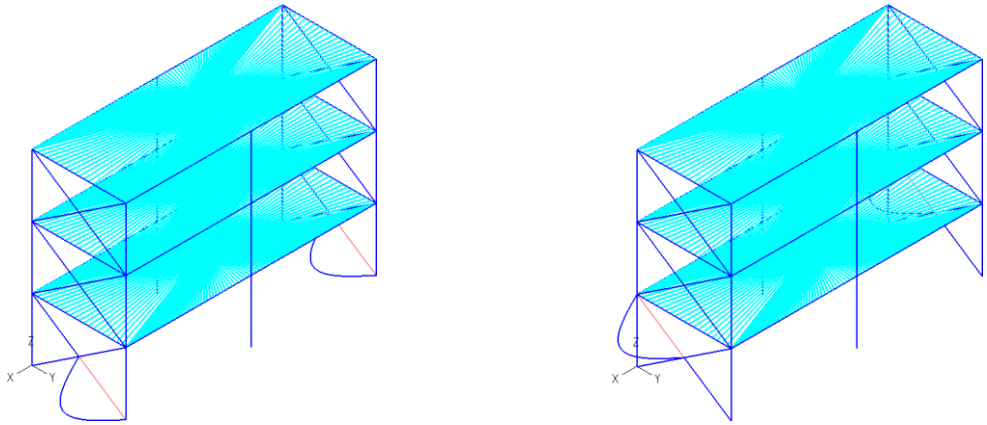

(a) (b)

Figure 3-13: Buckling modes, RHS100X60X5 (a) Mode 1, out of plane, λ_{cr} = 0.793 (b) Mode 3, out of plane, λ_{cr} = 0.797

For all buckling systems, the lower member of the compressed bracing requires slightly less critical load to buckle compared to the upper member of the same bracing system. This is because the lower member receives the dead load from the upper tension member, thus increasing its total axial force.

Considering that the braced members' cross-sections are RHS100X60X5, RHS100X60X4 and SHS70X3 from the bottom to the top, it is expected that the out of plane buckling modes precede the in plane ones, which is actually the case. In addition, the members' out of plane non-dimensional slenderness increases in height, because the buckling length is exactly the same both in and out of plane. However, it is impossible to determine directly which braced member is going to buckle first, as horizontal loads and, therefore, the axial forces that the bracings develop, decrease in height.

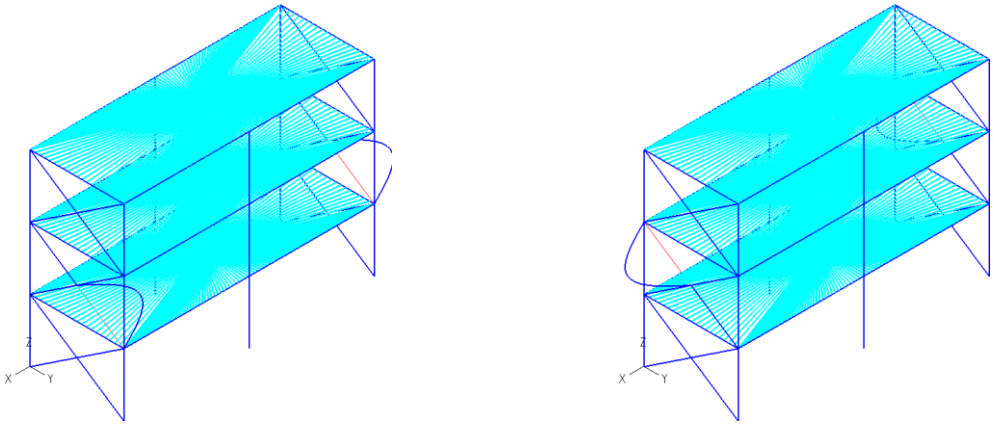

(a) (b)

Figure 3-14: Buckling modes, RHS100X60X4 (a) Mode 5, out of plane, λ_{cr} = 0.840 (b) Mode 7, out of plane, λ_{cr} = 0.844

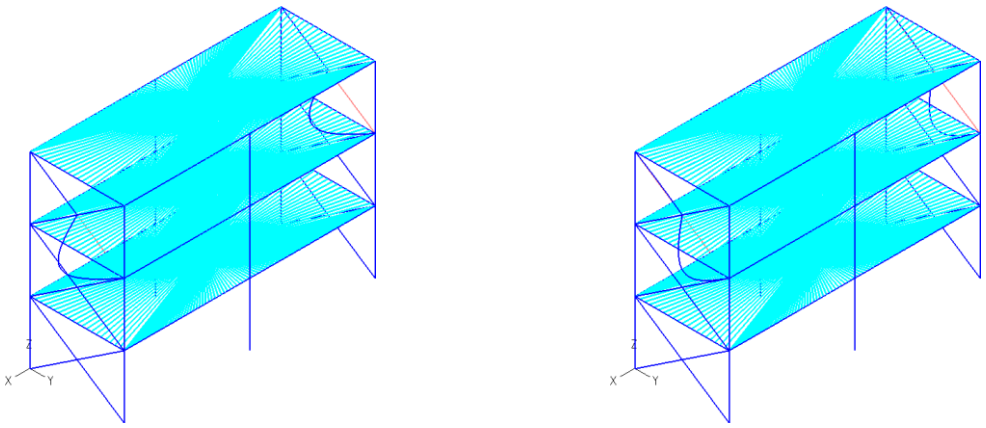

(a) (b)

Figure 3-15: Buckling modes, SHS70X3 (a) Mode 9, out of plane, λ_{cr} = 1.201 (b) Mode 11, in plane, λ_{cr} = 1.201

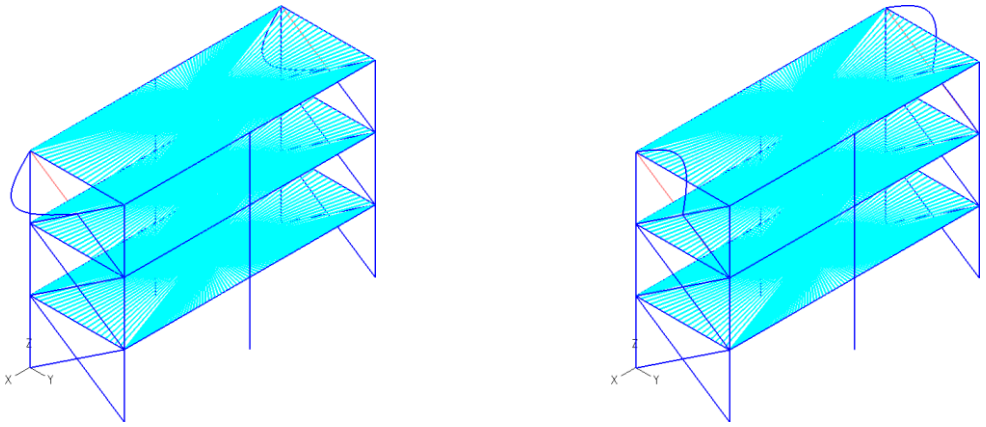

(a) (b)

Figure 3-16: Buckling modes, SHS70X3 (a) Mode 13, out of plane, λ_{cr} = 1.208 (b) Mode 15, in plane, λ_{cr} = 1.208

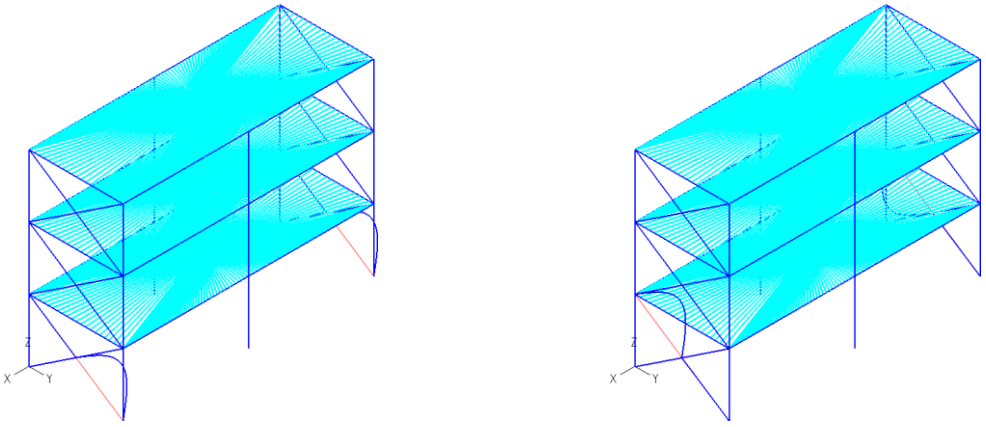

(a) (b)

Figure 3-17: Buckling modes, RHS100X60X5 (a) Mode 17, in plane, λ_{cr} = 1.804 (b) Mode 19, in plane, λ_{cr} = 1.813

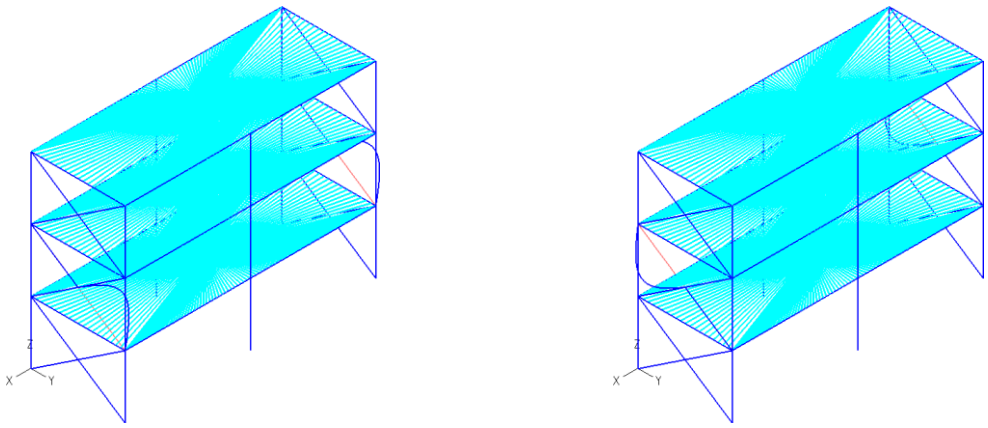

(a) (b)

Figure 3-18: Buckling modes, RHS100X60X4 (a) Mode 21, in plane, λ_{cr} = 1.890 (b) Mode 23, in plane, λ_{cr} = 1.900

3.3.3.2 Definition of initial imperfections

Considering that the braced members resist seismic loads only axially, the value of the initial imperfections can be estimated using the linear inelastic Ayrton – Pery buckling equation. Particularly, a simply supported beam is assumed under axial compression with the initial imperfections' shape to follow the in and out of plane buckling modal shape. Failure is defined by the maximum developed stress reaching the material's yielding stress. Moreover, the equation takes into consideration any kind of initial imperfection, including load eccentricity, residual stresses, the shape of the cross-section and the buckling axis (Ch. Gantes, 2015). More specifically:

$$e_o = \alpha \cdot (\bar{\lambda} - 0.2) \cdot \frac{W_{el}}{A} \qquad (3\text{-}1)$$

Table 3-3: Values for initial imperfections for each bracing system for Scenario 1

Ατέλειες	**RHS100X60X5**	**RHS100X60X4**	**SHS70X3**
e_z (mm)	7.1	7.2	6.9
e_y (mm)	6.1	6.1	6.9

For the introduction of initial imperfections in the non-linear model, all of the aforementioned buckling modes are selected with imperfections both in and out of plane. Since in the first two storeys RHS100X60X5 and RHS100X60X4 sections have been selected, whose in and out of plane non-dimensional slenderness values differ significantly, any form of interaction is not expected. However, in the upper storey's bracing SHS system, the in and out of plane non-dimensional slenderness coincide, thus resulting in the interaction of the two buckling modes with detrimental effects in the seismic capacity of the structure. Subsequently, in order to evaluate accurately the in and out of plane imperfections effects, geometric and material non-linear analyses were executed for the three most possible cases: (a) both in and out of plane initial imperfections are introduced to all bracing systems (b) only out of plane initial imperfections to all bracing systems and (c) both in and out of plane initial imperfections only in the upper SHS bracing system.

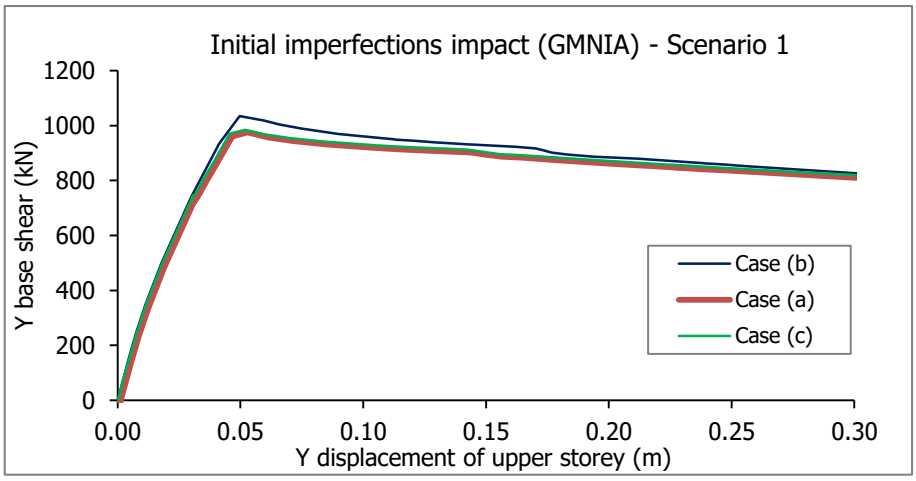

Figure 3-19: Case (a) both in and out of plane imperfections to all bracings, Case (b) only out of plane imperfections to all bracings and Case (c) both in and out of plane imperfections in upper SHS bracings only

Considering the results of the comparative diagram above, the assumption that the in and out of plane non-dimensional slenderness coincide in the upper SHS bracing system and, thus interact with each other, is confirmed. Cases (a) and (c) where both in and out of plane imperfections were taken into account, either in all or in the upper bracing system only, are completely identical. This outcome proves that the in plane imperfections to the compressed RHS bracings, do not effect at all the structure's response, as there is no interaction between the two directions. Consequently, the non-linear analyses of geometry and material are carried out by introducing only out of plane initial imperfections to the RHS bracing systems and both in and out of plane to the upper SHS.

The following figure is defined as a benchmark for any linear or non-linear analysis, as it accounts for the best approach of the structure's actual response. It should, also, be pointed out that the linear analysis curve is extracted only to confirm the initial rigidity of the structure. The required base shear that has to be adequately resisted by the structure includes only the tension diagonal, as the compressed bracing has lost its axial rigidity due to buckling.

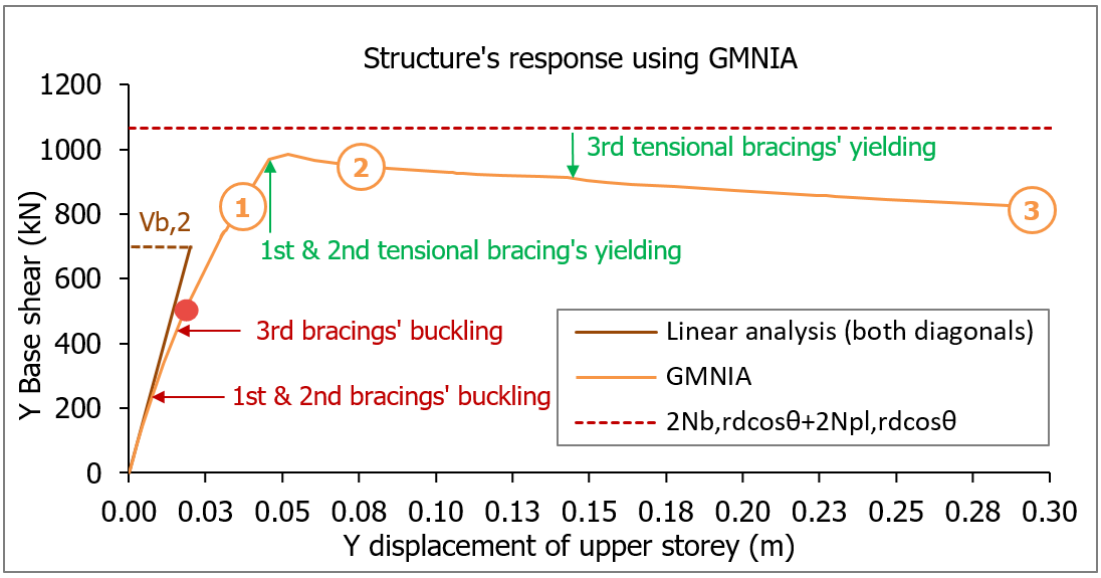

Figure 3-20: Structure's response for non-linear analysis of geometry and material considering both diagonals

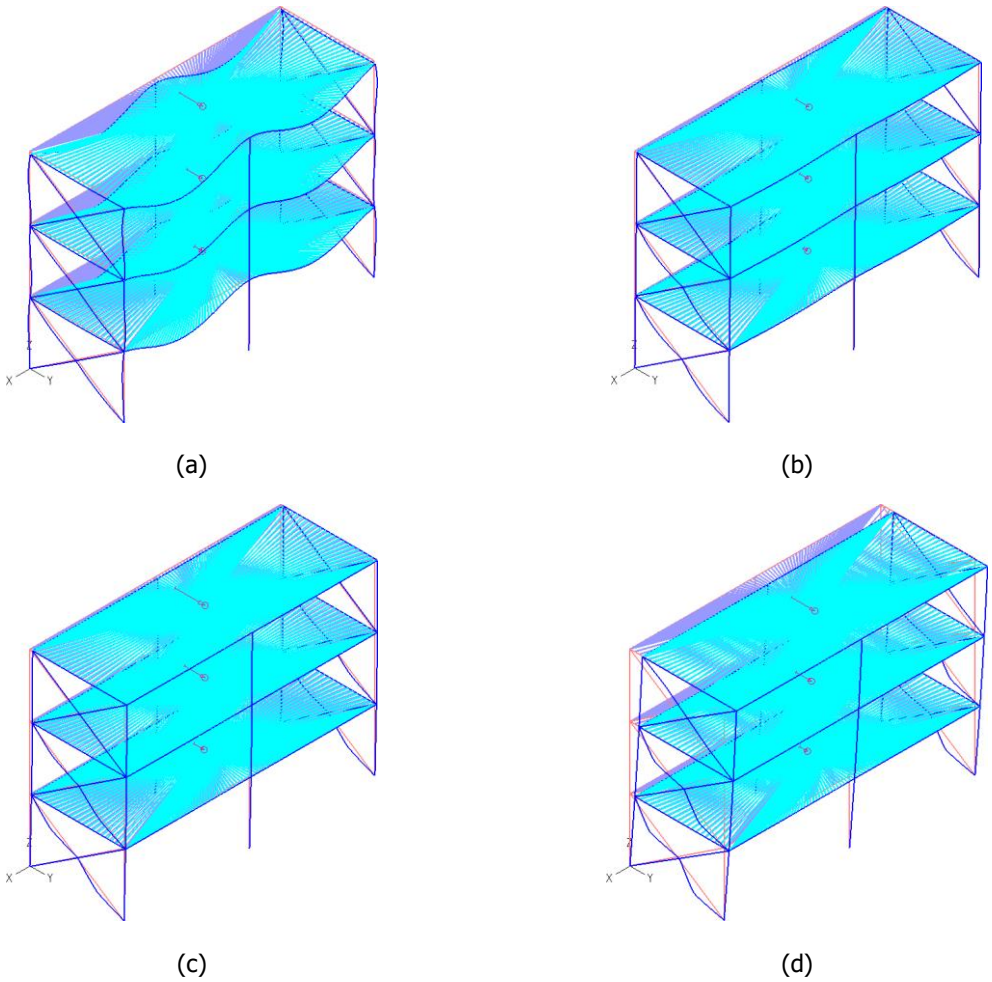

(a) (b)

(c) (d)

Figure 3-21: Deformed shape of the structure in characteristic points of the GMNIA (a) Point 1 for a magnification factor of 100 (b) Point 2 (c) Point 3 (d) Point 4

3.3.3.3 Investigation of the structure's response

The first conclusion after the comparison between the elastic and the non-linear analysis is that they retain the same tangent, therefore rigidity, for small values of the base shear. However, in order to reach with accuracy any conclusions regarding the non-linear behavior, it is important to locate the base shear values where the buckling and yielding of the bracings take place, as the response of the entire structure in the Y direction is primarily defined by the behavior of the bracing systems.

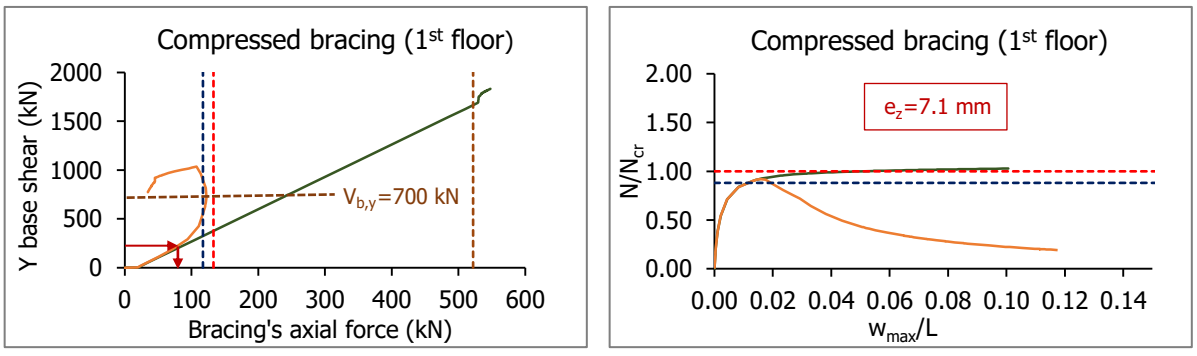

(a) (b)

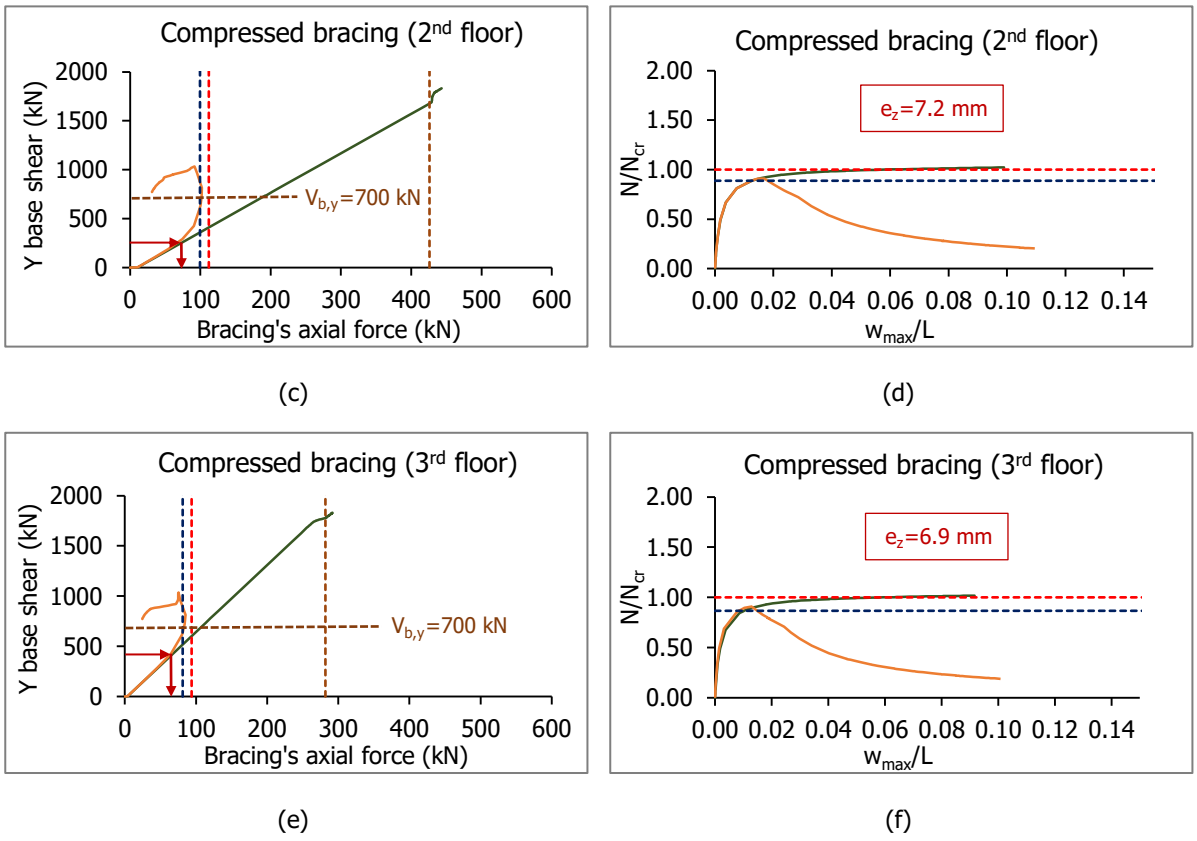

Figure 3-22: Compressed bracing's axial force to developed base shear with GMNIA and MNA analysis with both diagonals for the (a) 1st floor (b) 2nd floor (c) 3rd floor

In figures (b), (d) and (f) and for the GNIA analysis, the braced member's axial capacity is limited by the elastic critical load buckling, as the main assumption in the critical load buckling's definition is the linearity of material. The deformation w_{max} accounts for the out of plane displacement of the member's midpoint. The GMNIA analysis, on the other hand, illustrates the detrimental effect of the material non-linearity as the member's buckling takes place. The axial capacity reaches a maximum value and afterwards, the P-Δ effects advance rigorously. In conjunction with material non-linearity, the member's axial capacity decreases more and more as buckling advances.

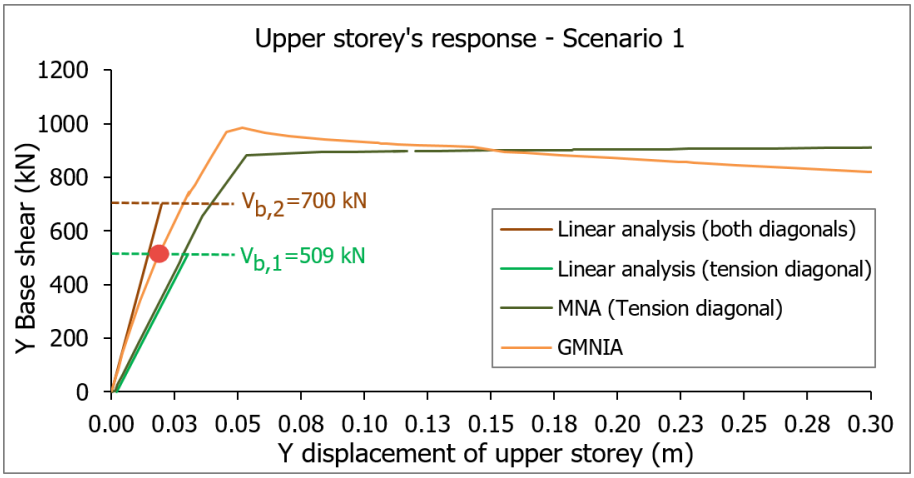

Figure 3-23: Comparison between linear and non-linear methods used to analyze structure's non-linear behavior

After the first buckling takes place for a base shear of 200 kN, the structure's response deviates from the elastic behavior and the two curves begin to separate from each other. In approximately 400 kN of base shear, when the last buckling has taken place, the rigidity of the GMNIA curve decreases and finally approaches the MNA's curve, where only one diagonal is considered. Despite the fact that all compressed braced members have lost their axial rigidity due to their buckling, the structure continues to withstand horizontal loads, as tension diagonals retain their rigidity. Consequently, after the buckling of all compressed bracings has taken place, the structure's ultimate load-bearing capacity depends entirely on the tension diagonals. Despite the material's hardening, after the GMNIA curve reaches its maximum possible base shear, the structure is unable to retain the maximum horizontal load; on the contrary, the base shear decreases, until the upper bracings yield as well.

Ultimately, an attempt for a simplified estimation of the structure's load-bearing capacity was made by taking into consideration the contribution of the compressed braced members before their buckling. Assuming that the axial components of the 1st level bracings are those who resist the earthquake's base shear ($2N_{b,Rd}\cdot\cos\theta = 2\chi A f_y \cos\theta$), along with the fact that the tension bracings have reached their plastic resistance ($2N_{pl,Rd}\cdot\cos\theta = 2Af_y\cos\theta$), the horizontal capacity of the structure can be estimated as $2N_{b,Rd}\cos\theta+2N_{pl,Rd}\cos\theta$. However, this simplified attempt seems to overestimate the maximum base shear of the structure, as the rigidity of the compressed bracing does not maintain a constant axial value of axial force since its buckling. The buckling of the compressed member precedes the yielding of the tension diagonal and, therefore, its axial rigidity decreases more and more as buckling advances. By the time the tension diagonal yields, the compressed bracing has developed an axial force which is slightly lower than its buckling resistance load $N_{b,Rd}$.

Furthermore, the structure's ultimate load (1000 kN) is almost twice as much as the required earthquake's base shear (509 kN). On one hand, this outcome is mainly based on the non-dimensional slenderness limitation of $1.3 \leq \bar{\lambda} \leq 2.0$ along with the 25% criterion for Ω, which result to an increased demand for cross-sections than axial resistance requires. On the other hand, the compressed braced members contribute since the very beginning to the structure's static configuration and, therefore, to the resistance of horizontal loads. For earthquakes which develop an inelastic base shear that do not cause any of the bracings to buckle, the developed base shear has a value of 700 kN, since both members contribute to the rigidity. However, for earthquakes with higher seismic shears, the required base shear has a lower value of 509 kN, since only the tension bracings contribute to the total rigidity and the applied seismic loads in general.

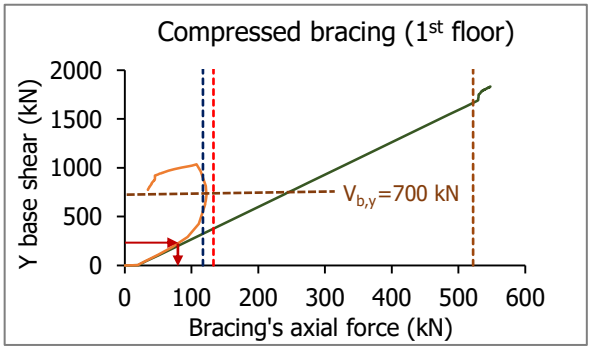

(a)

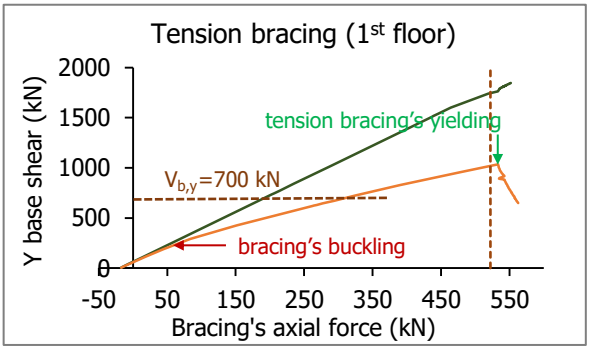

(b)

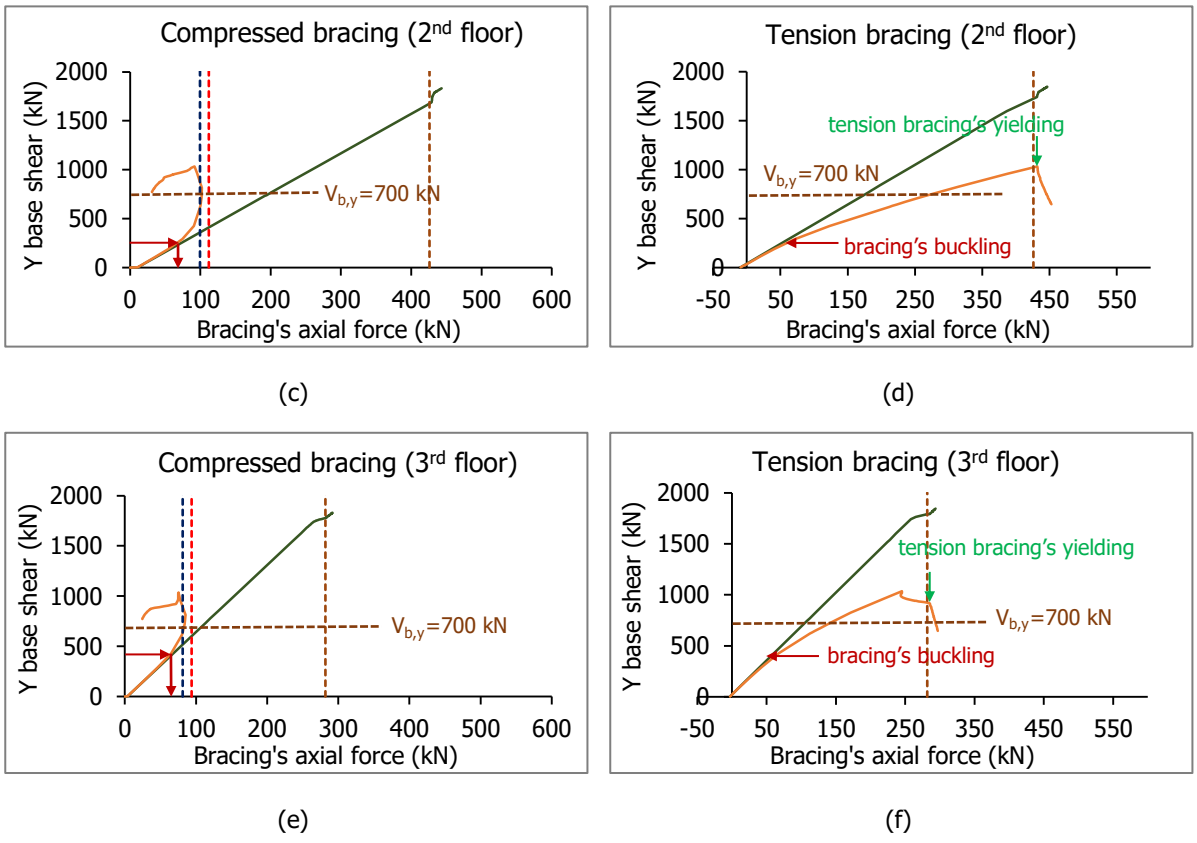

Figure 3-24: Compression and tension axial force versus the developed base shear with GMNIA and MNA analysis with both diagonals for (a) and (b) 1st floor (c) and (d) 2nd floor (e) and (f) 3rd floor

A variety of diagrams regarding the compression and tension axial force developed in the bracings are created in order to acquire a better understanding of the structure's non-linear behavior. First of all, the buckling resistance according to Eurocode 3 is represented, as well as the elastic critical buckling load and the plastic resistance of each bracing. The behavior of both compressed and tension bracings in an MNA with both diagonals is also illustrated, which is for all base shear values, linear. Nevertheless, when a member's plastic axial resistance takes place, its load-bearing capacity in terms of base shear, decreases significantly and the structure turns into a mechanism.

Subsequently, considering that the two diagonals under investigation are connected in their mid-length, they do not behave individually but, on the contrary, interact with each other. In addition, the maximum axial force compressed bracings are able to develop, is limited between the buckling and the elastic critical resistance of the member. However, the member's buckling has taken place for smaller values, as it declines from the linear curve before reaching its buckling resistance. After the compressed members' buckling begins to take place, the base shear increases significantly, whereas the developed axial force retains an almost constant value.

The tension diagonal, on the contrary, resists the same base shear by developing an axial force that increases gradually. In parallel with the compressed diagonals, the tension bracings' initial rigidity coincides with the linear curve for small base shear values. When buckling takes place, however, the tangent drops significantly and the tension diagonals retain this rigidity until their yielding.

3.3.3.4 Investigation of the CBF columns' behavior

In this paragraph, the CBF columns' behaviour during the buckling and yielding of the braced members that are directly connected to them, is examined. The CBF columns are mainly affected by the vertical axial component of the braced members and do not develop any shear or moment when horizontal loads are applied. This is due to the fact that all columns are pinned on the base and all connected beams in the Y direction are pinned on both ends. Because of the static system in the direction of the earthquake, the columns are not able to resist any horizontal loads and, therefore, develop shear and moment resistance. However, in the X direction, columns are activated in both shear and moment, as they are part of a moment resisting frame static configuration. It should be pointed out that columns are capacity designed and, therefore, any type of failure, either due to buckling or yielding, is not expected.

As observed by the following diagrams, the maximum developed axial force for the most compressed column is defined by the tension bracing's yielding. After the tension diagonal reaches its plastic axial resistance, the base shear's value drops significantly while the respective column's axial force retains a fixed value. In addition, the 1st floor's column approaches the linear behavior unlike the 3rd floor's, which presents a more intense non-linear behavior through its loading. The behavior of the columns remains linear, without any buckling or yielding taking place during the analysis. The following figures are representative of the effect the bracing's buckling and yielding have on the column's developed axial force.

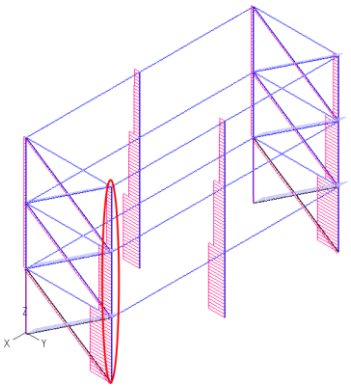

(a)

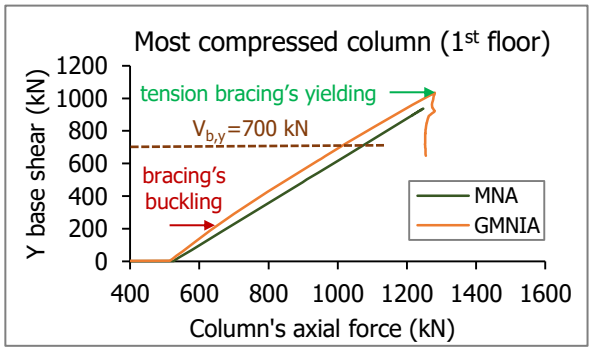

(b)

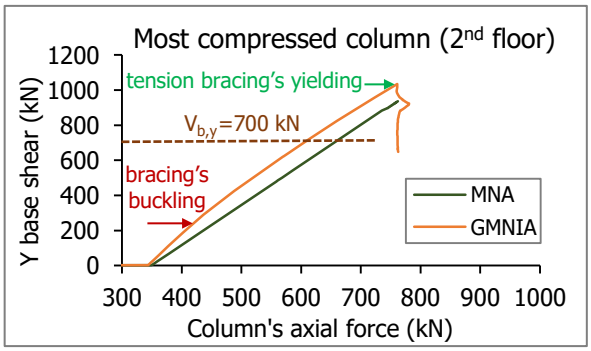

(c)

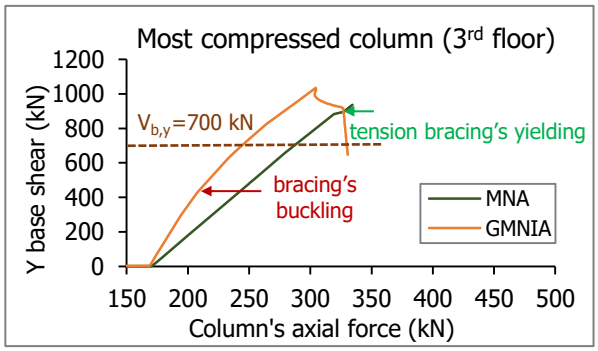

(d)

Figure 3-25: (a) Most compressed column (b), (c), (d) compression in CBF column VS base shear in each level

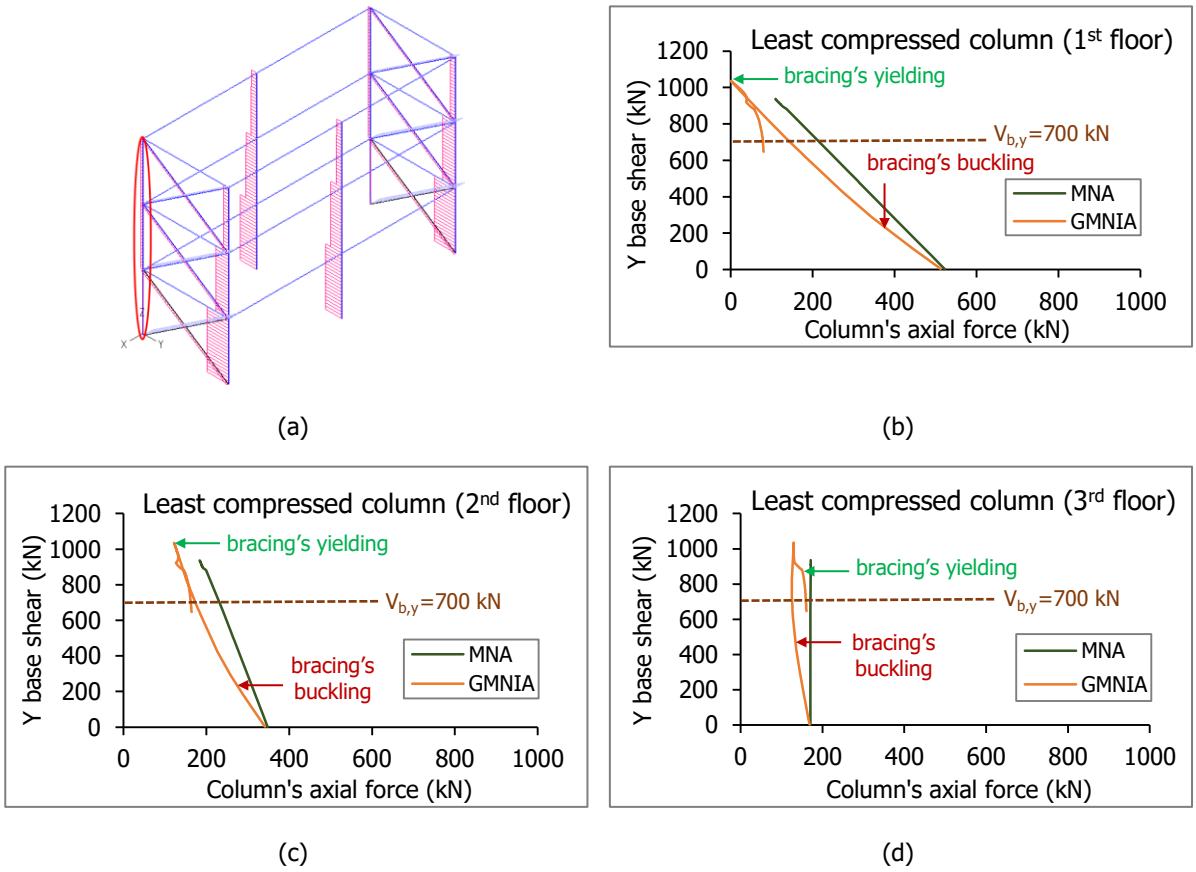

Figure 3-26: (a) Least compressed column highlighted (b), (c), (d) compression in CBF column versus base shear in each level

Regarding the most compressed CBF columns, since buckling takes place, the columns' axial force increases significantly, whereas the bracing's axial value remains almost the same. As for the column's axial force, after the yielding of the tension diagonal, it retains its value, while at the same time the bracing's axial force is reduced.

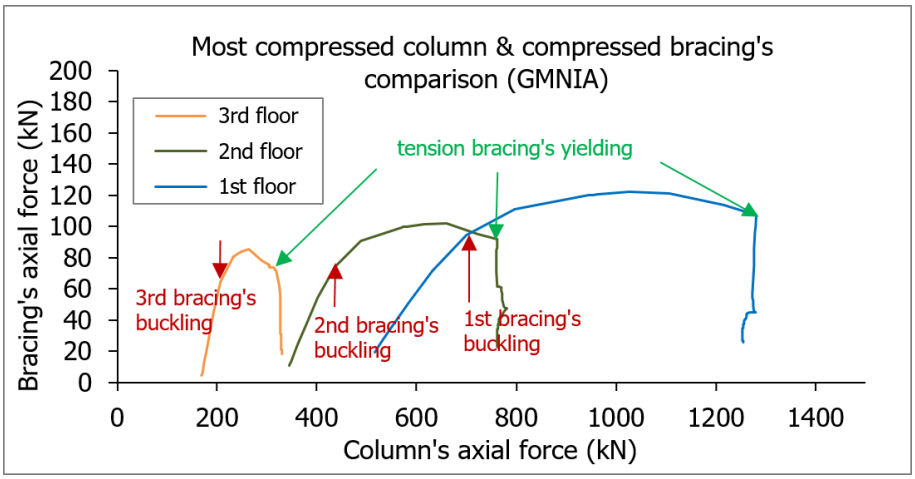

Figure 3-27: Connection between the most compressed CBF column and compressed bracing's behavior

The same conclusions apply for the least compressed CBF columns, with the exception that their axial force is reduced as horizontal loads increase in value. In fact, the column located in the 1st floor reaches a value of zero axial loading during the tension bracing's yielding.

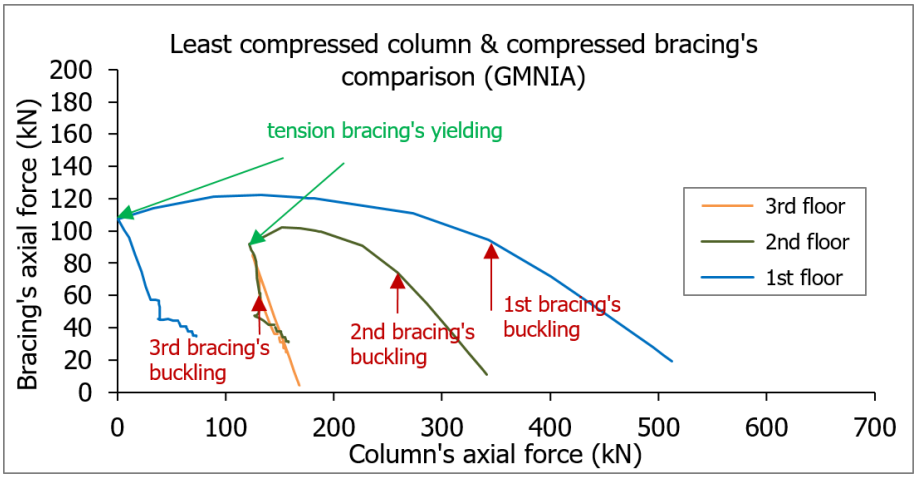

Figure 3-28: Connection between the least compressed CBF column and compressed bracing's behavior

As a consequence of the stern drift and stability requirements and the relative sensitivity of the steel moment frames in the X direction that govern the design, CBF columns lead to considerable over-strength. When, on one hand, the presence of over-strength reduces the ductility demand in dissipative zones, on the other, it also affects the imposed seismic forces. As a result, the examined columns demonstrate a perfectly linear behavior in both cases.

3.4 INVESTIGATION OF SCENARIO 2

This scenario examines the same structure as Scenario 1, with the exception that, although the design procedure was based on one diagonal only, the elastic analysis as well as the pushover analysis are now carried out with both bracings. Firstly, it should be taken into account that both braced members were included in the elastic analysis, which affects the structure's rigidity and, therefore, the applied seismic loads.

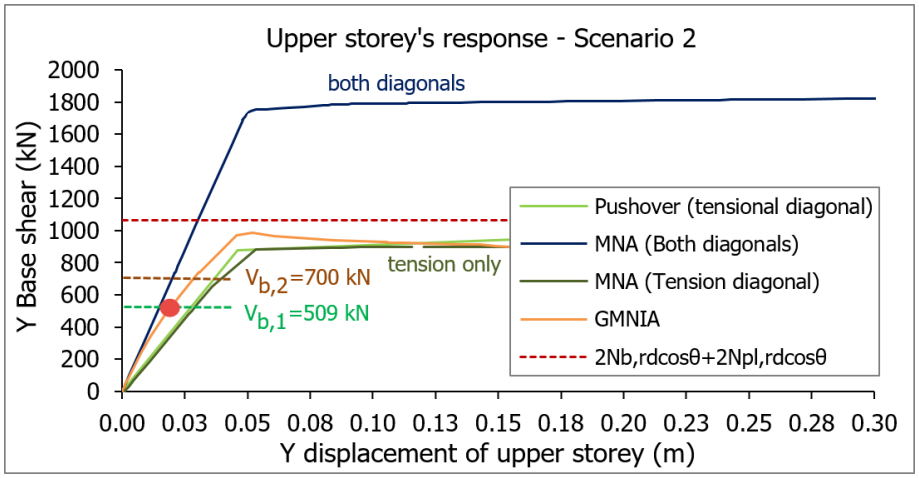

Figure 3-29: Comparative diagram of elastic and non-linear analysis for Scenarios 1 & 2

In an MNA analysis with both diagonals, the assumption of small displacements does not allow any form of buckling to take place. Therefore, despite the fact that the compressed diagonal is taken into account, the only possible type of failure is the yielding of both bracings. In the case of an MNA analysis with both bracings, the structure's load-bearing capacity is expected to be twice as high as in Scenario 1, an assumption confirmed by the comparative diagram below.

The ultimate base shear in the case where only the tension diagonal is considered is 900 kN, whereas in the situation where both of them are taken into account is 1800 kN. Moreover, both MNA analyses have the same yielding displacement of 5cm, therefore, the rigidity of the structure when both diagonals contribute is twice the rigidity of the pushover curve.

The guideline 6.7.2(3)(a) of Eurocode 8 states that both braced members can be taken into account if a non-linear static (pushover) global analysis is used. As indicated by the diagram above, however, a pushover analysis with both braced members overestimates the structure's ultimate horizontal load by a factor of 2, rendering this approach extremely unsafe. On the other hand, a pushover analysis considering only the tension diagonal, underestimates the seismic capacity of the structure by a factor of approximately 10%. Finally, the approach using the Eurocode's guideline to consider the compressed bracing's buckling resistance seems to overestimate the collapse load by a much smaller factor. Conclusively, after evaluation of the first 2 possible scenarios in terms of load-bearing capacity, the most effective method of analysis until now is proved to be the MNA (pushover) with one diagonal, as the GMNIA curve is located above the MNA curve and, therefore, the latter is considered to be safer.

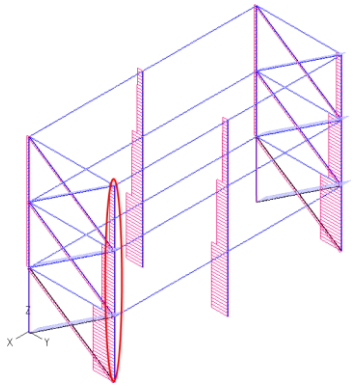

(a)

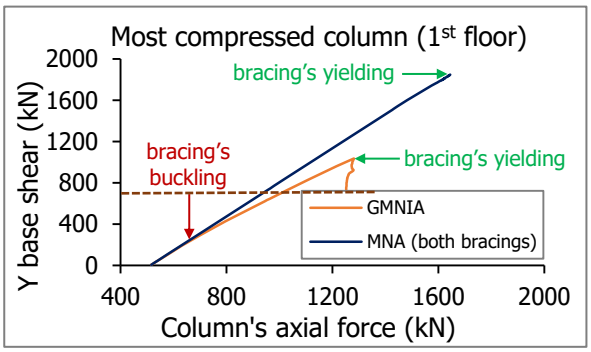

(b)

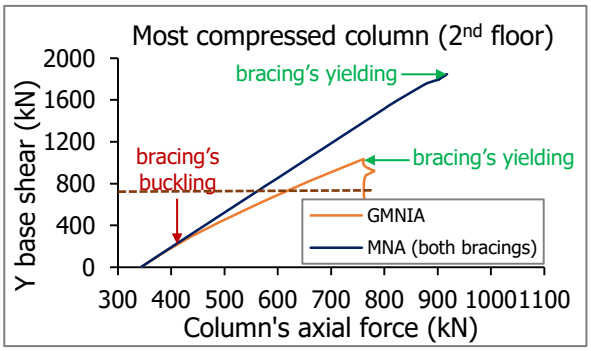

(c)

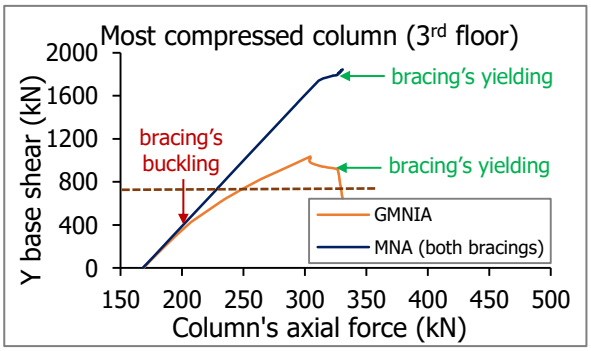

(d)

Figure 3-30: (a) Most compressed column highlighted (b) 1st floor (c) 2nd floor (d) 3rd floor

Same as in Scenario 1, the behaviour of the columns is also investigated in terms of axial forces, in order to evaluate their contribution to the non-linear behaviour of the structure. Concerning the case where both bracings are taken into account, the axial loading versus the seismic base shear retain a linear behavior, with the maximum load reaching two times higher values than in Scenario 1. In this scenario, the columns do not develop any failure due to yielding and, consequently, their behavior remains linear. Obviously, the possibility for buckling is eliminated in the MNA analysis, even though the columns' buckling loads are much higher than those developed. The diagrams for the least compressed columns do not result in any significant conclusions and, therefore, are not presented. Obviously, this scenario is unrealistic and proved that even for twice as high values of base shear, the behavior of the columns remains linear.

3.5 INVESTIGATION OF SCENARIO 3

This scenario approaches the matter under investigation by accounting the compressed bracing's contribution in the static configuration of the structure during the design procedure. The seismic loads, as well as the distribution of axial forces, result in different cross-sections for the braced members, thus leading to different cross-sections for the CBF columns as well. The following figure demonstrates the final outcome when both bracings are considered during the elastic analysis.

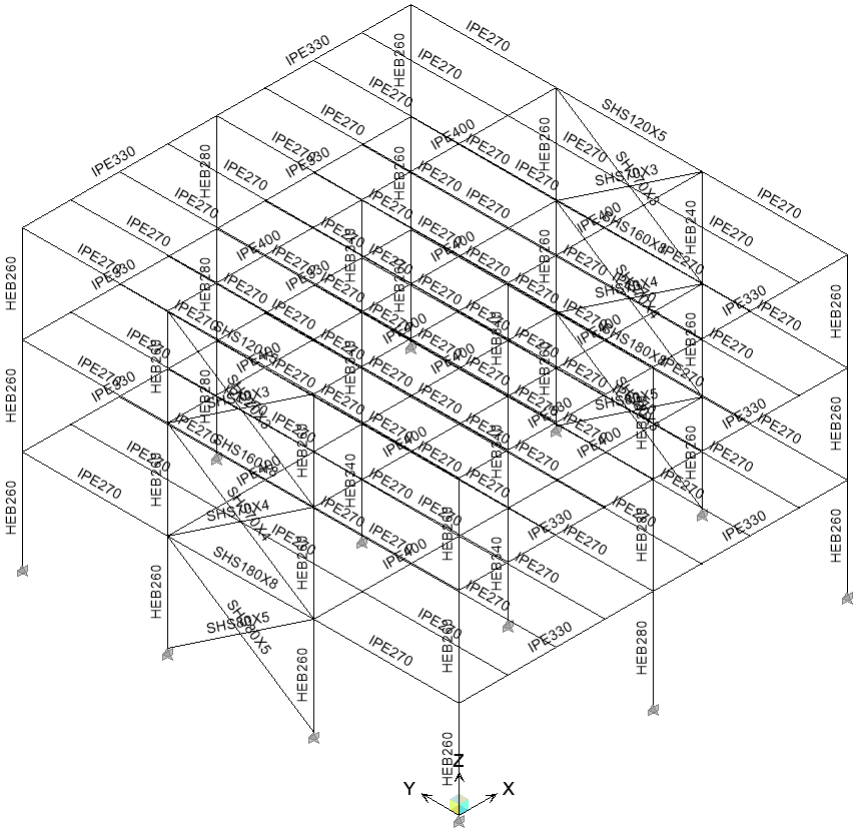

Figure 3-31: Design according to Eurocode based on elastic analysis considering compressed bracing

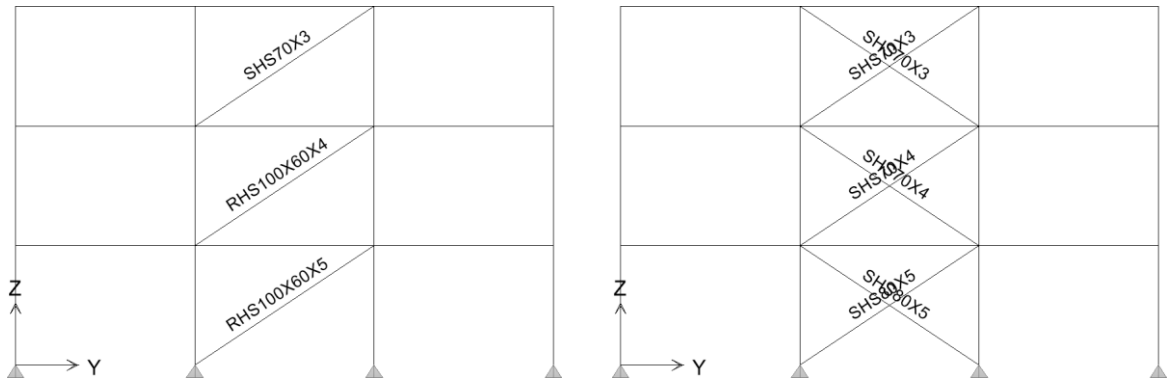

(a) (b)

Figure 3-32: Comparison in the design of the bracing systems for (a) Scenario 1 (b) Scenario 3

Before proceeding to the non-linear results, the following summary table is presented with the most significant characteristics of the braced members as designed in Scenario 3.

Table 3-4: Summary table of plastic axial resistance for compressed bracings

Storey	**Cross-section**	**A (cm^2)**	**L (m)**	**$N_{pl,Rd}$ (kN)**
1	SHS80X5	14.7	3.6	522
2	SHS70X4	10.4	3.6	369
3	SHS70X3	7.94	3.6	282

Table 3-5: Summary table of buckling resistance and elastic critical buckling load for compressed bracings

Storey	**Cross-section**	**i (cm)**	$\bar{\lambda}$	**χ**	**$N_{b,Rd}$ (kN)**	**N_{cr} (kN)**
1	SHS80X5	3.05	1.56	0.35	183	218
2	SHS70X4	2.68	1.77	0.28	103	119
3	SHS70X3	2.73	1.74	0.29	82	94

3.5.1 **Non-linear analysis of material**

A non-linear analysis of material is carried out in order to evaluate the structure's response in terms of a pushover curve, when both diagonals contribute to the design procedure of the structure. The rigidity of the structure in the Y direction is mainly defined by the axial rigidity of the bracings. In addition, the selected cross-sections in this scenario have a similar area to those in Scenario 1. This leads to the conclusion that the ultimate load in an MNA analysis is expected to result in similar maximum values for Scenarios 1 and 3. Additionally, the conclusion reached in Scenario 2, that a pushover curve for both diagonals is rendered unsafe for the structure's ultimate load, should be considered and, therefore, the MNA analyses are carried out from now on considering the tension diagonal only.

Since the ultimate load is defined by the yielding point of the bracings located in the base, a simplified approach is to receive the plastic axial resistance's horizontal component $2Af_y\cos\theta$. The contribution of the other bracing systems is not directly considered in terms of ultimate loading, but their behavior is taken into account in an entirely different manner.

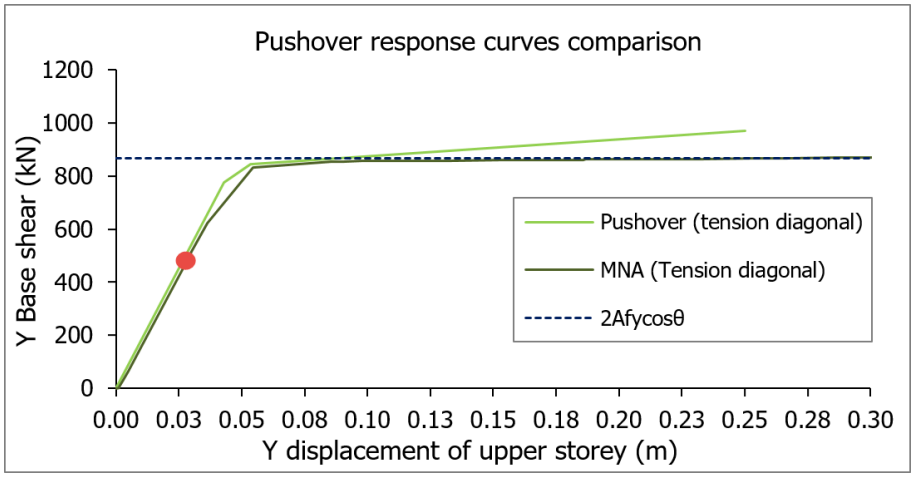

Figure 3-33: Comparison between the pushover curve, the non-linear analysis of material (MNA) and the developed seismic shear

Once the yielding of the upper diagonals takes place, the displacement of the respective storey and, thus, the axial forces of the lowest bracings in the base, increase. Therefore, the ultimate load of the structure is entirely defined by the yielding point of the bracings in the base, however the respective displacement relies on the behavior of all diagonals.

The following figure demonstrates the structure's response in an MNA analysis for the design Scenarios 1 and 3, where the contribution of the compressed bracing has been ignored in both cases. The assumption that the two ultimate loads were expected to be similar to each other, is confirmed.

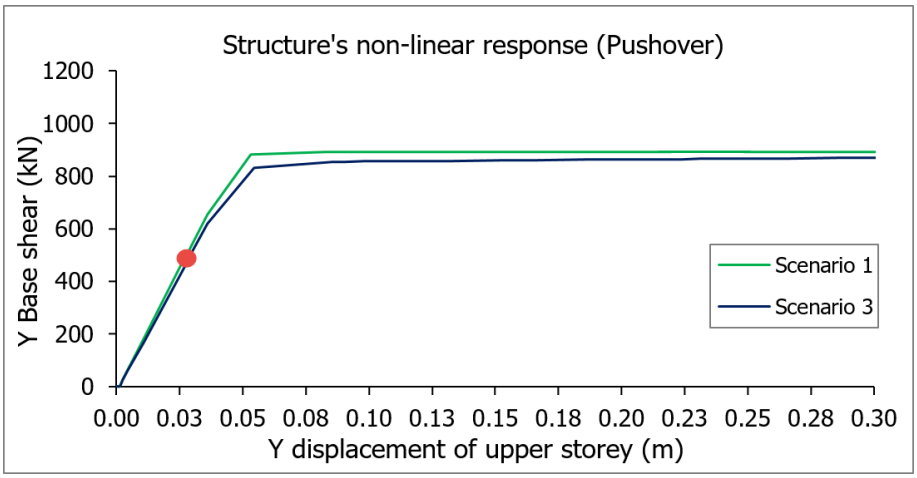

Figure 3-34: Comparison between pushover curves (MNA) for Scenarios 1 and 3

3.5.2 **Non-linear analysis of geometry and material with initial imperfections**

A full non-linear analysis is then carried out in order to examine the structure's response under the new braced members' cross-sections. Despite the fact that the axial rigidity of the bracings remains almost the same between Scenarios 1 and 2, their moment of inertia is entirely different, which results in higher values for the buckling resistance and elastic critical buckling load. Obviously, in the MNA analysis where the geometric non-linearity is not taken into account, the ultimate loads are almost the same, as illustrated in the comparative Figure 3-34. The same conclusion should not be made, however, for a full

non-linear analysis where the geometric non-linearity is considered, due to the different non-dimensional slenderness values in the two Scenarios.

A comparative table is presented afterwards, where typical quantities like non-dimensional slenderness, buckling resistance and elastic critical buckling load are compared for Scenarios 1 and 3.

Table 3-6: Summary table for slenderness, buckling and elastic critical load for Scenario 1

	Όροφος	**Διατομή**	**A (cm^2)**	$\overline{\lambda_y}$	$\overline{\lambda_z}$	**$N_{b,Rd}$ (kN)**	**N_{cr} (kN)**
Σενάριο 1	1	RHS100X60X5	14.7	1.33	1.99	117	133
	2	RHS100X60X4	12	1.31	1.95	99	112
	3	SHS70X3	7.94	1.74	1.74	81	94

Table 3-7: Summary table for slenderness, buckling and elastic critical load for Scenario 3

	Όροφος	**Διατομή**	**A (cm^2)**	$\overline{\lambda}$	**$N_{b,Rd}$ (kN)**	**N_{cr} (kN)**
Σενάριο 3	1	SHS80X5	14.7	1.56	183	218
	2	SHS70X4	10.4	1.77	103	199
	3	SHS70X3	7.94	1.74	82	94

3.5.2.1 Linearized buckling analysis

A linearized buckling analysis was carried out from the beginning, since the selected cross-sections for the selected braced members are different in the two scenarios. The figures located in the appendix demonstrate the buckling modes that were selected and introduced as buckling shapes to the initial imperfections. The critical buckling loads, especially for the first modes, are higher compared to Scenario 1, as the non-dimensional slenderness of the new bracings is decreased and, therefore, higher external loads are required to cause buckling.

3.5.2.2 Definition of initial imperfections

The values for the initial imperfections introduced to the non-linear model, are calculated using the Ayrton – Pery theory and equation (3-1), which assumes a linear inelastic buckling situation.

Table 3-8: Values of initial imperfections for each bracing systems for Scenario 3

Imperfections	**SHS80X5**	**SHS70X4**	**SHS70X3**
e_o (mm)	6.6	6.8	6.9

Since the structure is designed with braced members from the SHS range, the major and minor non-dimensional slenderness are expected to interact with each other. However, in order to decide accurately whether or not to consider both imperfections in the model, the two possible cases were examined. In the first case, a full non-linear analysis is carried out where both in and out of plane imperfections are introduced, whereas in the second no out of plane imperfections are considered in the analysis. The following comparative diagram illustrates the results for these two possible cases.

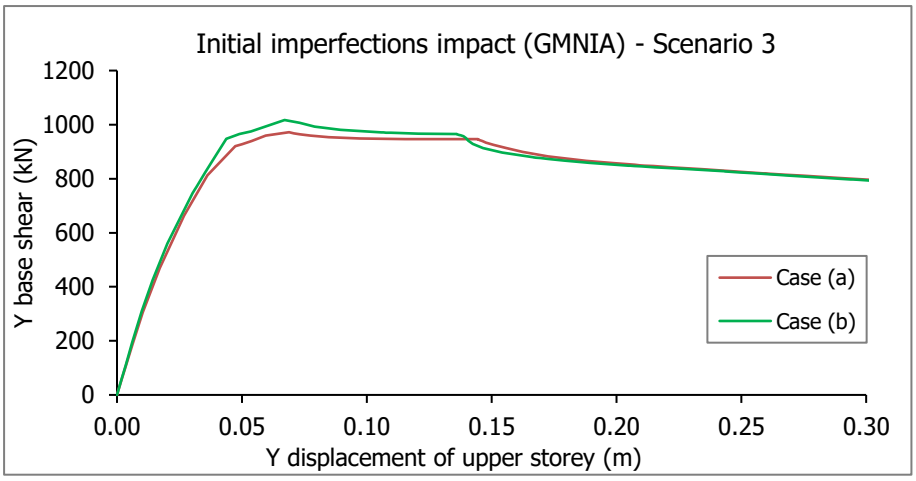

Figure 3-35: Case (a) both in and out of plane imperfections, Case (b) only out of plane imperfections

According to figure 1-37, the structure's behavior for base shear values up to 800 kN is almost identical for the two cases. As the base shear increases and the first buckling takes place, the two curves start to separate from each other. In particular, in case (a) where imperfections in both directions are considered, the ultimate load is 50 kN less than in case (b) where no in plane imperfections are introduced. This difference accounts for 5% of the structure's load-bearing capacity and, although it may seem insignificant in value, since the computational effort is the same for both cases, both imperfections are from now on considered in the full non-linear analysis of the structure.

Subsequently, in order to reach with accuracy any conclusions about the non-linear behavior of the structure, the base shear values for which the buckling and yielding of the bracings take place, are presented in the following figure.

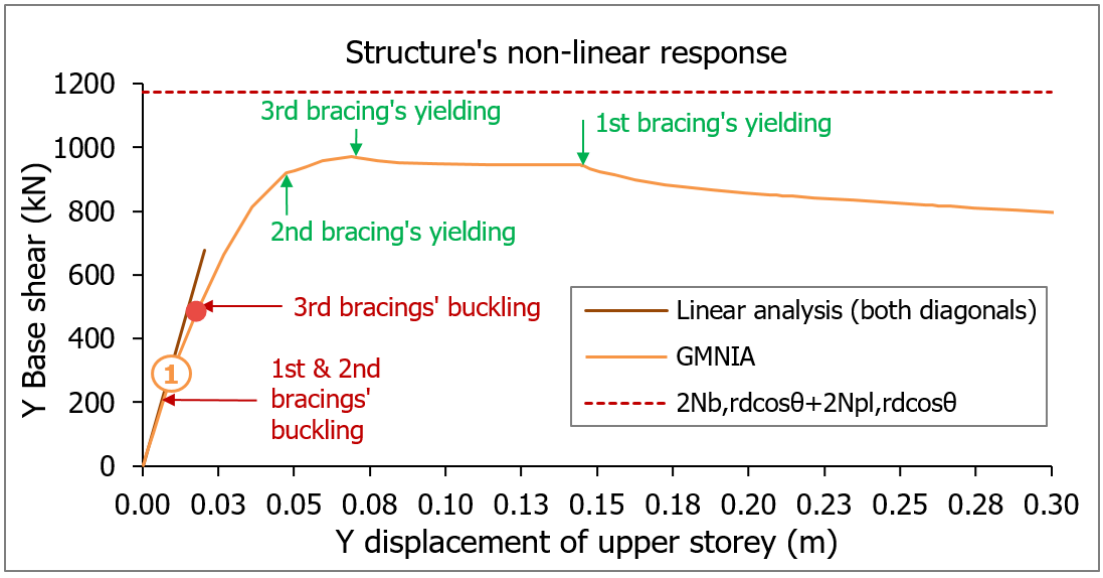

Figure 3-36: Structure's response for non-linear analysis of geometry and material considering both diagonals

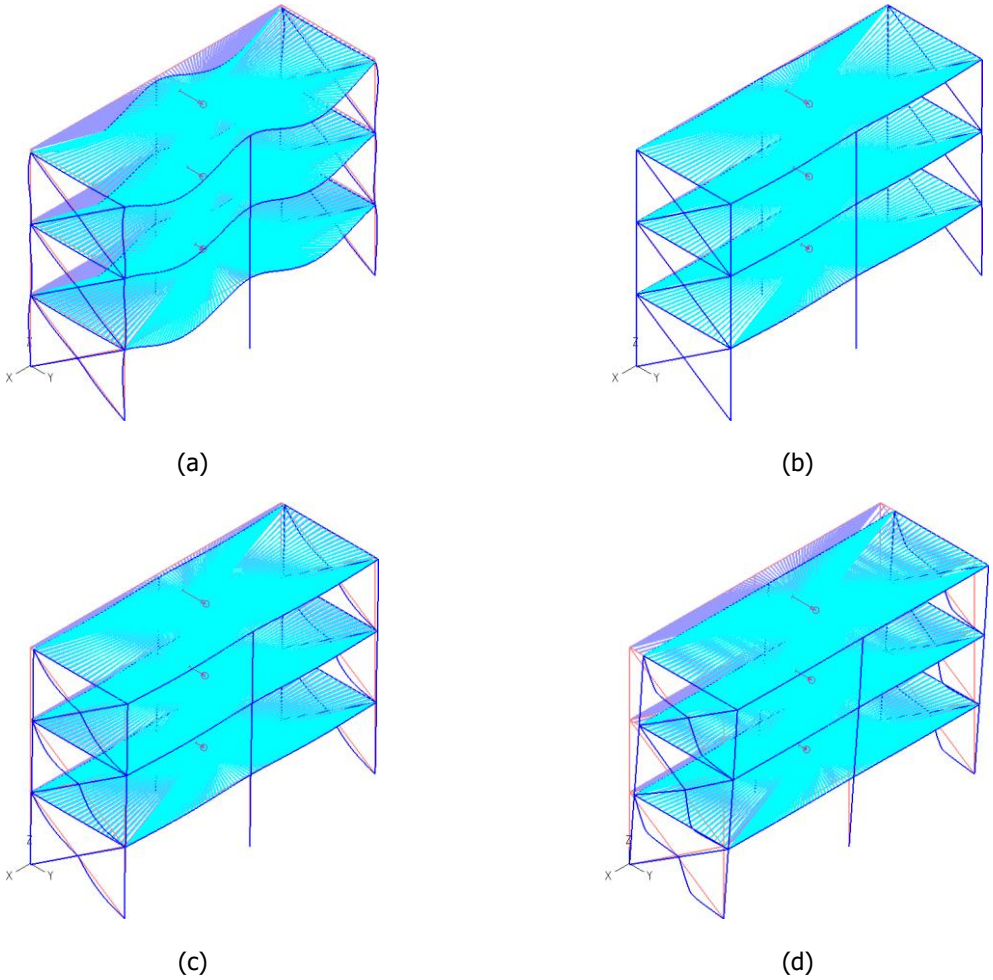

Figure 3-37: Deformed shape of the structure in characteristic points of GMNIA (a) Point 1 for a magnification factor of 10 (b) Point 2 (c) Point 3 (d) Point 4

3.5.2.3 Investigation of the structure's response

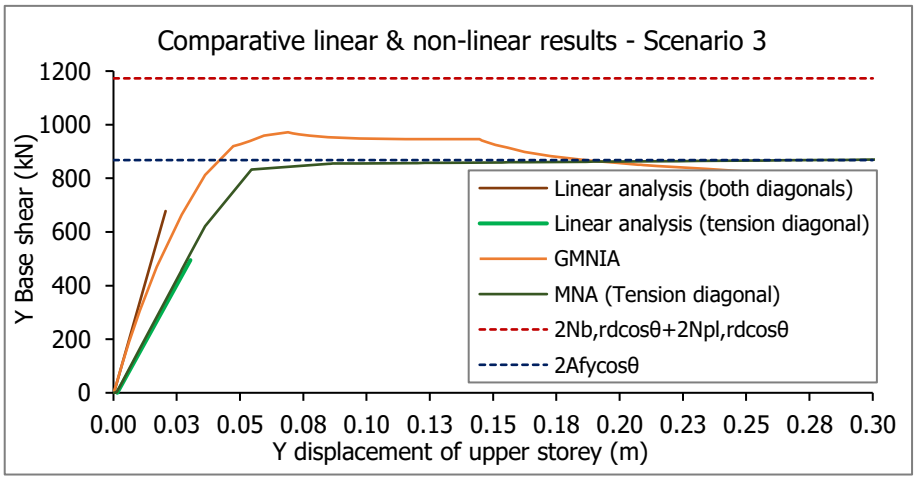

Figure 3-38: Comparison between linear and non-linear methods used to analyze structure's non-linear behavior

For small values of seismic shear, the structure retains its elastic rigidity according to the tangent of the elastic analysis. However, when the first buckling takes place, it starts to develop a non-linear behavior

by reducing the initial rigidity, until it finally approaches the rigidity developed when only the tension diagonal is accounted in the analysis. The following compressed bracings buckle successively, since the non-linear behavior is further amplified as the first bracing member's buckling advances.

Lastly, a simplified attempt was made to predict the ultimate horizontal load using the regulatories of Eurocode 3, in order to consider the contribution of the compressed bracing in the total resistance. Despite the fact that for both Scenarios 1 and 3 this approach predicted the collapse load accurately enough, in the case of Scenario 3, it is proved to be extremely unsafe. The ultimate predicted load reaches the value of 1180 kN, while the 'actual' capacity of the structure is almost 1000 kN, which is off by a factor of 18%. Consequently, in the case of Scenario 3, the approach of the base shear using $2N_{b,Rd}\cos\theta+2N_{pl,Rd}\cos\theta$ is not recommended, as the selected cross-sections include imperfections in both directions that interact with each other, thus resulting in an unexpectedly decreased capacity.

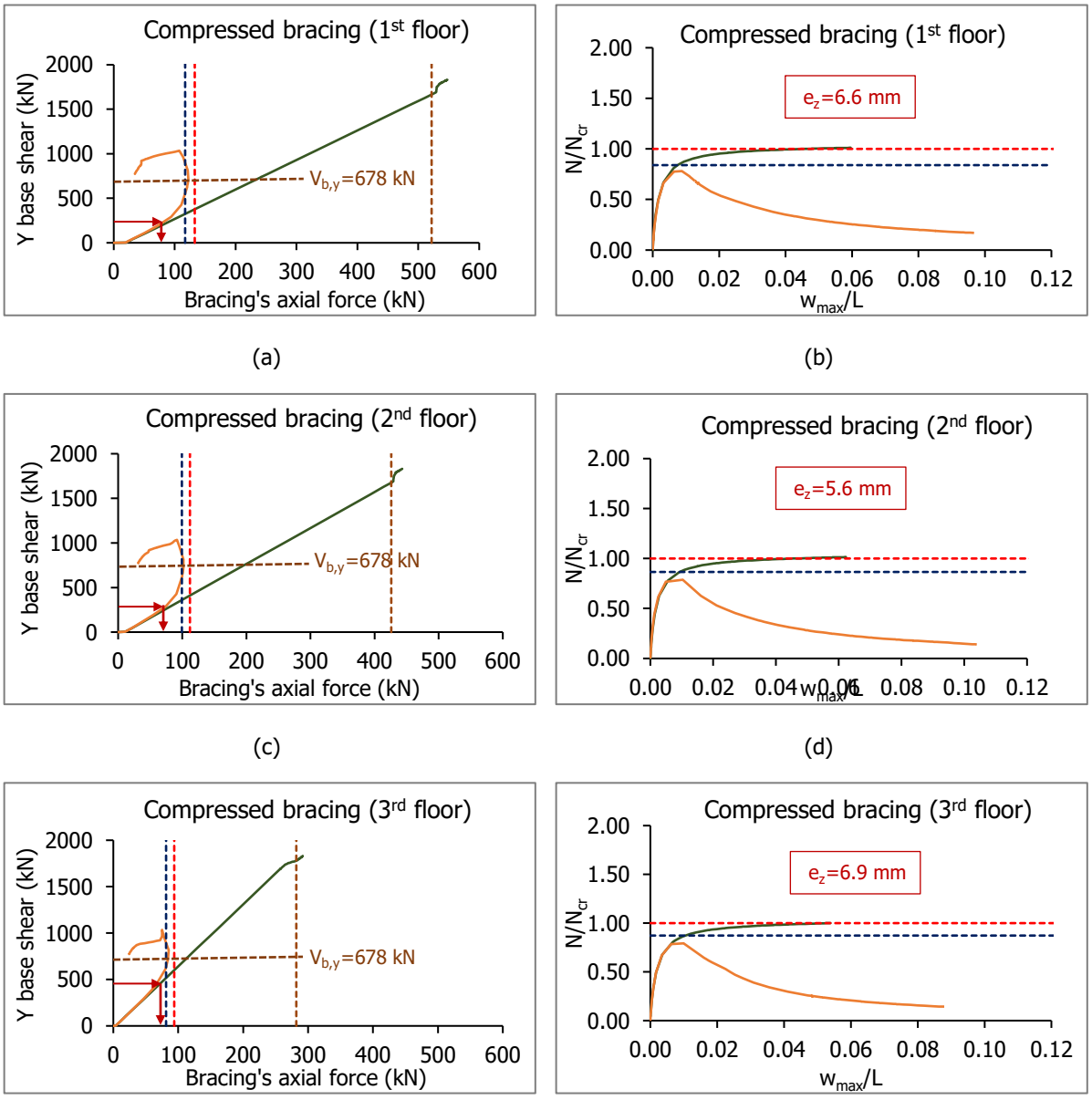

Figure 3-39: Compressed bracing's axial force versus the developed base shear with GMNIA and MNA analysis

Finally, deformation w_{max} accounts for the out of plane displacement of the member's midpoint, even though initial imperfections in both axes are introduced in the compressed member.

The comparison between the full non-linear analysis' maximum load and the member's buckling resistance, leads to the conclusion that the compressed member is unable to take full advantage of its buckling capacity. As opposed to Scenario 1, where the ultimate axial resistance was between the elastic critical load and the buckling resistance, the Eurocode's approach is rendered unsafe. It should be noted that in this case, both in and out of plane imperfections were included and, due to their interaction, the ultimate buckling resistance is lower than analytically calculated with the Eurocode.

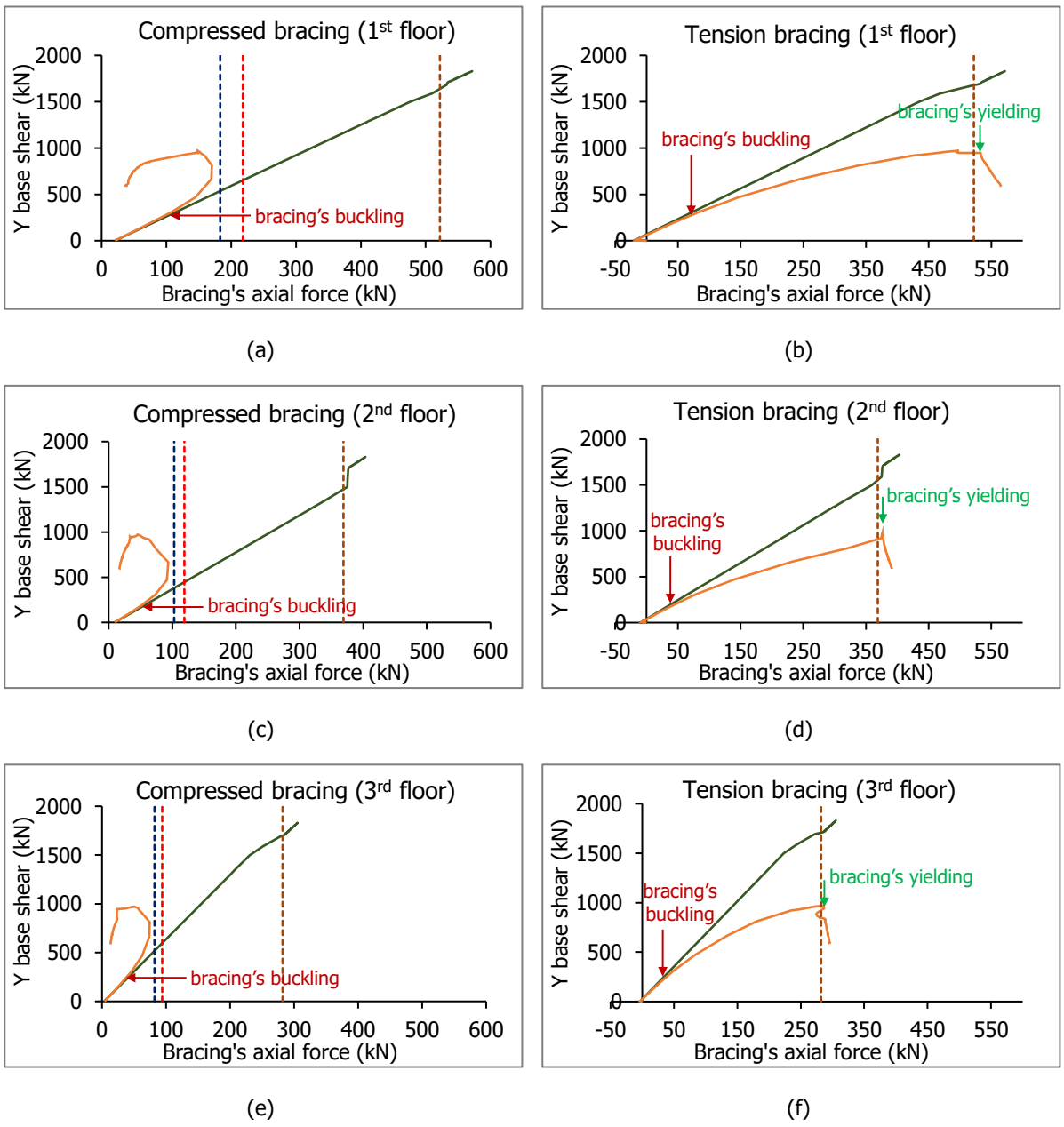

Figure 3-40: Compression and tension axial force versus the developed base shear with GMNIA and MNA analysis with both diagonals for (a) and (b) 1st floor (c) and (d) 2nd floor (e) and (f) 3rd floor of Scenario 3

The diagrams above confirm the assumption that the yielding of the tension diagonal sets the limit for the structure's maximum horizontal capacity. The compressed bracing is unable to resist higher base

shear due to its buckling and, obviously, decreasing axial resistance. Rather, it develops a non-linear behavior, way before its axial force reaches the buckling resistance value.

The compression force developed in the columns directly connected to the bracing systems versus the compressed bracing's resistance is presented in the following diagrams. In particular, the bracing's buckling takes place for small values, which actually delimits the beginning of the non-linear connection between the axial force of the column and the respective bracing. Since the buckling and the yielding of the two bracings do not occur at the same time, the behavior of the axial force of the column is primarily dominated by the compressed bracing. However, the tension diagonals stipulate the maximum axial force columns are subjected to develop during the entire analysis.

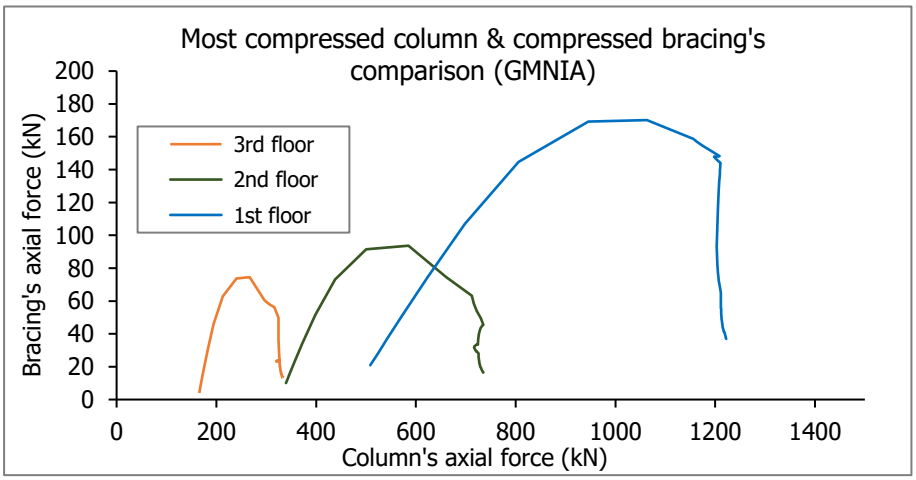

Figure 3-41: Connection between the most compressed CBF column and compressed bracing's behavior

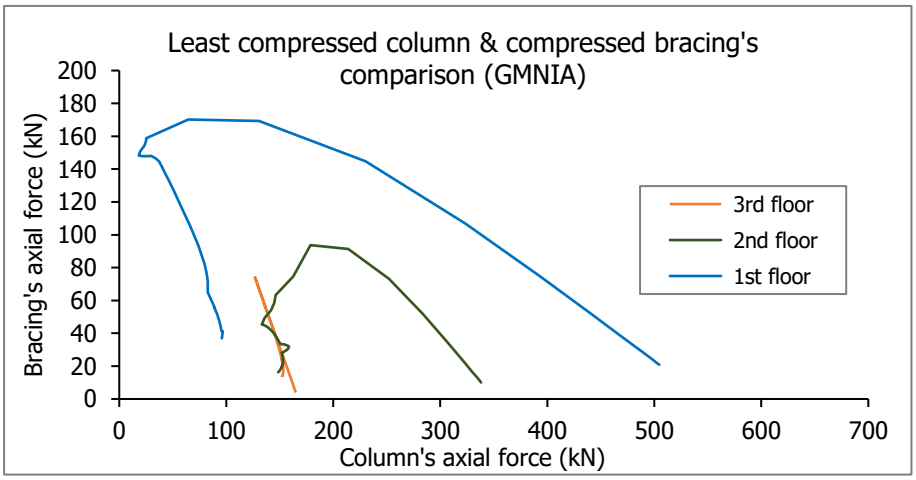

Figure 3-42: Connection between the least compressed CBF column and compressed bracing's behavior

As it has already been mentioned, the capacity design rule which is satisfied for all possible plastic joints positions ($\sum MR_c \geq 1.3 \cdot \sum MR_b$), in conjunction with the damage limitation checks ($dr \cdot v \geq \alpha \cdot h$), were definitive for the design of the columns. As a result, the behavior of the columns remains linear and they are not affected in terms of yielding or buckling for any seismic shear in this scenario as well.

3.5.3 Investigation of the non-dimensional slenderness limit

Another worth mentioning conclusion can be reached regarding the non-dimensional slenderness limitation or $1.3 \leq \bar{\lambda} \leq 2.0$. Eurocode 8 stipulates the lower limit in order to avoid overloading the columns in the prebuckling stage, where both compression and tension diagonals are active. In this case, however, where columns demonstrate an increased capacity in terms of internal forces, even for seismic shears above the design earthquake's value, this specific limit seems to have no practical meaning.

The most definitive parameter for the design of the braced members was the upper limit of the non-dimensional slenderness. Not only is it imposed so as to prevent the elastic buckling of the compressed bracing, but also to reduce the plastic out of plane deformation of gusset plates which are prone to low-cycle fatigue failure. As a matter of fact, especially in Scenario 3, the cross-sections of the bracings were increased entirely due to the non-dimensional slenderness limit. In the following paragraphs, the difference between the case where the bracings' design abides by the non-dimensional slenderness limitations and the situation where it does not, are examined.

It should be noted that the only parameter under investigation here, is the upper limit Eurocode 8 stipulates for the non-dimensional slenderness. Consequently, in order to focus our interest in this specific parameter, all other cross-sections in the structure remain identical for both cases. The difference concerning the seismic capacity of the structure between these two cases is illustrated below.

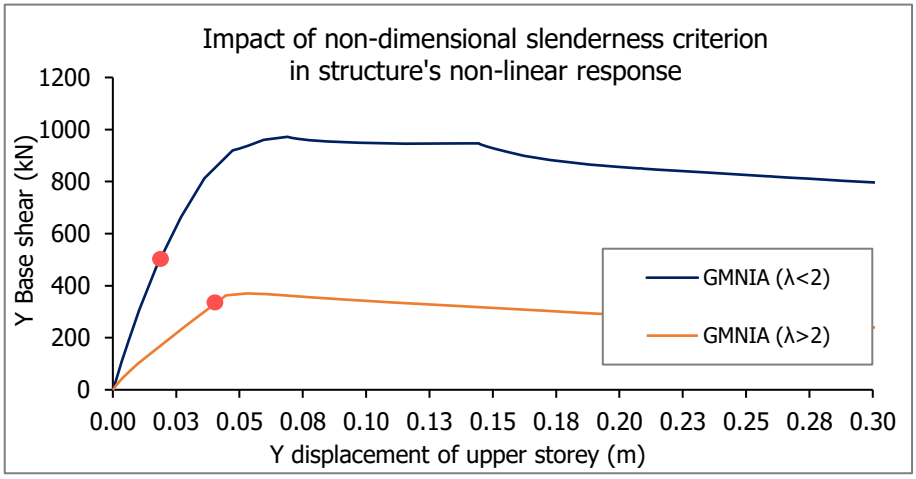

Figure 3-43: Structure's response between the cases when the non-dimensional slenderness limit is satisfied (λ<2) and not (λ>2)

Table 3-9: Summary table of characteristics for compressed bracings when slenderness limits are satisfied

	Storey	Cross-section	A (cm²)	$\bar{\lambda}$	$N_{b,Rd}$ (kN)	N_{cr} (kN)	e_o (mm)
Scenario 3 (λ < 2)	1	SHS80X5	14.7	1.56	183	218	6.6
	2	SHS70X4	10.4	1.77	103	199	6.8
	3	SHS70X3	7.94	1.74	82	94	6.9

Table 3-10: Summary table of characteristics for compressed bracings when slenderness limits are not satisfied

	Storey	Cross-section	A (cm^2)	$\bar{\lambda}$	$N_{b,Rd}$ (kN)	N_{cr} (kN)	e_o (mm)
Scenario 3 ($\lambda > 2$)	1	CHS60.3X3.2	5.74	2.35	34	38	6.2
	2	CHS48.3X4	5.57	3.02	20	22	6.1
	3	CHS33.7X3.2	3.07	4.39	5	6	6.1

The design of the bracings was carried out for all seismic combinations and for all checks according to Eurocode 8 for bracing systems, except for the non-dimensional slenderness check which is currently investigated.

In the case where the bracings' design abides by the non-dimensional slenderness limitation, the structure acquires overstrength in comparison to the design earthquake's shear. In particular, the first buckling takes places for a seismic shear of 200 kN, the required base shear has a value of 494 kN, while the structure's ultimate horizontal load is 1000 kN. It should be noted that although the slenderness limit refers to the compressed bracing, it defines the cross-section of the tension bracing as well. The design earthquake does not have a specific direction, the role of tension and compression alternates between the two bracings.

On the other hand, when the non-dimensional slenderness upper limit is not satisfied, the structure's seismic capacity is significantly reduced. The most important conclusion, however, lies on the fact that the structure seems marginally able to resist the required seismic shear and, consequently, the design earthquake. More specifically, the structure's ultimate load in the second case is 370 kN, whereas the design base shear accounts for 332 kN, with buckling taking place for extremely small earthquakes. The main reason for this non-acceptable behavior is the fact that the cross-sections were selected ignoring the non-dimensional slenderness' upper limit and their design was based merely on axial capacity and the limit of 25% Ω_{min}. No additional margin of capacity is left in case the seismic design actions exceed their nominal values.

Finally, the columns are not necessary to be checked for buckling or yielding, since not only smaller seismic actions are developed, but also because the compressed bracing's buckling in conjunction with the yielding of the tension diagonal take place for extremely small seismic shears.

Conclusively, the non-dimensional slenderness limitation $1.3 \leq \bar{\lambda} \leq 2.0$ and especially the upper limit that was investigated above, becomes very crucial for the design of the braced members. It goes without saying that both non-dimensional slenderness limits must be met, not only because Eurocode stipulates so, but also because its non-compliance has proved detrimental effects in the total capacity of the structure.

3.6 INVESTIGATION OF SCENARIO 4

As mentioned in §2.8, in an attempt to approach the matter of the compressed bracing and its contribution to the actual response of a regular steel building according to Eurocode 8, a different scenario which lies between Scenarios 1 and 3, is defined. Scenario 4, now, assumes that both bracings are considered in the structural configuration and, consequently, in the elastic analysis. However, the

design of the bracings is based on two basic assumptions: firstly, half of the cross-section's area is taken into account in order to consider the contribution of both bracings in the structural systems and, secondly, the design force is twice the maximum axial force developed only on the tension diagonal for all seismic combinations.

All seismic actions developed in the structure are calculated with the full area of the cross-sections and, thus, axial rigidity of the bracings. The final outcome under these two circumstances and when all checks and requirements according to Eurocodes are fulfilled, is demonstrated in the following figure. The design of all members in the structure reaches the same outcome as Scenario 3, so the aforementioned assumptions do not seem to have any effect. Since there was no particular change in the design, there is no point in investigating the structure's response from the beginning, as it has been extensively examined in paragraph 1.5.

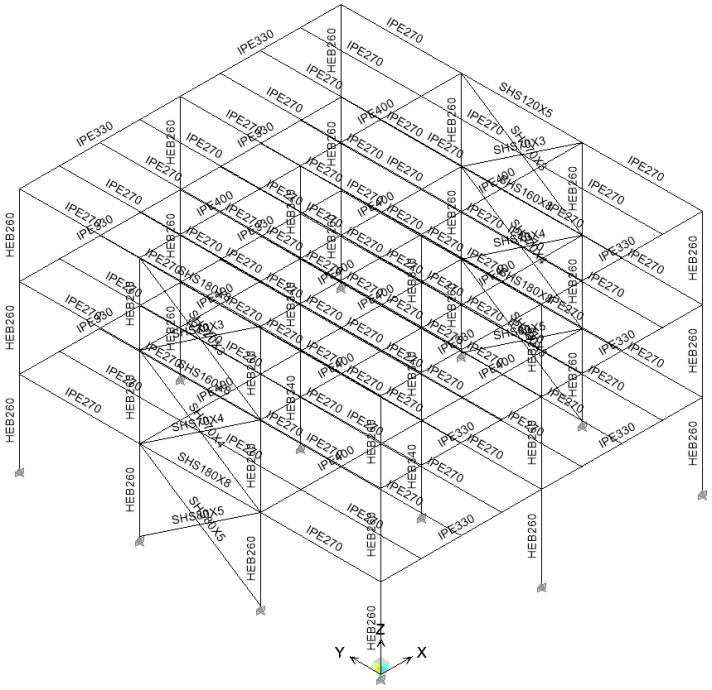

Figure 3-44: Design based on half cross-section area and twice the tension axial force according to Eurocodes

3.7 INVESTIGATION OF SCENARIO 5

The matter under investigation in this paragraph is to assess the influence of capacity design in the seismic response and not evaluate the performance of this scenario. No capacity design requirements are fulfilled and, consequently, the bracings are designed based on their axial resistance only. Obviously, due to the large deformations developed as a result of the premature buckling of the compressed bracing, the influence of P-Δ effects is expected to be very significant. It is worth mentioning that, although during the non-linear analyses only the direction of the CBF system is examined, where the columns do not participate actively in the structural configuration, their contribution is indirectly considered during the modelling of the bracings in §2.9.

Table 3-11: Summary table of useful characteristics for compressed bracings for Scenario 5a

	Storey	Cross-section	A (cm^2)	$\bar{\lambda}$	$N_{b,Rd}$ (kN)	N_{cr} (kN)
Scenario 5 (S355)	1	CHS60.3X3.2	5.74	2.35	34	38
	2	CH48.3X4	5.57	3.02	20	22
	3	CHS33.7X3.2	3.07	4.39	5	6

3.7.1 Non-linear analysis of material

First of all, a non-linear analysis of material is carried out in order to assess the ultimate horizontal load of the structure in terms of a pushover curve. For the same reasons already stated in §3.4, only one diagonal is considered in the analysis. Obviously, since there is no possibility for any form of buckling to take place, any of the compressed or tension bracings can be ignored. The maximum developed base shear reaches the value of 350 kN, which is higher than the design earthquake's base shear of 327 kN. Consequently, when the seismic code is ignored, the results extracted from a pushover curve where only the material non-linearity is considered, clearly illustrate the necessity of capacity design in case the nominal values of the seismic force are exceeded compared to the design.

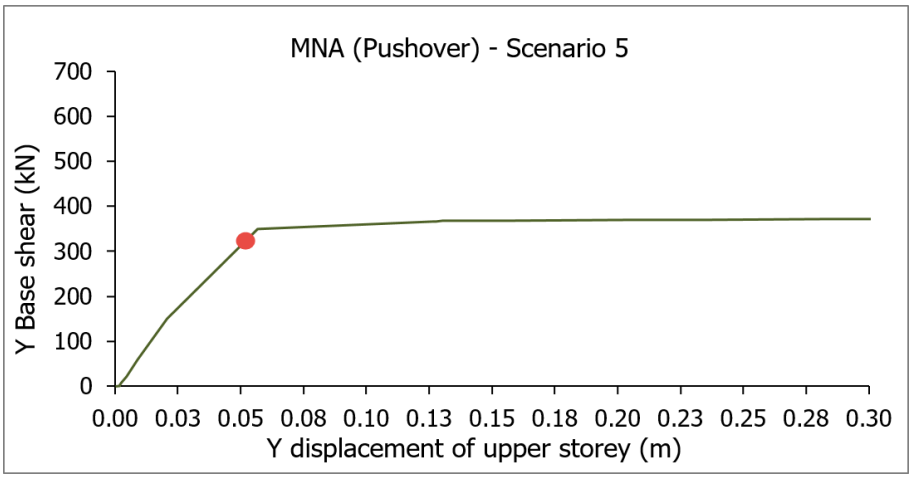

Figure 3-45: MNA response for Scenario 5 when only the tension diagonal is considered in the design

3.7.2 Non-linear analysis of geometry and material with initial imperfections

A pushover curve has been proved to underestimate the seismic capacity of the structure in all previous scenarios, thus becoming a trustful tool for the quick and effortless estimation of the structure's collapse load. Nevertheless, no matter how promising this conclusion seems, it cannot be blindly applied in scenario 5 as well, because the structure is designed using a completely different approach. Since the compressed bracings do not comply with the non-dimensional slenderness limits and the columns are not capacity designed, it is mandatory to examine the structure's response using a non-linear analysis.

According to the results of the following GMNIA curve, the maximum resisting load reaches a value of 590 kN first and then continues to increase. The required horizontal load is calculated for the tension diagonal only and has a value of 395 kN. The GMNIA analysis in comparison to the MNA results verifies the conclusion, that a pushover curve underestimates the 'actual' resisting horizontal load.

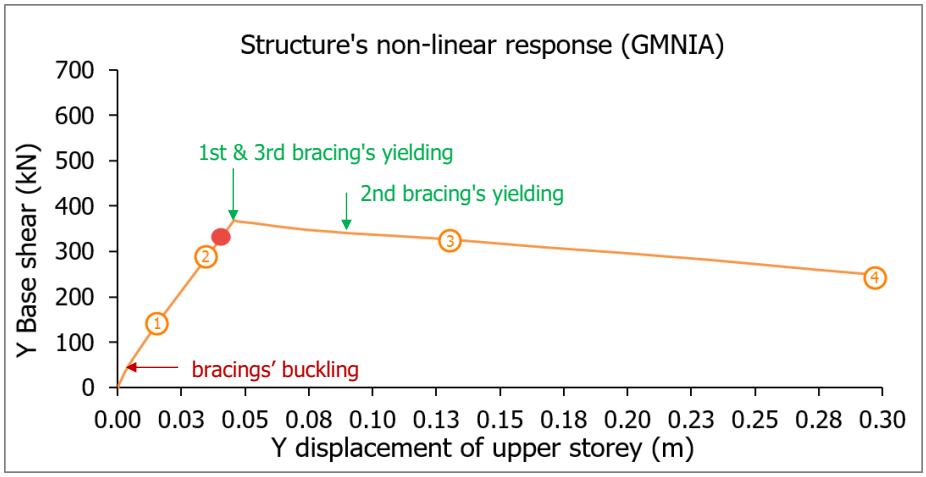

Figure 3-46: GMNIA response for Scenario 5 when only the tension diagonal is considered in the design

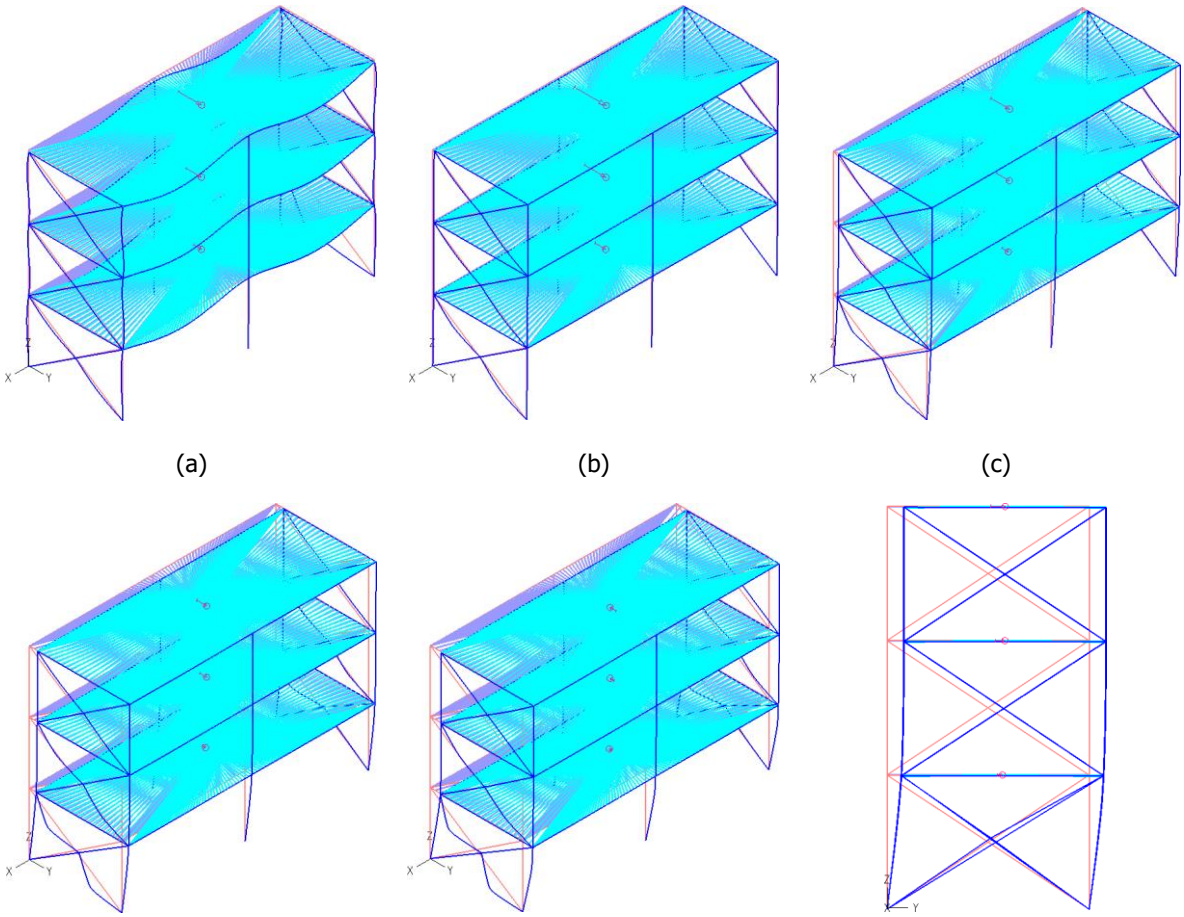

Figure 3-47: Deformed shape of the structure in characteristic points of GMNIA (a) Point 1 for a magnification factor of 50 (b) Point 2 (c) Point 3 (d) Point 4 (e) Point 5 (f) Elevation in Point 5

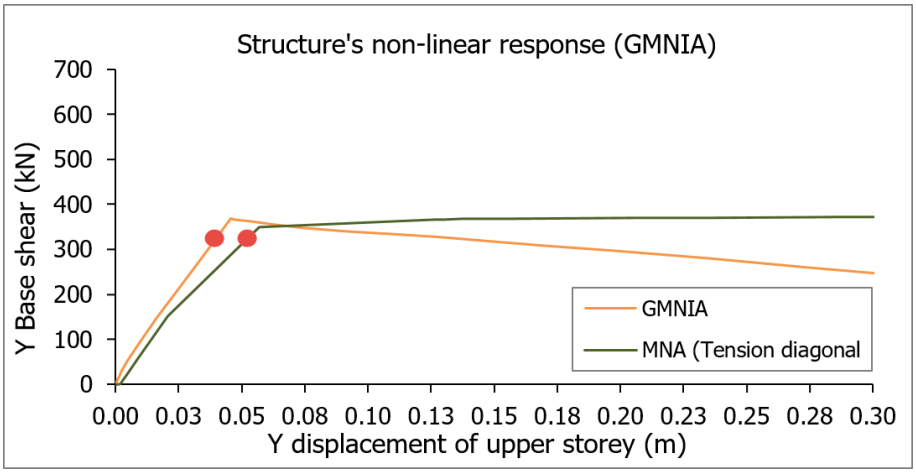

Figure 3-48: Comparison between MNA and GMNIA approaches of the structure in Scenario 5

After the evaluation of the structure's total response, comparative diagrams for the three predominant scenarios concerning the loading of the columns, are presented. Scenario 5 is the most favorable in terms of compression, as the bracing's buckling takes place for very small values of the base shear. Scenarios 1 and 3, on the other hand, are the most unfavorable for the most compressed column because the seismic loads are increased due to the increased cross-sections. On the other hand, the lower the non-dimensional slenderness, the higher the load-bearing capacity of the structure as both bracings remain active before buckling for increased seismic shears. As a result, the compression the columns directly connected to the bracings have to resist, is significantly increased as well.

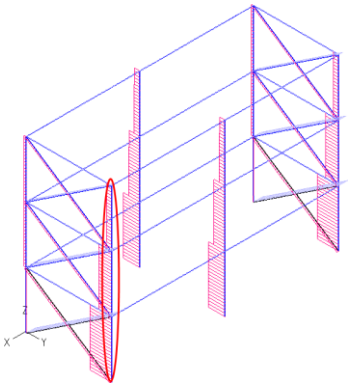

(a)

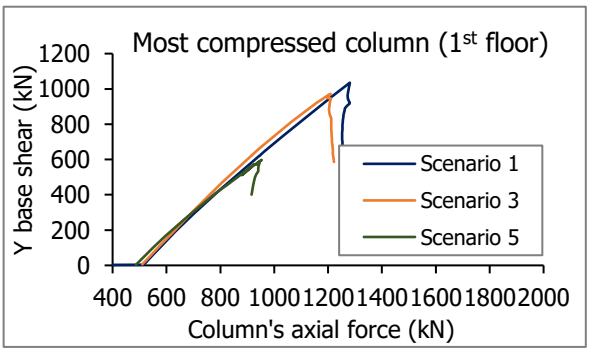

(b)

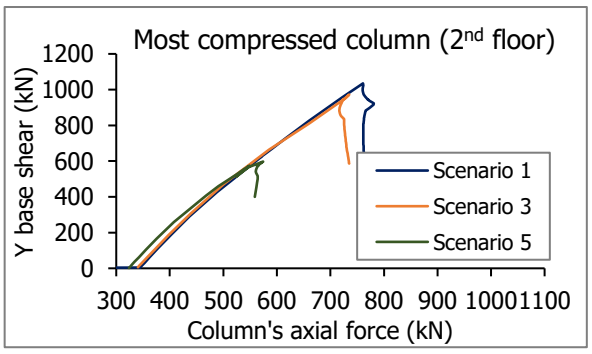

(c)

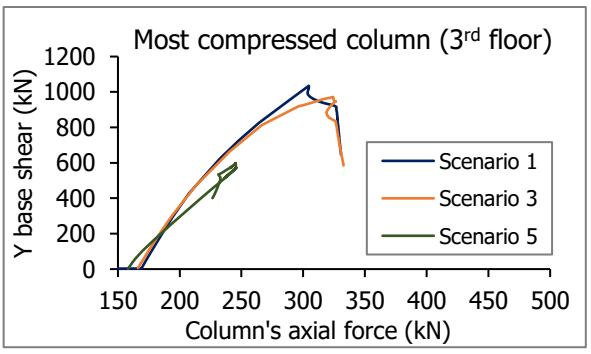

(d)

Figure 3-49: (a) Most compressed column highlighted (b) 1st floor (c) 2nd floor (d) 3rd floor for all Scenarios

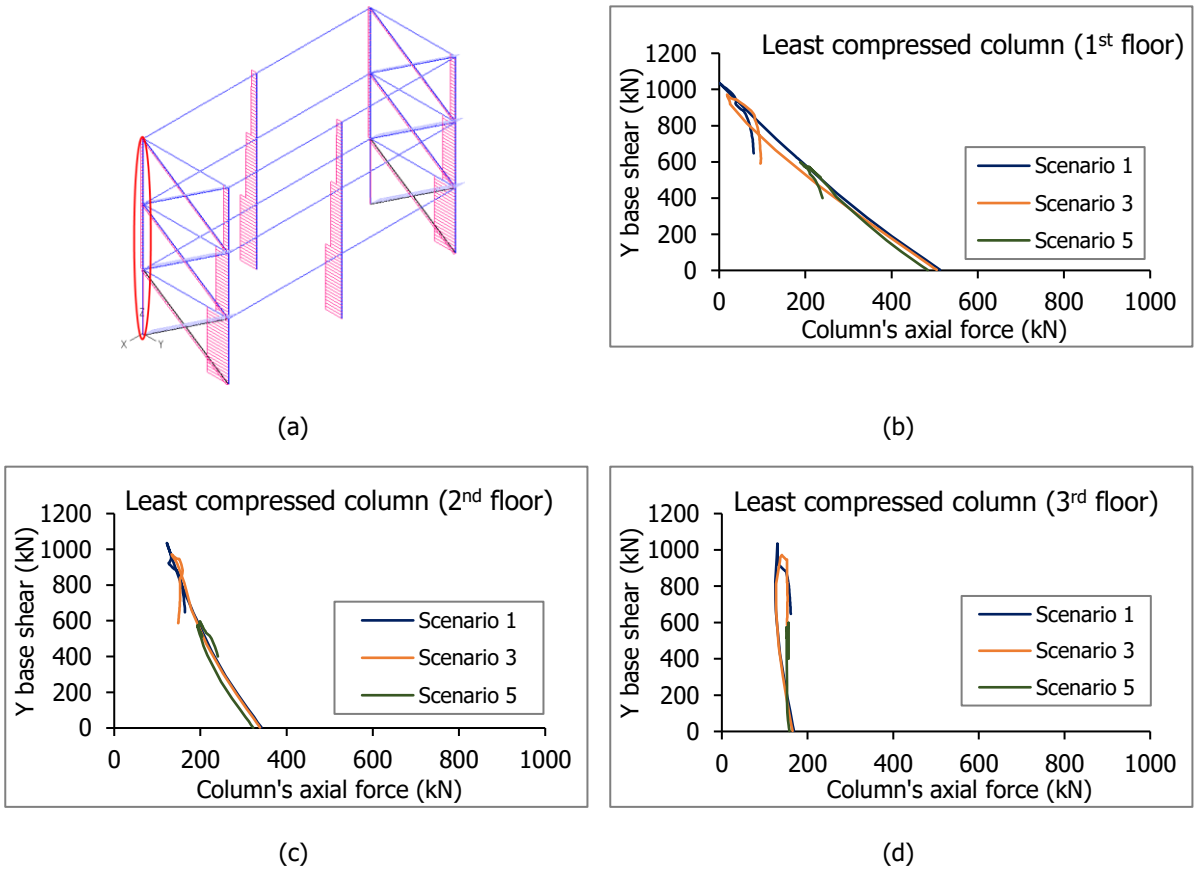

Figure 3-50: (a) Least compressed column highlighted (b) 1st floor (c) 2nd floor (d) 3rd floor for all Scenarios

The investigation of the diagrams concerning the most compressed columns, create a more comprehensive picture about this scenario, where the columns have been designed by considering their capacity only in terms of internal forces. It is very important to decide whether or not any yielding takes place in the CBF columns. Any possibility for buckling does not exist, due to the fact that the maximum axial force developed in the columns during the analysis is far from its buckling resistance load. In order to reach, although, the conclusion concerning their yielding, an additional non-linear analysis is carried out using elastic material with a maximum yielding strength of 355 MPa without any hardening and with negligible plastic strain in the CBF columns and inelastic for the bracings.

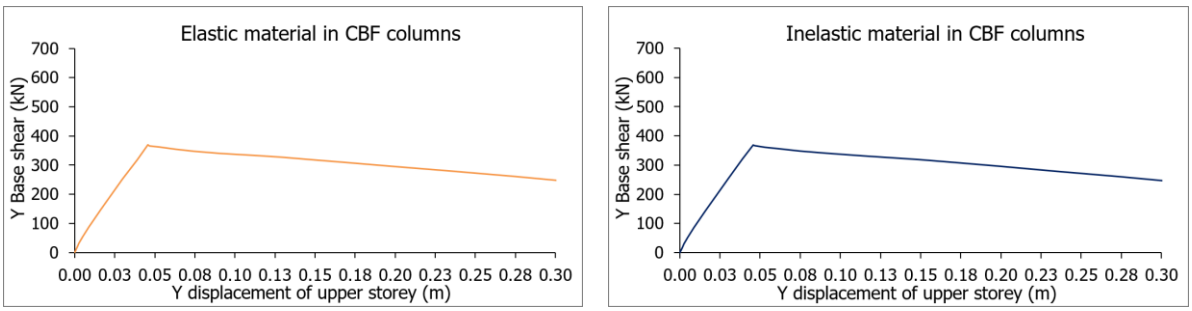

Figure 3-51: GMNIA analysis of the structure for (a) inelastic material to all members (b Elastic material to CBF columns and inelastic to all other members

The two non-linear analyses of the structure come to absolute agreement and, therefore, prove that even in this case where columns do not comply with the capacity design concepts, both buckling and yielding behaviors are prevented.

3.7.3 **Parametric study for the material**

Up to this point, the contribution of the seismic code to the structure's load-bearing capacity has not been highlighted yet. Figure 3-48 demonstrates the ability of the structure to resist marginally the required seismic loads for either type of non-linear analysis, which raises questions regarding the necessity of the application of seismic codes. In order to address the answer to such concerns, the basic concepts and foundations revolving around the capacity design should be addressed.

One of the main principles in the philosophy of capacity design is to avoid the possibility of partial or total collapse of the structure and, thus, the following two factors should be taken into consideration:

- the structure should be able to resist seismic loads for the design earthquake or in case the seismic actions exceed the design earthquake's, without any danger of partial or total collapse (avoidance of the development of soft storey mechanism)
- the structure should be able to resist the developed seismic loads in case the members' nominal resistance is less than calculated during the design, by preventing any danger of partial or total collapse

The first point is satisfied through the weak beam/strong column checks in the X direction, whereas in the main direction of the earthquake, through the internal force capacity checks of the CBF columns. The second point, however, is separately examined under the assumption that the characteristic yielding value of the material in design differs from that in reality. In particular, a variety of different grades of steel and for all possible scenarios is investigated, starting from grade S355 and resulting in S275, which is of course an unrealistic approach, studied only to develop a more comprehensive picture of the phenomenon. The two main structural elements activated in the direction of the earthquake are the CBF columns and the braced members. Finally, a reduction in the grade of the bracings has a favourable effect in the capacity design of the CBF columns, while, on the other hand, leads to the reduction of the structure's total seismic capacity.

3.7.3.1 Parametric study for the material of the CBF columns

The current seismic design practice and codes penalize the non-dissipative members, such as the CBF columns, with high overstrength demand in order to safeguard the occurrence of plasticity only in the braces. Furthermore, it has to be ensured that the braces undergo plastic deformations on each floor in order to utilize the maximum available capacity of dissipation.

The following diagrams aim to represent the effect to the load-bearing capacity of the structure for all scenarios, when the CBF columns' material is modified. The reason for modifying the material exclusively in the CBF columns and not in all existing columns, is because the only columns affected axially during an earthquake in the Y direction, are those directly linked to the bracings. The rest of the members retain their yielding strength of the initially selected steel grade of S355. It appears that the parametric

study for the material of the CBF columns illustrates that any modification to the grade of the steel has absolutely no effect in the seismic capacity of the structure. The main reason for this outcome is based on the fact that the CBF columns are capacity designed in such a way that, even for extremely low grades of steel, no form of yielding or buckling takes effect.

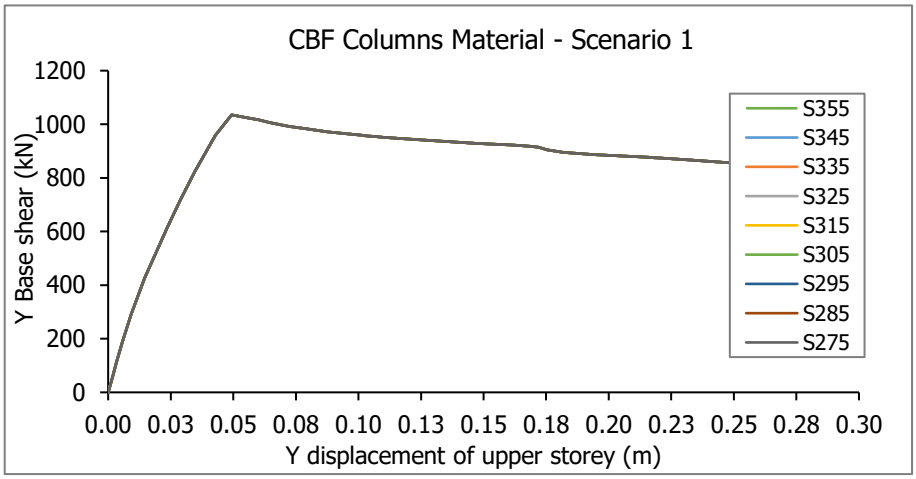

Figure 3-52: Parametric study for all steel grades for the material of the CBF columns in Scenario 1 using GMNIA

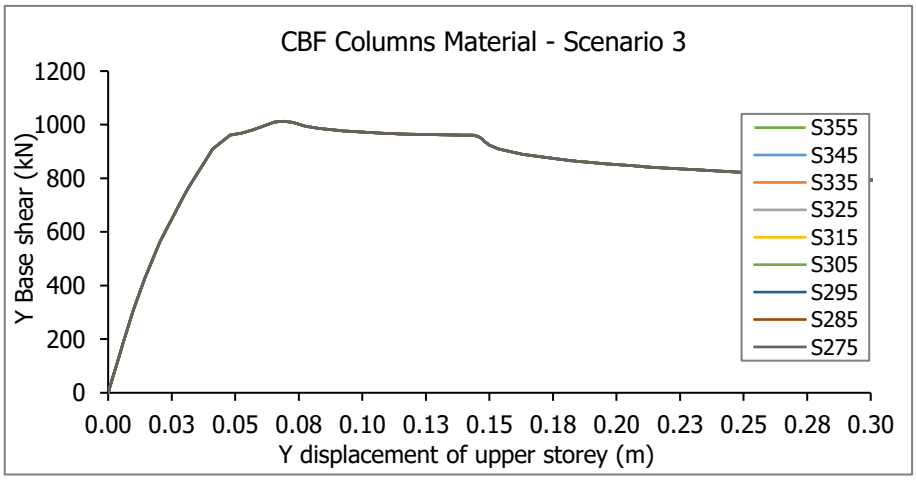

Figure 3-53: Parametric study for all steel grades for the material of the CBF columns in Scenario 3 using GMNIA

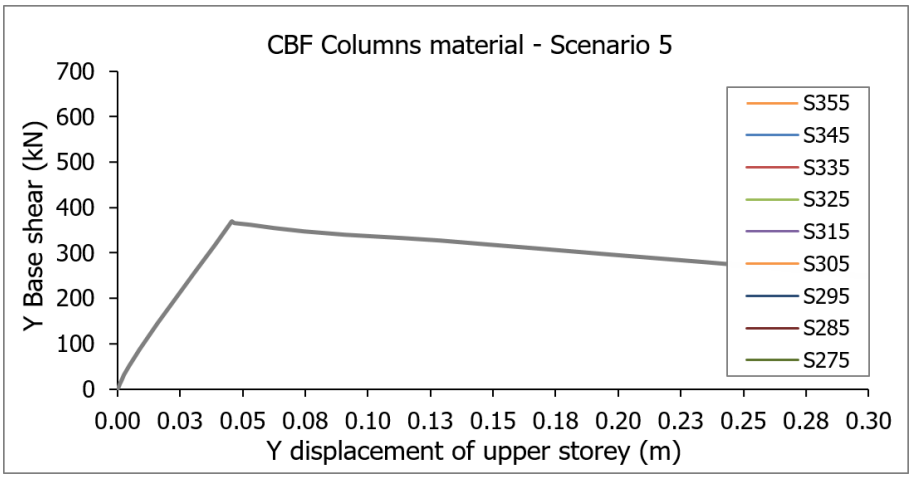

Figure 3-54: Parametric study for all steel grades for the material of the CBF columns in Scenario 5 using GMNIA

3.7.3.2 Parametric study for the material of the bracings

This paragraph examines the effect in the load-bearing capacity of the structure, where the material of the bracings is modified. Since the bracings are the only elements responsible to resist the seismic loads in the Y direction, they are expected to be significantly affected by the reduction in the yielding strength of their material. The parametric studies below are carried out for all scenarios and lead to the conclusion that the structure's ultimate load drops almost analogically as the grade of the steel is reduced. In both Scenarios 1 and 3, even for the lowest grade of S275, the structure retains its ability to resist the required base shear. In addition, all curves coincide in the 3 scenarios, almost until the first yielding takes place. Finally, the design base shear when only the tension diagonal is considered is defined as a benchmark for the evaluation of the structure's horizontal capacity, since the compressed bracing has already lost its axial rigidity due to buckling during the design earthquake.

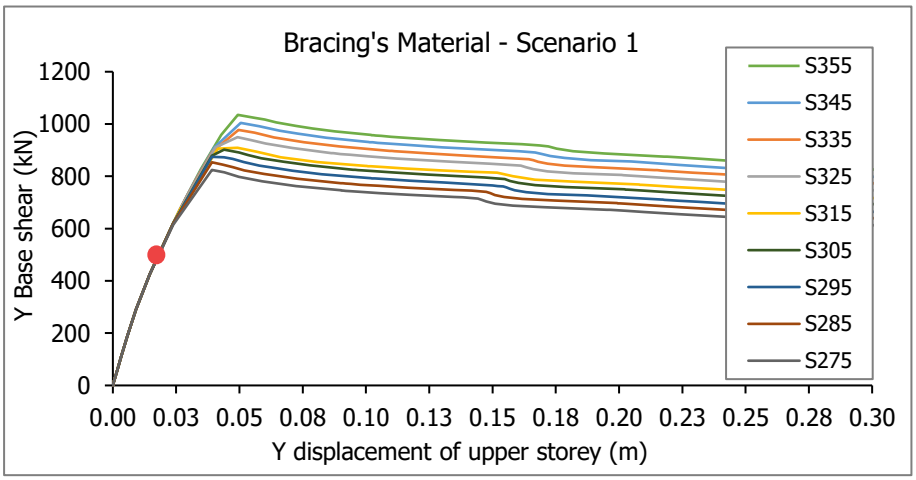

Figure 3-55: Parametric study for all steel grades for the material of the bracings for Scenario 1 using GMNIA

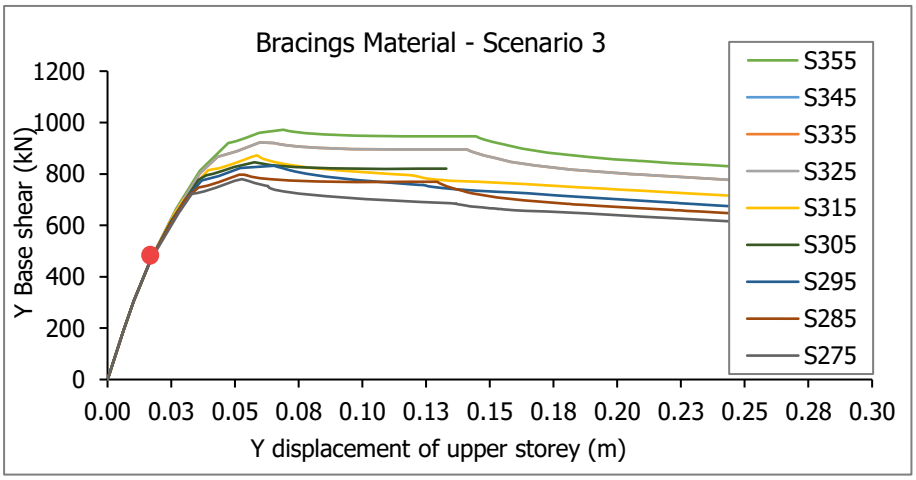

Figure 3-56: Parametric study for all steel grades for the material of the bracings for Scenario 3 using GMNIA

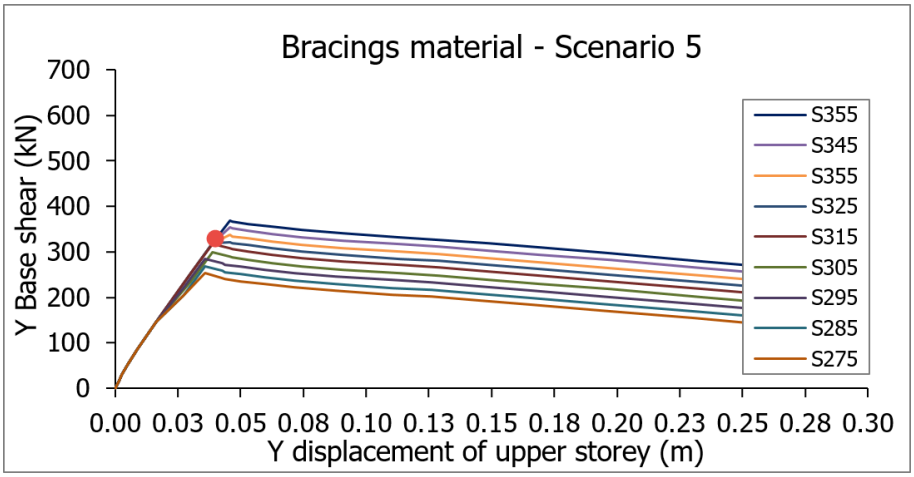

Figure 3-57: Parametric study for all steel grades for the material of the bracings for Scenario 5 using GMNIA

The parametric diagram above illustrates the necessity of seismic codes in the structure's total seismic capacity. The two main principles of capacity design mentioned in the beginning of the paragraph should be fulfilled at the same time. This means that in case the actual yielding strength of the bracings is lower that specified during the design, the structure should still be able to resist adequately the design seismic loads without any danger of partial or total collapse. Considering the diagram above, this requirement is not met in the cases of S355, S345 and S335, where the structure's maximum horizontal load comes very close to the required base shear, thus leaving no adequate margin for the design earthquake. Moreover, the structure is completely unable to resist the required seismic shear in the cases of S315, S305, S295, S285 and S275 grade, thus demonstrating the invaluable necessity of capacity design, especially in the bracings. The CBF columns, on the other hand, even when they are not capacity designed, due to the fact that the developed shear is very close to the ultimate load, do not present any failure either due to buckling or yielding.

3.8 COMPARATIVE DEMONSTRATION OF ALL SCENARIOS

In previous paragraphs, the most possible approaches and attempts were presented in order to develop a more comprehensive understanding regarding the actual behavior of a concentric bracing system. In particular, 5 scenarios focusing on different methods of design were created and, afterwards, compared and evaluated using non-linear analyses. Scenario 5 was established only for the parametric investigation of the material's impact and to highlight the necessity of capacity design.

The response of the structure investigated in each case is illustrated in the following diagrams for a pushover and a GMNIA analysis as well. It should be reminded that in Scenario 1, initial imperfections were introduced in both directions only to the upper bracing system, whereas in Scenarios 3 and 5 to all existing bracings. Scenarios 1 and 3 display almost the same horizontal capacity, even though the design philosophy was different in each case. Since the pushover analysis includes only material non-linearity, the parameter that played the most important role was the area of the selected cross-sections. Particularly, in Scenarios 1 and 3, the yielding of the tension diagonals takes place for almost the same seismic shears.

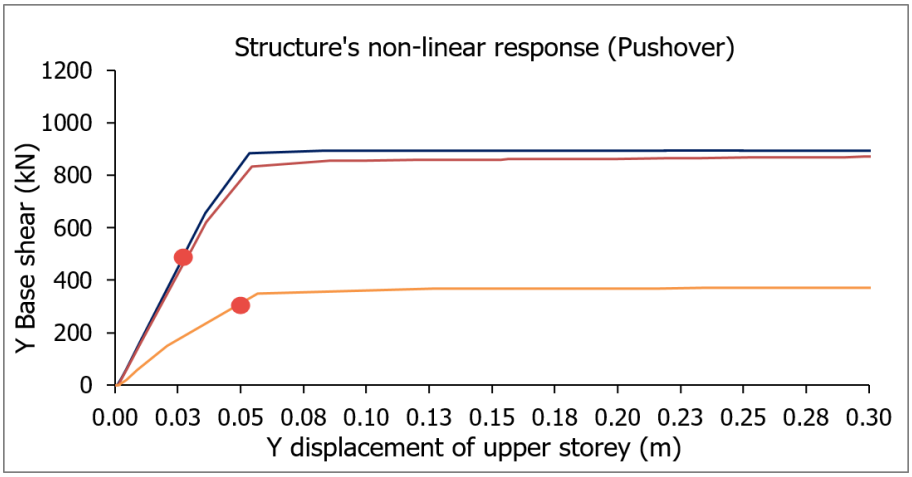

Figure 3-58: Comparison of MNA (Pushover) curves for all scenarios

In the case of the GMNIA analysis, where both area and non-dimensional slenderness contribute to the total response of the structure, the response of the structure in Scenarios 1 and 3 is very similar. Despite the different values in slenderness, as well as the interaction of the two directions, the seismic shears for which the buckling of the bracings takes place, as well as the ultimate loads do not differ significantly in those two scenarios. In addition, the yielding of the tension diagonals seems to remain unaffected, as it is developed for almost the same seismic loads in both cases. The results of the analyses and design methods are evaluated only in terms of load-bearing capacity, without considering target displacements and ductility.

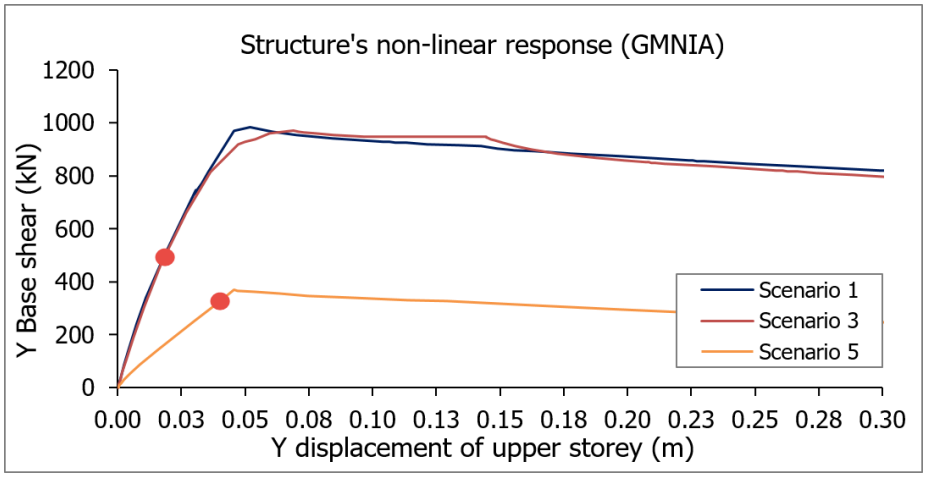

Figure 3-59: Comparison of GMNIA (actual response) curves for all scenarios

However, the seismic capacity should not be evaluated based entirely on the absolute value of their ultimate loads, but, in spite, on their performance concerning the resistance of the respective seismic loads. Consequently, the design base shear is also presented for each scenario and the total capacity is assessed using a dimensionless quantity. This index could be defined as $C = V_u/V_b$, where V_u is the ultimate load in each type of analysis (MNA or GMNIA) and V_b is the developed base shear for the tension diagonal only in the seismic design situation.

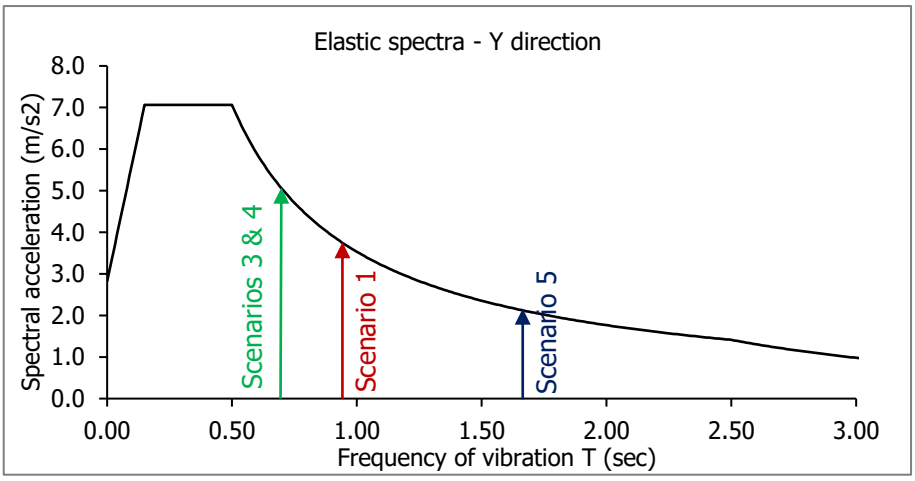

Figure 3-60: Elastic spectra and Y periods of vibration for the design scenarios

The conclusive decision concerning the most recommended scenario of elastic analysis should be based on the balance of the following two indexes; index C that demonstrates the ability of the structure to resist the developed seismic loads in the design situation and, secondly, index R that introduces the accuracy in the prediction of the ultimate loads using the quantity $(2N_{b,Rd}+2N_{pl,Rd})\cos\theta$ and is defined as $R = 2N_{pl,Rd}\cos\theta/V_{b,max}$ for the MNA analysis and $R' = (2N_{b,Rd}+2N_{pl,Rd})\cos\theta/V_{b,max}$ for the GMNIA.

Table 3-12: Comparison of characteristic quantities according to the non-linear analyses

Scenario	**$V_{b,max}$ MNA**	**C MNA**	**$2N_{pl,Rd}$ MNA**	**R MNA**	**$V_{b,max}$ GMNIA**	**C' GMNIA**	**$(2N_{b,rd}+2N_{pl,Rd})*\cos\theta$ GMNIA**	**R' GMNIA**
1	900	1.77	868	0.96	1000	1.96	1066	1.07
2	1800	3.54	1736	0.96	1000	1.96	1066	1.07
3	850	1.72	868	0.98	1.02	1.98	1173	1.20
4	850	1.72	868	0.98	1.02	1.98	1173	1.20

According to Table 3-12 and for the MNA or pushover type of analysis, the values of index C are much greater than 1, meaning that the structure displays an increased ability to resist the required base shear in the seismic design situation, where the buckling of the compressed bracings has taken place. Regarding the approximation of the ultimate load in an MNA analysis, the approach of $2N_{pl,Rd}$ in the first two cases underestimates the ultimate load as index R is greater than 1, while in Scenarios 3 and 4 it overestimates it. Moreover, according to index R', the approach of $(2N_{b,Rd}+2N_{pl,Rd})\cos\theta$ is extremely unsafe for all scenarios as it overestimates their ultimate load.

In the more representative and realistic case of the full non-linear analysis, the values of index C' are much greater compared to the correspondent index in MNA, leading to the conclusion that the actual load-bearing capacity of the structure, where the buckling of the compressed bracing takes place, is relatively higher than the one calculated using a pushover analysis. The existence of compressed bracings, although they buckle for small seismic shears, delays the yielding of the tension diagonals. As a result, their yielding occurs for higher base shear values, thus increasing the capacity of the structure which is primarily defined by the yielding point of the tension diagonals.

Consequently, the best approach of the 'actual' ultimate load in the GMNIA analysis, is considered

Scenario 1, which abides by the Eurocode's guideline that ignores entirely the compressed bracing. In correspondence to the ultimate load received from the GMNIA analysis, the seismic capacity in the MNA is underestimated by a factor of 10%, while the approximation of the ultimate load by calculating the horizontal components of the braced members in the base is satisfactorily accurate. In addition, Scenario 3 displays an increased 'actual' capacity compared to the pushover analysis, although the approach of its ultimate load in the MNA analysis is considered unsafe (R<1).

The conclusive definition of the most suitable scenario lies on the available analysis tools and their trustworthiness. In case the software used for the analysis of the structure is assumed to carry out trustworthy pushover curves, then the selection between Scenarios 1 and 3 is at the discretion of the designer, since both cases present increased load-bearing capacity in the seismic design situation, while the total weight of the steel in use and, thus, cost is very similar. In any case, though, it is recommended to assess the ultimate load received from a pushover analysis using quantity $2N_{pl,Rd}$. If there is no convergence between the two ultimate loads, then Scenario 1 is considered a safer approach, since ultimate load can be safely approached through quantity $2N_{pl,Rd}$. Concerning Scenario 3, since both approaches of $(2N_{b,Rd}+2N_{pl,Rd})\cos\theta$ and $2N_{pl,Rd}$ are rendered unsafe, it would be rather against safety to assume that the ultimate load of the structure in this case is equal to $2N_{pl,Rd}$. Therefore, in case no solid approach of the ultimate load using pushover analysis is available, it is recommended not to design according to Scenario 3 and choose Scenario 1 instead.

3.9 CONCLUSIONS

In this chapter, the load-bearing capacity of a three-storey steel building with concentrically braced frames is extensively investigated in the seismic design situation through non-linear analyses for all design scenarios. In particular, a non-linear analysis of material is carried out and compared to the respective pushover curves received from the commercial software. Subsequently, geometric non-linearity with initial imperfections is also considered, while the total behavior of the structure is examined in each scenario. The behavior of the CBF columns is investigated independently, although they do not present any type of failure and their behavior remains linear, since they are capacity designed. The braced members, though, dominate the behavior of the structure, as the buckling of the compressed bracing in conjunction with the upcoming yielding of the tension diagonals define the ultimate load.

Finally, the effect of the rather definitive non-dimensional slenderness criterion to the design of the bracings is investigated in terms of load-bearing capacity and displacements, which inspired the need to highlight the necessity of the entire concept of capacity design. Therefore, a fifth design scenario is introduced, where the structure under investigation is designed based entirely on the resistance checks, thus ignoring completely the requirements of the seismic code. A parametric study for the material of the bracings as well as the columns directly connected to them is carried out, leading to the conclusion that only the material of the bracings influences the capacity of the structure. Ultimately, the load-bearing capacity of the structure in correspondence to the developed seismic shear is assessed for each design scenario and type of analysis, while the safest scenario is suggested as a realistic approach of the 'actual' behavior of the structure, using only linear analyses and commercial too

4 CHAPTER 4: GENERAL CONCLUSIONS

4.1 SUMMARY

The present diploma thesis aims to investigate the influence in the design and the behavior of the compressed bracings in the load-bearing capacity of regular multi-storey steel buildings under seismic loading. In particular, guideline §6.7.2(2) of Eurocode 8 is under investigation, which stipulates that in concentrically braced framing systems only the tension diagonal should be taken into account. In order to address this matter under realistic conditions, 4 possible design scenarios are created that represent different approaches and interpretations of the aforementioned guideline. The fundamental principles and requirements of capacity design are summarized and presented in the first chapter, with emphasis on the understanding of their application. For the purposes of this thesis, a methodology in the form of a design algorithm with specific checks was developed, that integrates all design requirements for the modelling of regular multi-storey steel building according to Eurocodes 3 and 8.

In the following chapter, the direct application of the basic principles of capacity design presented in the first chapter is carried out for the design of a three-storey steel building with MRF as well as CBF systems. The developed optimum design method is used for the modelling of all scenarios, while its detailed application is demonstrated for the first scenario, step by step, from the preliminary to the final design. The most definitive checks for the modelling of the primary seismic members, such as the columns and the bracings, are also summarized, while comparative results in terms of internal forces, displacements and selected cross-sections are illustrated between the different scenarios.

In the third chapter, the contribution of the compressed bracings is taken into account in the structural configuration and the behavior of the structure is extensively investigated through non-linear analyses. The effects of the compressed bracing's buckling and the yielding of the tension diagonals concerning the response of the building as well as the columns directly connected to the bracing systems are examined. An investigation of the non-dimensional slenderness limitation is also carried out, while the importance of capacity design is highlighted in the design and load-bearing capacity of steel buildings.

Finally, the load-bearing capacity of the structure in correspondence to the developed seismic shear is assessed for each design scenario and the most effective scenario is suggested as a more realistic approach of the contribution of the compressed bracing.

4.2 CONCLUSIONS

The direct application of the basic principles of Eurocode 8 in the three-storey steel building in conjunction with the development of the optimum design method, result in the following conclusions concerning the design of regular steel buildings using elastic analyses.

- The design of the main, as well as the secondary beams, is based on the Ultimate and the Serviceability Limit states which are rendered more unfavorable compared to the seismic situation.
- The upper limit of the non-dimensional slenderness is the most definitive criterion for the design of the bracings, in correspondence to the damage limitation checks for the design of the columns due to the increased lateral flexibility of the moment resisting frames.
- The non-dimensional slenderness limitation $1.3 \leq \bar{\lambda} \leq 2.0$ in conjunction with the 25% criterion for the uniform distribution of ductility across the bracings increases the demand for cross-sections and, therefore, results in higher load-bearing capacity compared to the design base shear.
- In the direction of a typical CBF structural configuration, the columns directly connected to the bracings are mainly affected by their vertical axial component and they do not develop any shear or bending moment for horizontal loads across the Y direction.
- The alternative approach of the assumption of half cross-section area and twice design axial force reaches the same outcome as Scenario 3, where the compressed bracing is included in the elastic analysis.

Subsequently, the structure's response is evaluated and interpreted through non-linear analyses, while the behavior of both braced members as well as the columns directly connected to them is also investigated. Both non-linear analyses of material (MNA) and geometry (GMNIA) are carried out as an attempt to approach the results received from a typical pushover curve and the structure's actual response respectively. The following conclusions are reached according to the non-linear analyses:

- The elastic and non-linear analysis retain the same tangent and, therefore, rigidity for small values of base shear in the GMNIA analysis. In the case of the MNA analysis, their tangents are completely identical, as no buckling takes place that reduces the rigidity of the structure.
- Despite the fact that all compressed bracings lose their rigidity due to global buckling in the seismic design situation, the structure continues to resist horizontal loads as tension diagonals retain their rigidity. Considering that the buckling of the compressed bracings precedes the yielding of the tension diagonals, the structure's ultimate load-bearing capacity depends entirely on the tension diagonals after all bracings have buckled.
- The stringent damage limitation checks that govern the design of the columns due to the relative

sensitivity of the steel moment frames in the X direction, eliminate the possibility of failure due to global buckling or yielding, while the classification requirements limit the possibility of local buckling.

- The stern drift and stability requirements lead to considerable overstrength of the CBF columns, which reduces the ductility demand in dissipative zones. Due to the capacity design of the CBF columns, their behavior is perfectly linear in all cases.
- A pushover analysis should be carried out with the tension diagonal only, in spite of the number of bracings considered in the elastic analysis. A pushover analysis with both bracings overestimates the ultimate load of the structure by a factor of 2.
- In case only the tension diagonal is taken into account during the modelling of the structure, a pushover analysis underestimates the load-bearing capacity by a factor of 10% compared to the 'actual' ultimate load acquired using a GMNIA.
- The pushover curve with the tension diagonal only is considered a safe approach of the structure's ultimate load, as the GMNIA curve is located above the MNA curve for all scenarios.
- The ultimate load of the structure when a pushover analysis is carried out is almost the same in Scenarios 1 and 3, where the contribution of the compressed bracing has been ignored in the first case, while in the latter it is considered.

Ultimately, the influence and necessity of capacity design are also investigated through the introduction of a final scenario, where the seismic code is ignored and the structure is designed based entirely on the resistance checks. The importance of capacity design is highlighted in the following two cases. Firstly, the load-bearing capacity of the structure is evaluated in correspondence to the required seismic shear with due account to the possibility of exceedance of the nominal values of the seismic actions during the design. Secondly, a parametric study for the material of the columns as well as the bracings is carried out for all scenarios.

- Scenario 5, where the seismic code is completely ignored, illustrates the detrimental effects of the non-compliance to the capacity design requirements in the load-bearing capacity of the structure.
- According to the parametric study for the material of the columns, it is clearly illustrated that any modification to the grade of steel in the CBF columns has absolutely no effect in the seismic capacity of the structure. The main reason lies on the stern drift and stability requirements imposed in the CBF columns according to capacity design.
- According to the parametric study for the material of the bracings, in both Scenarios 1 and 3, even for the lowest grade of S275, the structure retains its ability to resist adequately the required seismic shear.
- In Scenario 5, though, where the principles of capacity design are not satisfied, the structure presents a reduced ability to resist the design seismic shear as the grade of material reduces. The columns, however, do not present any failure due to buckling or yielding, since the design seismic shear is very close to the structure's ultimate load.

- The seismic capacity of the structure should not be evaluated based on the ultimate load, but rather, on its relative ability to resist the developed seismic shear in each case. The cross-sections of the bracings and, therefore, the rigidity of the structure defines the value of the imposed seismic loads.
- In case the software used for the elastic analysis is considered trustworthy, then the selection between Scenarios 1 and 3 is at the discretion of the engineer, since the structure presents almost the same load-bearing capacity in both cases (in both pushover and GMNIA curves). However, in case there is no convergence between the ultimate load received from the pushover analysis and the simplified approach, it is preferable to design according to Scenario 1.

4.3 SUGGESTIONS FOR FURTHER RESEARCH

In the present diploma thesis, the modelling and investigation of the behavior of a regular multi-storey steel building with concentrically braced frames under seismic loading was carried out. One of the first initial assumptions is regarding to the buckling length of the bracings, which is considered equal to half the diagonal's length, due to the defined moment end-releases, both in and out of plane. A more detailed approach could include the parametric study of the bracings' buckling length in correspondence to the load-bearing capacity of the structure. Taking into consideration that the very definitive non-dimensional slenderness criterion depends on the effective buckling length as well as the radius of gyration of the bracing's cross-section, the investigation of the buckling length affects directly the radius of gyration and, therefore, the available cross-sections.

An alternative approach could include the investigation of the load bearing capacity of buildings that do not comply with the criteria for regularity and, especially, those considered irregular in elevation which is a significant prerequisite for the application of the lateral force method of analysis. In particular, no conclusions can be reached concerning the consideration or not of the compressed bracings in case a modal response spectrum analysis should be carried out, according to this thesis. Since the current building is categorized as regular, a modal response spectrum analysis would only modify the developed internal forces, due to the participation of higher modes of vibration. The seismic loads are imposed in the centre of mass of each storey, which in this case coincides with the respective centre of rigidity, and, therefore, no torsional effects are taken into account. Consequently, in the case of a modal response spectrum analysis, the building under investigation should be considered irregular in order to increase the contribution of higher modes of vibration as well as the torsional effects, due to the difference between the center of mass and the center of rigidity of the storeys.

Especially in the case of a pushover analysis in irregular buildings where the contribution of higher modes of vibration is significant, it is rather inaccurate to carry out a pushover analysis only for the fundamental period of vibration. This problem can be mitigated, but not eliminated, by applying more than one load patterns that account for higher elastic mode effects (Krawinkler & Seneviratna 1998). Consequently, the developed seismic loads of each mode shape are imposed in the structure and a pushover curve is received for the respective mode shape. Afterwards, all the extracted curves are superpositioned (using the SRSS or the CQC method) according to the modal pushover methodology and the final pushover curve is received. However, this approach is only suitable when material non-

linearity is considered and is, therefore, extremely inaccurate to introduce geometric non-linearity, rendering the superposition of the GMNIA results impossible. An entirely different approach is required in this case, where the structure is subjected to dynamic time-history analysis with material non-linearity, where the mode shapes are calculated based on the assumption of elastic material.

Additionally, the benchmark for the interpretation of the non-linear results in the present thesis is defined as the ultimate load. It is as crucial to assess the seismic capacity of the structure in terms of displacements and, more specifically, the available and demand ductility. Moreover, the capacity curve could be checked to fulfill the requirements of the target displacements regarding immediate occupancy, life safety and structural stability.

Lastly, the development of the respective methodology for the design as well as the investigation of the behavior of both regular and irregular buildings using non-linear analyses can be expanded to the examination of frames with eccentric bracings instead of concentrically braced framing systems.

5 REFERENCES

A. Elghazouli, 2008: Seismic Design of Steel-Framed Structures To Eurocode 8. The 14th World Conference on Earthquake Engineering (14WCEE).

A. Elghazouli, 2004: Seismic design procedures for concentrically braced frames

A. Elghazouli, 2009: Seismic design to Eurocode 8, CRC Press.

Ch. Gantes, 2015: Elastic and inelastic buckling of compressed members, pp.1–38.

EN1993-1-1, 2011: Eurocode 3 (2005).

EN 1998-1:, 2004: Eurocode 8, pp.1–229.

I. Psycharis, 2016: Earthquake Engineering Notes - Part 1.

JRC European Commission, 2012: Eurocode 8 : Seismic Design of Buildings Worked examples

Krawinkler, H. & Seneviratna, G.D.P.K., 1998: Pros and cons of a pushover analysis of seismic performance evaluation. Engineering Structures, 20(4–6), pp.452–464.

Kumar, Stafford & Elghazouli, 2013: Influence of ground motion characteristics on drift demands in steel moment frames designed to Eurocode 8. Engineering Structures, 52, pp.502–517.